Six-rowed spike 4 (*Vrs4*) regulates spike architecture and lateral spikelet fertility in barley (*Hordeum vulgare* L.)

Dissertation

zur Erlangung des

Doktorgrades der Agrarwissenschaften (Dr. agr.)

der

Naturwissenschaftlichen Fakultät III
Agrar- und Ernährungswissenschaften,
Geowissenschaften und Informatik

der Martin-Luther-Universität Halle-Wittenberg

vorgelegt von

Herrn M.Sc. Ravi Koppolu

geb. am: 12.08.1982 in Santhanuthalapadu, India

Gutachter:

Prof. Dr. Andreas Graner

Dr. Takao Komatsuda

Verteidigt am

13/10/2014

Halle/Saale

Acknowledgements

At the outset, i convey my heartfelt thanks to my supervisor, Dr. Thorsten Schnurbusch (Research group leader, Plant Architecture, IPK) for giving me the opportunity to work in the exciting field of barley inflorescence development. I sincerely admit that my research project would not have been at its present state without his unabated support, fruitful scientific discussions, advices, and encouragement. My special thanks to Dr. Takao Komatsuda (NIAS, Japan) for giving motivation to work on this project, his collaborative efforts and fruitful scientific discussions were indispensable in achieving the project goals.

I sincerely thank Prof. Dr. Andreas Graner (Director, IPK), for accepting me as a PhD student at the Martin-Luther-University (MLU), Halle-Wittenberg. I am very thankful for his appreciation of my research results, great encouragement and guidance during the course of the project.

I would like to thank different people at IPK for helping me with their scientific expertise, and knowledge, especially Dr. Twan Rutten for helping with the scanning electron microscopy, Dr. Nese Sreenivasulu, and Dr. Christiane Seiler for the microarray work, Dr. Ruvini Ariyadasa for physical mapping, and Dr. Nicolas Heinzel for the metabolite analysis. I am beholden to an anonymous reviewer of the PNAS paper (published based on the present thesis) for his/her valuable ideas, and suggestions in performing the phylogenetic analysis.

I would like to thank all of my present and former colleagues from research group Plant Architecture for creating a friendly and scientific environment and constant support. My special thanks to office mates Dr. Piotr Gawroński, Tina Seidensticker, Dr. Helmy Youssef, and other group members Dr. Naser Poursarebani, Ahmad Alqudah, Zifeng Guo, Gizaw Wolde Metaferia, and Arash Fazeli for being wonderful to me. I sincerely and greatly acknowledge the technical assistance rendered by, Corinna Trautewig, Claudia Weissleder, Mechthild Peurschel, Mandy Püffeld, and Annette Bayer. My sincere thanks are also to the technical staff from the research group Genome Diversity. The technical help offered by the greenhouse staff is invaluable. I thank all of the administrative staff at IPK, especially Dr. Britt Leps for their kind help with the work and family related matters.

I thank all of my Indian and cross-continental friends for creating a friendly and joyous atmosphere in Gatersleben.

I deem that my achievements are incomplete without my family support. I especially thank my parents Koppolu Murahari and Koppolu Chinna Durga Prasad for nurturing me to my present day status. I wholeheartedly thank my dear wife Koppolu Jahnavi, for her constant support and encouragement all through my PhD and also for giving a lovely daughter Koppolu Arnavi SriSai.

At the end I would like to conclude by giving a quote that I firmly believe in,

"A hundred times every day I remind myself that my inner and outer life are based on the labors of other men, living and dead, and that I must exert myself in order to give in the same measure as I have received and am still receiving".

– Albert Einstein.

Contents

1.0. Introduction **1**

1.1. Inflorescence development in grasses **2**

1.1.1. Rice **4**

1.1.2. Maize **5**

1.1.3. Wheat and Barley **6**

1.2. Genetic regulation of inflorescence development in rice and maize **7**

1.2.1. Control of inflorescence meristem identity and development **8**

1.2.2. Control of branch meristem identity and development **9**

1.2.2.1. Maize *RAMOSA* pathway **12**

1.2.3. Control of spikelet meristem identity **14**

1.2.4. Control of floral meristem identity **15**

1.3. Genetic regulation of inflorescence development in barley **16**

1.3.1. Control of lateral spikelet fertility and row–type **16**

1.3.2. Control of spikelet meristem identity and spike branching **19**

1.3.3. Control of rachis internode elongation and spike density **20**

1.3.4. Control of glume development **21**

1.3.5. Control of lodicule and stamen development **22**

1.3.6. Control of lemma and awn development **23**

1.3.7. Control of caryopsis type **24**

1.4. Genomics resources for gene cloning in barley **25**

1.4.1. Structural genomics tools **26**

1.4.1.1. ESTs and FLcDNAs **26**

1.4.1.2. BAC libraries **26**

1.4.1.3. Genetic and physical maps **27**

1.4.1.4. Gene expression arrays **28**

1.4.1.5. Barley whole exome capture **29**

1.4.2. Functional genomics tools **29**

1.4.2.1. Forward genetic tools **29**

1.4.2.2. Reverse genetic tools **30**

1.5. Aims of the present thesis **33**

2.0. Materials and Methods **34**

2.1. Plant materials and growing conditions **34**

2.1.1. Spike phenotype analysis **34**

2.1.2. F_2 mapping populations **34**

2.1.3. Allelic *vrs4* mutants **34**

2.1.4. *Vrs4* candidate gene re-sequencing **35**

2.1.5. Microarray and qRT–PCR analyses **36**

2.1.6. Metabolite analysis **36**

2.2. DNA preparation **37**

2.3. Genetic linkage and physical mapping of *vrs4* locus **37**

2.3.1. Molecular marker development **37**

2.3.2. Phenotyping of mapping populations **38**

2.3.3. Linkage analysis of genotypic and phenotypic data **38**

2.3.4. High resolution mapping **39**

2.3.5. BAC sequencing, assembly, and annotation **39**

2.4. mRNA expression analyses **40**

2.4.1. RNA extraction **40**

2.4.2. Microarray hybridization and data analysis **41**

2.4.3. qRT–PCR **42**

2.5. Metabolite analysis of trehalose biosynthesis intermediates and precursors **43**

2.6. Re-sequencing and haplotype analysis of *vrs4* in diverse barley genotypes **43**

2.7. Phylogenetic analysis of RAMOSA2 orthologs/homologs **44**

2.8. Data contributions by the author and the collaborators towards the present thesis **44**

3.0. Results **47**

3.1. Spikelet development in *Vrs4* wild type and mutant inflorescences **47**

3.1.1. Scanning electron microscopy showed early developmental changes in inflorescences of *vrs4* mutants leading to indeterminate spikelet development with altered axillary meristem identity **48**

3.1.2. Different types of additional axillary structures produced by *vrs4* mutants **50**

3.1.3. Lateral spikelet fertility is completely restored in *vrs4* mutant inflorescences **53**
3.2. Genetic and physical mapping of *vrs4* locus **55**
3.2.1. Low resolution mapping in F_2 populations localizes *vrs4* to chromosome 3HS **55**
3.2.2. High resolution and fine-scale mapping of *vrs4* locus on 3HS **58**
3.2.3. Establishment of barley physical BAC contig around *vrs4* locus **58**
3.3. Identification of candidate gene responsible for *vrs4* phenotype and its validation **60**
3.3.1. *Vrs4* underlies a barley ortholog of maize inflorescence architecture gene *RAMOSA2* (*HvRA2*) **60**
3.3.2. Validation of *HvRA2* gene candidate in allelic *vrs4* mutants by re-sequencing **60**
3.3.3. Validation of *HvRA2* gene candidate by qRT–PCR **64**
3.3.4. *HvRA2* encodes a LOB domain transcription factor with grass specific domains **65**
3.4. Phylogenetic analysis of RAMOSA2 orthologs/homologs from grasses and eudicots groups them into two distinct and respective clades **67**
3.4.1 *HvRA2* is unique among the barley LBD gene family members **71**
3.5. Re-sequencing of *HvRA2* shows reduced nucleotide diversity **73**
3.6. Identification of downstream target genes of *Vrs4* by mRNA expression analysis **77**
3.6.1. *Vrs1* is highly down-regulated in *vrs4* mutants **79**
3.6.2. *vrs4* mutants showed down regulation of genes involved in trehalose biosynthesis **80**
3.6.3. *EGG APPARTUS1–LIKE* is highly up-regulated in *vrs4* mutants **81**
3.6.4. *vrs4* mutants showed differential regulation of transcripts involved in cytokinin biosynthesis and auxin transport **81**
3.7. Metabolite analysis in *vrs4* mutants showed unaltered pools of Trehalose–6–Phoshate, Glucose–6–Phosphate, and UDP–glucose **87**
4.0. Discussion **89**
4.1. *Vrs4* (*HvRA2*) regulates two distinct genetic pathways in barley inflorescence development **90**

4.1.1. *HvRA2* regulates spikelet determinacy at barley's TSM **90**
4.1.2. *HvRA2* regulates barley row–type pathway **92**
4.1.2.1. Converging evidence for transcriptional regulation of *Vrs1* by *Vrs4* **92**
4.2. Genetic regulation of *RAMOSA* pathway in barley may differ from that of maize and other Andropogoneae species **96**
4.2.1. Evolution of *RAMOSA2* **99**
4.2.2. *HvRA2* is co–opted for regulating row–type phenotype in barley **100**
4.3. Gene expression analysis using microarray indicated that *HvRA2* may regulate phytohormones and trehalose-6-phosphate biosynthesis and metabolism **101**
4.3.1. *HvRA2* may control trehalose-6-phosphate homeostasis **101**
4.3.2. *HvRA2* may regulate active cytokinin pools and polar auxin transport **104**
4.4. The reduced variation at *HvRA2* may represent a purifying selection **107**
5.0. Outlook **108**
6.0. Summary **112**
7.0. Zusammenfassung **114**
8.0. References **116**
9.0. Supplementary information **131**
10.0. Curriculum Vitae **136**
11.0. Eidesstattliche erklärung **139**

List of Figures

Figure 1.1.1. Schematics showing panicle and inflorescence meristem differentiation **4**
Figure 1.1.2. Schematics showing maize tassel inflorescence and meristem differentiation in tassel and ear **5**
Figure 1.1.3. Schematics showing wheat, barley spikes and their inflorescence meristem differentiation **7**
Figure 1.2.1. Genetic control of inflorescence development in rice and maize **11**
Figure 1.2.2. Tassel and ear phenotypes of maize *ramosa* mutants **14**
Figure 1.3.1. Spike morphology of different *vrs* loci **18**
Figure 1.3.2. Spike phenotypes of *compositum* and *rattail* mutants **20**

Figure 1.3.3. Phenotypes of *dense spike* (*dsp*) and laxatum (*lax*) mutants **22**
Figure 1.3.4. Barley *third outer glume* (*trd*) phenotype **22**
Figure 1.3.5. Phenotypes of cleistogamous and chasmogamous barley spikes **23**
Figure 1.3.6. Spike phenotype of *Hooded* (*Kap*) barley **24**
Figure 1.3.7. Kernel and spike phenotypes of hulled and hull less barley **25**
Figure 3.1.1. SEM analysis of BW-NIL(*mul1.a*) and BW-NIL(*vrs4.k*) **50**
Figure 3.1.2. Spike morphology of Six-rowed spike 4 (*vrs4*) mutants **51**
Figure 3.1.2-1. Glume, lemma and tillering defects in *vrs4* mutants **53**
Figure 3.1.3. Spike phenotypes of *vrs4* mutant alleles **54**
Figure 3.2.1. Linkage maps for the *vrs4* locus on barley chromosome 3H **57**
Fig. 3.2.3. High resolution linkage and physical map of *vrs4* **59**
Figure 3.3.2a. *HvRA2* gene model localized with lesions in *vrs4* mutant alleles **62**
Figure 3.3.2b. *HvRA2* (*Vrs4*) nucleotide and protein sequences showing mutated positions and effects for sixteen *Vrs4* mutant alleles **63**
Figure 3.3.3. Relative expression of *HvRA2* in BW-NIL(*vrs4.k*), MHOR 318 and MHOR 345 compared to their progenitors **65**
Figure 3.3.4. RA2 and RA2-like proteins in grasses and eudicots **67**
Figure 3.4.0. Phylogenetic analysis of RAMOSA2 orthologs/homologs and other LBD proteins **70**
Figure 3.5.0. Resequencing of *HvRA2* in diverse barley genotypes **76**
Figure 3.6.1. Relative *mRNA* expression of *Vrs1* in *vrs4.k* mutant **80**
Figure 3.6.2. Gene expression analysis in *vrs4* using microarray **83**
Figure 3.6.4. qPCR validation of differentially regulated genes identified in the *vrs4* microarray experiment **84**
Figure 3.6.5. Expression of *HvCKX2*, *HvSRA* and *HvPIN1-LIKE* in *vrs4* mutants **86**
Figure 3.7.0. Trehalose biosynthesis in higher plants **87**
Figure 3.7.1. Metabolite analysis of trehalose biosynthesis precursors, intermediates **88**
Figure 4.1.1. Branching phenotype in *vrs4* mutant, MC(*mul1.a*) **91**
Figure 4.1.2. Model of *Vrs4* interaction with *Vrs1* **93**
Figure 4.1.2-1. HvRA2 functions as a transcriptional regulator of *Vrs1* **95**
Figure 4.2.0. *HvBAD1* expression in *vrs4* mutants **99**

Figure 4.3.0. Models of *Vrs4* interactions showing putative targets of *HvRA2* **106**

List of Tables

Table 1-1. Barley *vrs* loci, their occurrence and chromosomal location **17**

Table 1-2. Gene cloning and characterization in barley **32**

Table 2-1. *vrs4* mutant allele descriptions **35**

Table 2-2. BAC clones sequenced in *Vrs4* gene region on 3HS **40**

Table 3-1. *vrs4/Vrs4* segregation analysis in the two F_2 mapping populations **55**

Table 3-2. *vrs4* mutant alleles with type of molecular lesion in *HvRA2* and its position within ORF **64**

Table 3-3. List of barley LOB domain (LBD) encoding genes **72**

Table 3-4. Barley accessions used for *Vrs4* haplotype analysis with their haplotypes **74**

Table 3-5. Characterization of *X*-ray induced deletion in MHOR 318 & MHOR 345 **78**

Supplementary Information

Supplementary Table 1a. List of markers used for genetic mapping of *vrs4* **131**

Supplementary Table 1b. Primer pairs for *HvRA2* resequencing and haplotype analysis **132**

Supplementary Table 1c. qRT-PCR primer pairs used in the present study **132**

Supplementary Table 2. Monocot RAMOSA2 orthologs, RAMOSA2-LIKE proteins from dicots and LBD proteins used for phylogenetic analysis **133**

Supplementary Text **135**

Supplementary Table 3. Complete set of genes regulated in MHOR 318 and MHOR 345, respective progenitors AD and HH (**Data provided as Compact Disc**.)

Supplementary Table 4. Expression patterns of genes regulated in MHOR 318 and MHOR 345, respective progenitors AD and HH (**Data provided as Compact Disc**.)

Supplementary Table 5. Genes commonly regulated in HH and AD in comparison to respective MHOR 345 and MHOR 318 mutants (**Data provided as Compact Disc**.)

Supplementary Figure 1. Microarray heat maps of MHOR 318 and MHOR 345, respective wild types AD and HH (**Data provided as Compact Disc**.)

List of Abbreviations

AA	Amino Acid
AD	Ackermann's Donaria
AF	Additional Floret
AM	Axillary Meristem
AP	Awn Primordium
AS	Additional Spikelet
At	*Arabidopsis thaliana*
BAC	Bacterial Artificial Chromosome
Bd	*Brachypodium distachyon*
BIM	Branch Inflorescence Meristem
BLAST	Basic Local Alignment Search Tool
BLASTn	Nucleotide BLAST
BLASTp	Protein BLAST
BLASTx	Translated nucleotide BLAST against protein database
BM	Branch Meristem
BOPA	Barley Oligo Pool Assay
bp	base pair
BR	Brassinosteroid
BW–NIL	Bowman Near Isogenic Line
˚C	Celsius
CAPS	Cleaved Amplified Polymorphic Sequence
cM	centi Morgan
cm	centimeter
cRNA	complementary RNA
CS	Central Spikelet
CSM	Central Spikelet Meristem
Cy3	Cyanine3
DArT	Diversity Arrays Technology
dCAPS	derived CAPS
DNA	De-oxyribo Nucleic Acid
DR	Double Ridge
EMS	Ethyl Methyl Sulfonate
EST	Expressed Sequence Tag
F_2	Second filial generation

FLcDNA	Full Length cDNA
FM	Floret Meristems
GA	Green Anther
Gb	Gigabase
GP	Glume Primordium
GWAS	Genome Wide Association Study
G6P	Glucose-6-phosphate
h	hour
HH	Heine's Haisa
Hv	*Hordeum vulgare*
IM	Inflorescence Meristem
INDEL	Insertion Deletion
IPK	Leibniz Institute of Plant Genetics and Crop Plant Research
LC-MS/MS	Liquid Chromatography-Mass Spectrometry
LBD	LOB Domain
LBM	Long Branch Meristem
LOB	Lateral Organ Boundary
LP	Lemma Primordium
LS	Lateral Spikelet
LSM	Lateral Spikelet Meristem
μg	Microgram
μl	Microlitre
μm	Micrometre
mm	Millimetre
mRNA	messenger RNA
miRNA	micro RNA
Mya	Million years ago
NCBI	National Centre for Biotechnology Information
NIAS	National Institute of Agrobiological Sciences
ORF	Open Reading Frame
Os	*Oryza sativa*
PBMs	Primary Branch Meristems
P-value	Probability value
QC	Quality Control
qRT–PCR	quantitative Real Time-Polymerase Chain Reaction
RFLPs	Restriction Fragment Length Polymorphisms

RIN	RNA Integrity Number
RNAi	RNA interference
s	Second
SAM	Shoot Apical Meristem
SBMs	Secondary Branch Meristems
SE	Standard Error
SEM	Scanning Electron Microscopy
SFP	Single Feature Polymorphism
ShBM	Short Branch Meristem
SIM	Secondary Inflorescence Meristem
SM	Spikelet Meristem
SNP	Single Nucleotide Polymorphism
SP	Stamen Primordium
SPM	Spikelet Pair Meristem
SSRs	Simple Sequence Repeats
syn	*synonymous*
TALENs	Transcriptional Activator–Like Effector Nucleases
TF	Transcription Factor
TILLING	Targeting Induced Local Lesions IN Genomes
TM	Triple Mound
TPP	Trehalose-6-phosphate phosphatase
TPS	Trehalose-6-phosphate synthase
TSM	Triple Spikelet Meristem
UDP	Uridine di-phosphate
USDA–ARS	United States Department of Agriculture-Agricultural Research Service
UTRs	UnTranslated Region
VIGS	Virus Induced Gene Silencing
WA	White Anther
WD40	Tryptophan (W) Aspartic acid (D) dipeptide 40
WT	Wild Type
Zm	*Zea mays*
60K	60 Thousand

1.0. Introduction

Cereals are the major and most important food source for human beings and also animal kind. The current cereal production amounts to 2.3 billion tonnes, of which approximately 1.0 billion tonnes is destined for human consumption, 750 million tonnes is used as animal feed, whereas the remaining 500 million tonnes serve as source to industrial usage, seed, or get wasted [(http://faostat3.fao.org/faostat-gateway/go/to/home/E), (FAO Statistical year book 2013)]. Barley (*Hordeum vulgare* L.), is the fourth most important cereal food crop after maize (*Zea mays* L.), rice (*Oryza sativa* L.), and wheat (*Triticum spp*.) in terms of global production (http://faostat.fao.org/site/339/default.aspx). Barley belongs to tribe Triticeae (family Poaceae) which also includes other economically important crops such as wheat, rye (*Secale cereale* L.), and triticale (× *Triticosecale* Witt. ex A. Camus). Barley was mainly cultivated for human food supply in the last century but nowadays it is significantly grown for animal feed, malt production and human food respectively (Baik and Ullrich, 2008). However, in some parts of Asia and Northern Africa, barley has still remained as a major food source (Newman and Newman, 2006). Interest in barley for food has increased in the recent past mainly because of the health benefits associated with its beta-glucan (an anticholesterol substance), acetylcholine (a substance which nourishes nervous system) contents, easy digestibility (due to low gluten contents), high lysine, thiamine and riboflavin (Marwat et al., 2012). Genetically barley is a diploid (2n=14), (vonBothmer, 1992) and self-pollinating annual plant with a comparatively smaller genome size [(DNA content = 5.1 Gb; (Dolezel et al., 1998)]. Among all of the Triticeae species, barley encompasses a rich collection of genetic and genomic resources (discussed in detail in section **1.4**). A draft genome sequence of barley was recently made available by the International Barley Sequencing Consortium (IBSC, 2012) which provides an essential reference gene space for

genetic research and breeding. Because of these facts barley can serve as a wonderful model plant for the tribe Triticeae.

1.1. Inflorescence development in grasses

The external appearance of flowering plants is determined to a large extent by the forms of flower–bearing branch systems (inflorescences), and their position and spatial orientation on the plant axis (Vollbrecht et al., 2005). In flowering plants the vegetative Shoot Apical Meristem (SAM) transforms into a reproductive Inflorescence Meristem (IM) after perceiving an intrinsic signal from the plant to flower. The architecture of inflorescence depends upon the function and fate of the IM. The IM produces groups of meristematic cells (stem cell-like plant cells) which differentiate to produce flower bearing branches, and reproductive floral organs. Thus, inflorescence architecture ultimately reflects meristem number, arrangement and also duration of meristem activity which correlates with inflorescence branch length.

In comparison to model dicot species such as Arabidopsis with simple inflorescence architecture, grasses (the Poaceae family) show complex inflorescence architecture (Kellogg, 2007). In Arabidopsis, when appropriate endogenous signal is perceived, the SAM transforms into a reproductive IM. The IM differentiates into a Secondary Inflorescence Meristem (SIM), which further differentiates into floral meristem (Amasino, 2010; Irish, 2010). This simple categorization of meristems seen in Arabidopsis is, however, insufficient to describe the great diversity of grass inflorescences, which have multiple types of meristems, each with a distinct fate and genetic control (Kellogg, 2007). In grasses, flowers are produced on a specialized short branch called spikelet. Before the formation of spikelet, inflorescence axis undergoes multiple iterations of branching depending upon species. Different grass species morphologically vary

from each other in their arrangement of inflorescence branches, spikelets, and florets (Clifford, 1987). Thus, the ultimate architecture is determined by the extent of branch iterations. In grasses, after transition from vegetative to the reproductive phase, the SAM converts into IM, as also seen in Arabidopsis. However, the IM in grasses further initiates the Branch Meristems (BMs) and forms the main axis of the inflorescence. The BMs initiate Spikelet Meristems (SMs) which further initiate Floret Meristems (FMs), the FM produces florets containing floral organs (carpel, stamen, and lodicules) and two outer organs lemma and palea which enclose the floral organs. The floral organs together with lemma and palea subtended by two rudimentary bract leaves (glumes) constitute the grass spikelet which serves as a building block of grass inflorescence (Clifford, 1987). The florets are initiated on an axis known as rachilla, which is specific to grasses. The spikelet is composed of one to several florets depending upon species (Sakuma et al., 2011). Although this represents the general scheme of inflorescence and flower development in grasses, various levels of branch iterations in different grass species result in diverse inflorescence structures. The three predominant inflorescence types that can be distinguished by branching architecture in grasses include (1.) simple raceme, where spikelets are born individually on short pedicels attached directly to the inflorescence axis. There are no branches (e.g. tassel inflorescence of maize (*Zea mays* L.), inflorescences of *Paspalum spp*. L., and *Echinocloa spp* L.), (2.) branched panicle: pedicelled spikelets are born on primary, secondary and tertiary branches arising from the inflorescence axis (e.g. *Oryza sativa* L., and *Sorghum bicolor* L.), (3.) spike: unbranched, sessile spikelets are directly attached to the inflorescence axis (e.g. *Hordeum spp.* L, *Triticum spp.* L, *Lolium spp.* L, and *Brachypodium spp*. L). It is thought that the panicle is the primitive grass inflorescence form, from which the spike inflorescence evolved at a later time (Ward and Leyser, 2004). Several variants of these three inflorescence

types exist in grasses. A detailed overview of reproductive meristem differentiation and organization in four of the major and commercially important grass species that bear one or the other inflorescence types mentioned above is described in the following sections.

1.1.1. Rice

The rice inflorescence is a panicle. Flower bearing spikelets in rice are produced after multiple rounds of branching which itself is indicative of a prolonged IM activity. The IM in rice initially produces several Primary Branch Meristems (PBMs) and degenerates after producing PBMs. The PBMs initiate Secondary Branch Meristems (SBMs), both PBMs and SBMs elongate to produce the typical panicle architecture in rice (Bommert et al., 2005) (**Figure 1.1.1.A**). The PBMs and SBMs produce SMs in their flanks and terminate in a SM. The SM differentiates into a single FM (**Figure 1.1.1.B**). In rice both, IM and axillary branch meristems (PBMs and SBMs), terminate with a determinate SM.

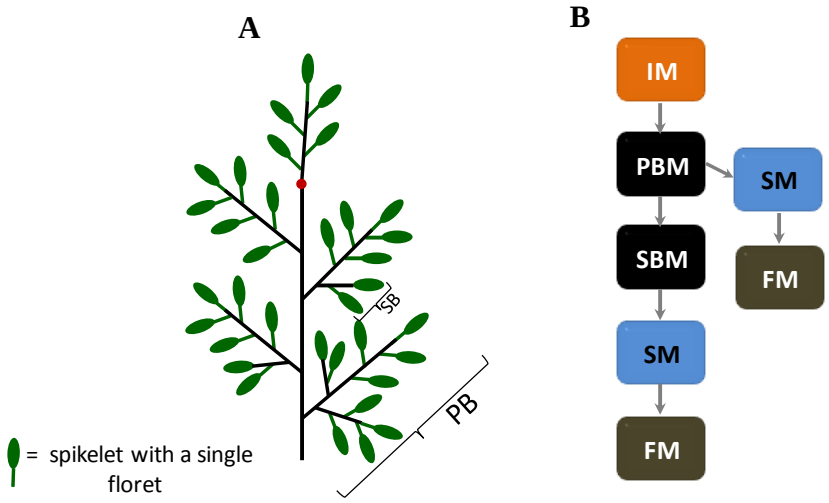

Figure 1.1.1. Schematics showing panicle and inflorescence meristem differentiation.
Mature panicle (**A**), and inflorescence meristem differentiation and organization (**B**) in rice. The red circle (**A**) denotes the degenerate tip of the panicle, which is indicative of IM degeneration. IM: Inflorescence Meristem: PBM: Primary Branch Meristem; SBM: Secondary Branch Meristem; SM: Spikelet Meristem; FM: Floret Meristem.

1.1.2. Maize

A more complex inflorescence meristem differentiation and organization can be seen in maize. Maize is a monoecious plant producing male flowers on a racemose inflorescence known as tassel (at the plant apex) (**Figure 1.1.2.A**), whereas the female flowers are born on a spike–type inflorescence called ear or cob (in vegetative leaf axils). In maize and other species of tribe Andropogoneae, spikelets are produced in pairs, (one pedicelled spikelet and one sessile spikelet) (**Figure 1.1.2.A**). The indeterminate tassel IM first initiates several indeterminate lateral Long Branch Meristems (LBMs) at the base, which themselves produce a large number of Short Branch Meristems (ShBMs) also known as Spikelet Pair Meristems (SPMs). After producing several LBMs the apical meristem shifts to produce ShBMs (SPMs). SPMs produce a pair of SMs (**Figure 1.1.2.B**). SMs produce sterile leaves, called bracts, and two staminate FMs. Unlike tassel the ear does not produce basal LBMs; the IM directly produces ShBMs which differentiate into SMs (**Figure1.1.2.C**). The SMs differentiate into a pair of pistillate floral meristems, in the maize ear only one FM remains fertile and the other FM is aborted (**Figure1.1.2.C**).

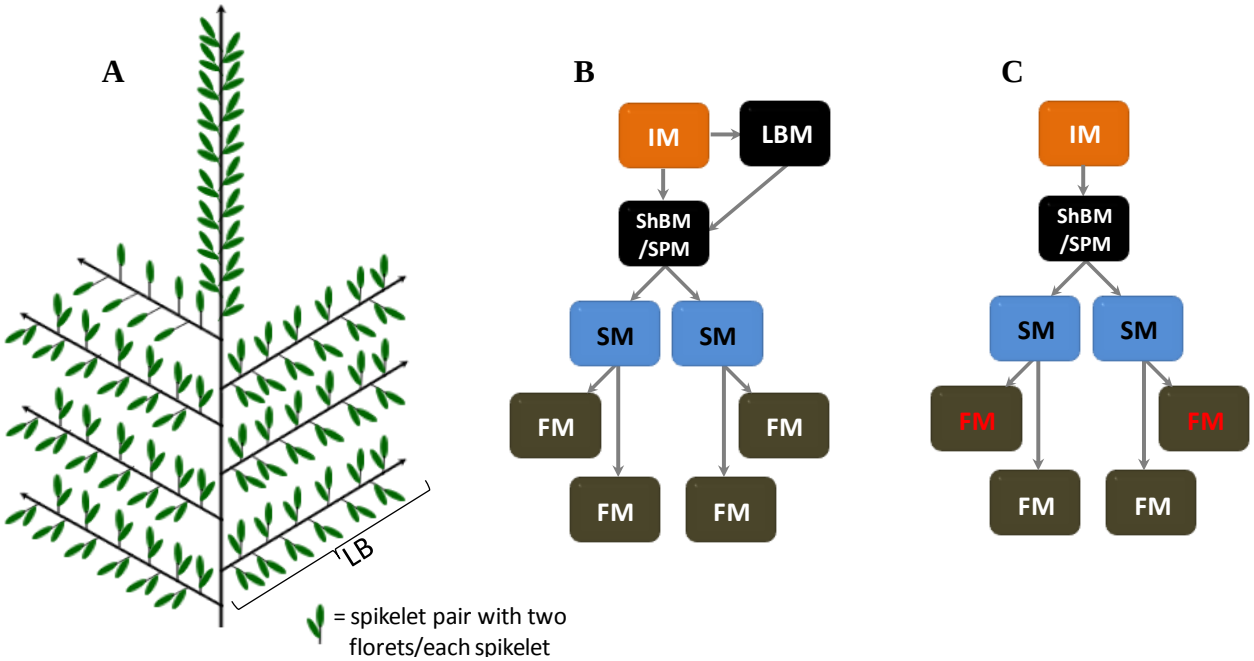

Figure 1.1.2. Schematics showing maize tassel inflorescence and meristem differentiation in tassel and ear.

Mature tassel with indeterminate long branches at the base followed by determinate spikelet pairs (**A**). Inflorescence meristem differentiation and organization in tassel (**B**) and ear (**C**) inflorescences of maize. IM: Inflorescence Meristem: LBM: Long Branch Meristem; ShBM/SPM: Short Branch Meristem/Spikelet Pair Meristem; SM: Spikelet Meristem; FM: Floret Meristem. The FM indicated in red font (**C**) depicts the abortion in ear inflorescence.

1.1.3. Wheat and barley

Wheat, barley and other species belonging to tribe Triticeae are characteristic for a branchless inflorescence called spike, the sessile spikelets are produced directly on the inflorescence axis (**Figure 1.1.3.A** for wheat, and **1.1.3.C** for barley). The meristem differentiation and organization is comparatively less complex than in panicle and tassel inflorescences of rice and maize respectively, due to the absence of branching. In wheat the determinate IM differentiates into the first axillary meristem called Double Ridge (DR) which has a lower leaf ridge and upper spikelet ridge. The spikelet ridge differentiates into a SM; whereas the leaf ridge remains suppressed. The SM produces more than ten FMs in a distichous manner on the indeterminate rachilla (**Figure 1.1.3.B**). Barley, however, shows a peculiar meristem differentiation and organization. Here the inderminate IM differentiates into a DR meristem but then develops into a *Hordeum*-specific, determinate Triple Spikelet Meristem (TSM). Each SM produces only one FM, always resulting in three single-flowered spikelets per rachis internode (**Figure 1.1.3.D**). Differences in the fertility of the *Hordeum*-specific spikelet triplet (arising from TSM) confer unique row–type identity to barley spikes (row–types are discussed in **section 1.3.1**.)

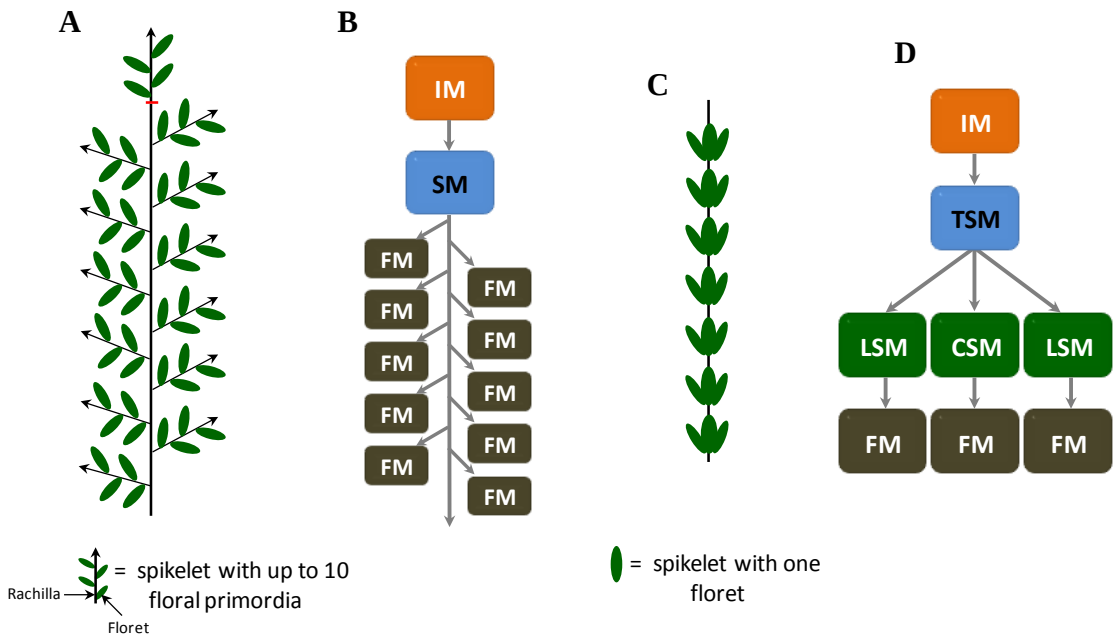

Figure 1.1.3. Schematics showing wheat, barley spikes and their inflorescence meristem differentiation.

(**A**) Determinate wheat spike. Within the spikelet, florets are produced on indeterminate rachilla, each spikelet produces up to 10 floral primordia in a distichous manner. (**B**) Meristem differentiation and organization in wheat spike. (**C**) Schematic diagram showing an indeterminate barley spike, with in the spikelet, a single floret is produced on determinate rachilla. (**D**) Schematic diagram showing inflorescence meristem differentiation and organization in barley. IM: Inflorescence Meristem; TSM: Triple Spikelet Meristem; SM: Spikelet Meristem; LSM; Lateral Spikelet Meristem; CSM: Central Spikelet Meristem; FM: Floret Meristem. The red bar (**A**) indicates the degenerate IM in wheat.

1.2. Genetic regulation of inflorescence development in rice and maize

Maize and rice are unquestionably the best models for studying the genetic regulation of inflorescence development and architecture due to the multiplicity of meristem types (Kellogg, 2007). The extent of IM differentiation and organization is already indicative of the complex nature of genetic regulation underlying inflorescence development in these two species. As described in earlier sections, in maize and rice the typical reproductive development starts with initiation of IM followed by different types of BMs, SMs and FMs. A large number of mutants

that are affected in discrete stages of different meristem developmental phases and corresponding genetic determinants responsible for initiation, maintenance, and transition of these meristems have been identified and characterized in these two species (Bommert et al., 2005; Malcomber et al., 2006; Pautler et al., 2013; Sreenivasulu and Schnurbusch, 2012; Tanaka et al., 2013; Yoshida and Nagato, 2011). In the following sections, rice and maize genes that are responsible for the initiation, maintenance and transition of these meristem types are discussed.

1.2.1. Control of inflorescence meristem identity and development

In rice the IM development is induced by the accumulation of the florigen producing gene *Heading date3a* (*Hd3a*) and its homolog *RICE FLOWERING TIME LOCUS1* (*RFT1*). *Hd3a* and *RFT1* are homologs of Arabidopsis *FLOWERING TIME1* [(*FT1*) (Komiya et al., 2008; Tamaki et al., 2007)]. In maize *Zea CENTRORADIALIS8* (*ZCN8*), which also encodes an FT1–LIKE protein, induces IM formation (Lazakis et al., 2011). In Arabidopsis, *CLAVATA1* (*CLV1*) and *CLV3*, together with *CLV2* [(a Leucine Rich Repeat (LRR) protein)], constitute the CLAVATA signaling pathway, which restricts the *WUSCHEL* (homeodomain transcription factor) gene expression domain to maintain shoot and floral meristems (Yoshida and Nagato, 2011). The architecture of IM in rice is maintained by two genes, *FLORAL ORGAN NUMBER1* (*FON1*) and *FON2*. *FON1* is an ortholog of Arabidopsis *CLV1*, encodes an LRR receptor–like kinase (Suzaki et al., 2004), *FON2* is a CLE protein similar to Arabidopsis *CLV3* (Chu et al., 2006; Suzaki et al., 2006). Mutations in these genes cause IM fasciations and a corresponding increase in floral organ number. In maize the mutants *thick tassel dwarf1* (*td1*) and *fasciated ear2* (*fea2*) underlie the *CLV1* (Bommert et al., 2005) and *CLV2* (Taguchi-Shiobara et al., 2001) homologs respectively (**Figure 1.2.1**). The mutants, *td1* and *fea2* also result in IM fasciations. Recently Bommert et al. (2013) showed that the maize *COMPACT PLANT2* (*CT2*) encoding G subunit of

a heterotrimeric GTP binding protein functions as a signaling molecule for LRR receptor kinases (*CLV1* & *CLV2*) thus controlling IM architecture. In the mutants of rice *aberrant panicle organization1* [(*apo1*), F–box protein, ortholog of Arabidopsis *UNUSUAL FLORAL ORGANS* (*UFO*)], *apo2* (ortholog of Arabidopsis *LEAFY*), the IM is precociously converted to SM resulting in a sparse inflorescence (Ikeda-Kawakatsu et al., 2007; Ikeda-Kawakatsu et al., 2012). Thus, *APO1* and *APO2* [(*syn. RICE FLORICAULA* (*RFL*); (Rao et al., 2008)] appear to be important for IM maintenance in rice. *APO1* and *APO2* interact with each other, where *APO2* negatively regulates the transcription of *APO1* (Ikeda-Kawakatsu et al., 2012). Recently it has been shown that over expression of *TAWAWA1* (*TAW1*) is also important for prolonged IM activity and delayed BM specification (Yoshida et al., 2012b).

1.2.2. Control of branch meristem identity and development

In rice a number of genes that regulate different branch meristems (PBMs, SBMs and SMs) have been identified and characterized (**Figure 1.2.1**). Because of the precocious conversion of IM to SM the number of PBMs and SBMs are reduced in rice *apo2* and *apo1* mutants resulting in a shorter panicle (Ikeda-Kawakatsu et al., 2007; Ikeda-Kawakatsu et al., 2012). The activity of PBMs and SBMs is also regulated by two genes *GRAIN NUMBER1a* (*GN1a* – encodes cytokinin oxidase2, OsCKX2) and *LONELYGUY* (*LOG* – encodes cytokinin riboside 5′–monophosphate phosphoribohydrolase) involved in cytokinin catabolic and biosynthetic pathways, respectively (Ashikari et al., 2005; Kurakawa et al., 2007). The *GN1a* mutants show increased activity of PBMs, and SBMs due to abundant levels of cytokinin. However the mutants of *LOG* with low cytokinins show reduced number of PBMs, SBMs and subsequently less number of SMs. Recently Yoshida et al. (2012b) showed that over expression of *TAW1* is important for prolonged IM activity which results in production of more PBMs, SBMs and in turn SMs. Number of

Primary Branches (PB), Secondary Branches (SB) and spikelets are also regulated by genes like *DENSE AND ERECT PANICLE1* (*DEP1*) and *IDEAL PLANT ARCHITECTURE* (*IPA*)/*WEALTHY FARMERS PANICLE* (*WFP*) which encode PHOSPHATIDYL ETHANOLAMINE–BINDING PROTEIN (Huang et al., 2009) and SQUAMOSA PROMOTER BINDING LIKE14 (OsSPL14) (Jiao et al., 2010; Miura et al., 2010), respectively. The *OsSPL14* is negatively regulated by micro RNA *OsmiR156*. *DEP1* transcriptionally controls *GN1a* (Huang et al., 2009), whereas the IPA/WFP directly binds with *DEP1* and *LOG* genes, and activate their transcription (Lu et al., 2013). *ABERRANT SPIKELET AND PANICLE1* (*ASP1*) encoding a transcriptional co–repressor similar to *TOPLESS* of Arabidopsis, is also important for phase transition from BM to SM, the mutants of *ASP1* show reduced number of BMs (Yoshida et al., 2012a). Recently Zhang et al. (2013a) showed that *OsmiR397* promotes different orders of panicle branching in rice by down-regulating an enzyme called LACCASE (OsLAC) involved in brassinosteriod metabolism.

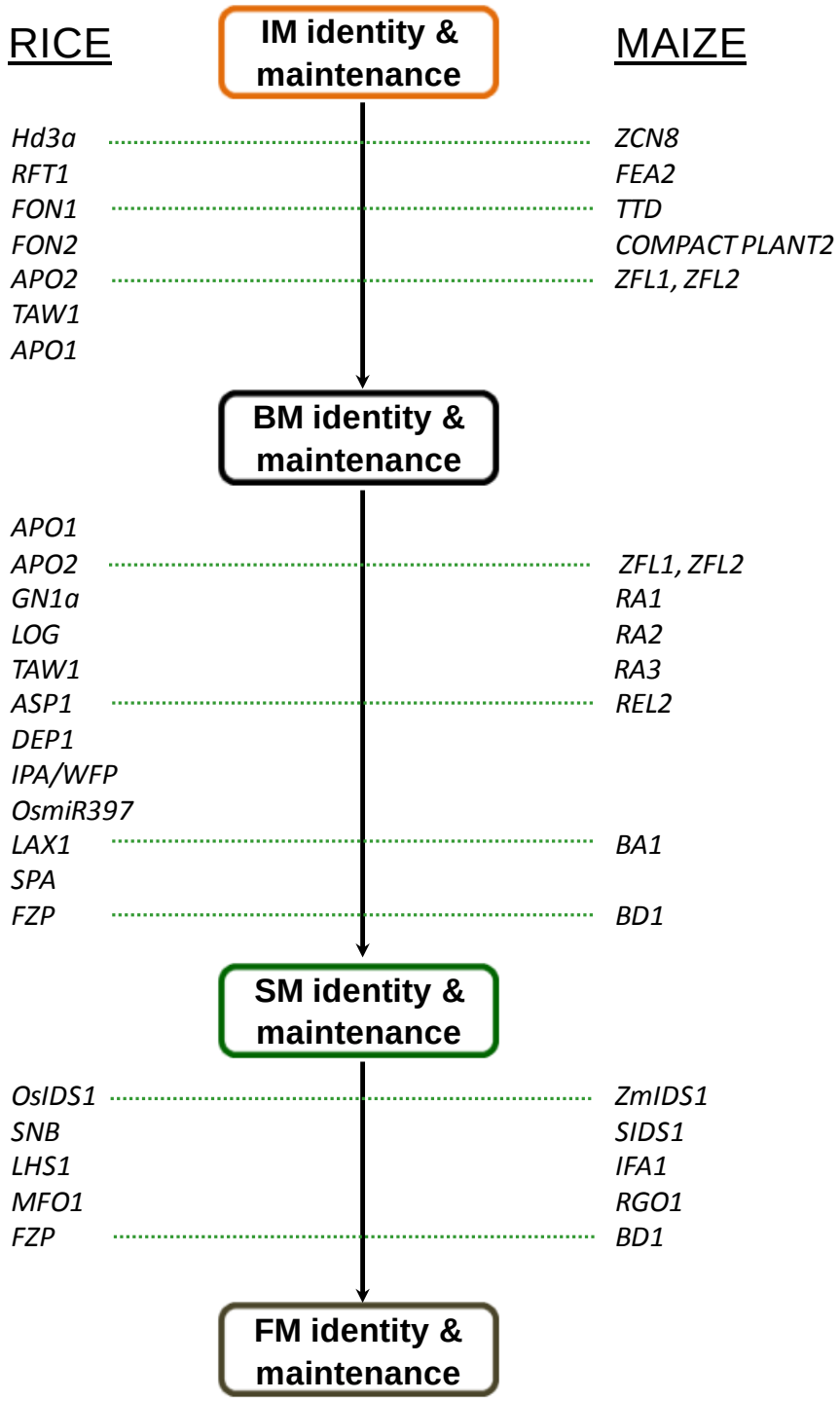

Figure 1.2.1. Genetic control of inflorescence development in rice and maize.

Figure modified after Tanaka et al. (2013). Genetic regulation of inflorescence meristem, branch meristem, spikelet meristem and floret meristem specification, maintenance, and transition in rice and maize. The dotted lines indicate the presence of potential ortholog in rice and maize. IM: Inflorescence Meristem; BM: Branch Meristem; SM: Spikelet Meristem; FM: Floret Meristem.

LAX PANICLE1 (*LAX1*) and *SMALL PANICLE* (*SPA*) are two other major regulators of panicle branching in rice. *LAX1* encodes a basic HELIX–LOOP–HELIX (bHLH) transcription factor (Komatsu et al., 2003a). The mutants of *lax1* and *spa* show reduced number of PBMs, SBMs, and SMs where as the *lax1/spa* double mutants show highly degenerated panicles without any branches indicating that *LAX1/SPA* operate in a genetic pathway promoting panicle branching in rice. *BARREN STALK1* (*BA1*) is the corresponding maize ortholog of *LAX1*. *BA1* regulates the development of BMs in maize, the maize *ba1* mutants completely shut down the production of all axillary meristems including LBMs and ShBMs on tassel and ear (Gallavotti et al., 2004). A similar barren phenotype is also seen in the mutants of *barren inflorescence2* (*bif2*) which encodes a serine–threonine kinase PINOID (McSteen et al., 2007). In contrast to *LAX /SPA*, the rice *FRIZZY PANICLE* (*FZP*) functions as a negative regulator of branching after SM identity is specified. *FZP* encodes an APETALA2/ETHYLENE RESPONSE FACTOR (AP2/ERF) family transcription factor and in *fzp* mutants several branches containing rudimentary glumes are formed in place of spikelets (Komatsu et al., 2003b). The maize *BRANCHED SILKLESS1* (*BD1*) is an ortholog of *FZP*; the *bd1* mutants in maize also produce indeterminate long branches instead of spikelets (Chuck et al., 2002).

1.2.2.1. Maize *RAMOSA* pathway

The BM formation and regulation in maize is under the co–ordinated regulation of the *RAMOSA* pathway which is operated by four genes, *RAMOSA1* (*RA1*), *RA2*, *RA3*, and *RAMOSA1 ENHACER LOCUS2* (*REL2*) (**Figure 1.2.1**). In the maize tassel, the branches are either long or short without any intermediates (Kellogg, 2007). In the tassels of maize *ramosa* mutants, shift from LBMs to ShBMs/SPMs is disrupted, with branches being produced that are intermediate in

length between the long and short branches (**Figure 1.2.2**). Thus, the normal function of the *RAMOSA* gene products is to control BM outgrowth. *RA1* encodes a C2H2 zinc finger transcription factor with an EAR (Ethylene-responsive element binding factor – Associated amphiphilic Repression) domain (Vollbrecht et al., 2005). *RA1* is unique to the species of tribe Andropogoneae, where spikelets are produced in pairs (SPM). *RA2* encodes a Lateral Organ Boundary (LOB) domain transcription factor and is found in all grass species (Bortiri et al., 2006). Interestingly *RA3* encodes a Trehalose–6–phosphate phosphatase (TPP), an enzyme involved in trehalose biosynthesis (Satoh-Nagasawa et al., 2006). It appears that *RA3* is unique to Andropogoneae species, however, a *RA3–LIKE* gene known as *SISTER OF RAMOSA3* (*SRA*) is present in all grass species. *RA1* is under the transcriptional control of RA2 and RA3. The other *RAMOSA* pathway gene *REL2* is a transcriptional co–repressor, which is similar to Arabidopsis *TOPLESS* and is found in other grass species (Gallavotti et al., 2010). The REL2 protein contains three domains: the N-terminal LisH (lyssencephaly type1-like homology) and CTLH (C–terminal to LisH) and 11 WD-40 repeats in the C-terminal region. The CTLH domain of REL2 physically interacts with C–terminal EAR domain of RA1. The RA1/REL2 protein complex appears to be transcriptionally controlled by *RA2* and *RA3* resulting in the expression or repression of target genes, and promote the determinacy of SPM (Gallavotti et al., 2010). *ABERRANT SPIKELET AND PANICLE1* (*ASP1*) is the rice ortholog of REL2. The mutants of *ASP1* display precocious conversion of BM to SM resulting in reduced BM indeterminacy. However, the IM, which generally degenerates after PBM initiation, is active even after the production of SBMs resulting in indeterminate IM in *asp1* mutants (Yoshida et al., 2012a). Thus, the inflorescence branching regulated by the *RAMOSA* pathway appears to be unique to maize

and other Andropogoneae species because true orthologs of *RA1* and *RA3* are not present in other grass species (Vollbrecht et al., 2005; Satoh-Nagasawa et al., 2006).

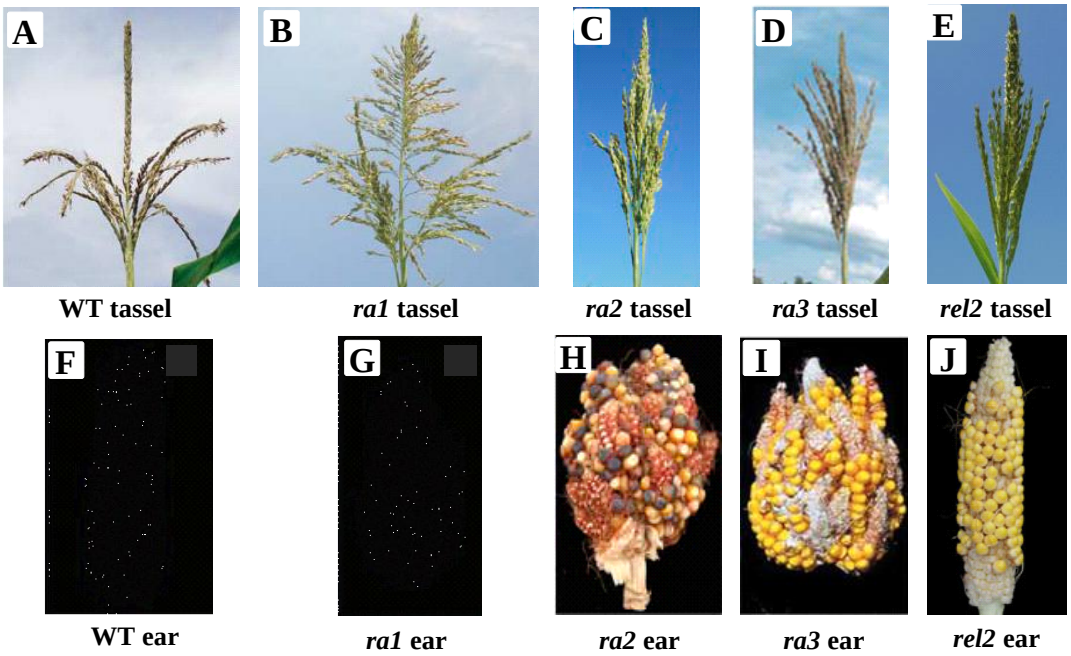

Figure 1.2.2. Tassel and ear phenotypes of maize *ramosa* mutants.
Wild type tassel (**A**) and ear (**F**). *ra1* tassel with indeterminate basal long branches (**B**) and deformed ear (**G**). *ra2* tassel with indeterminate long branches (**C**) and highly branched ear (**H**). *ra3* tassel with indeterminate long branches (**D**) and highly branched ear (**I**) *rel2* mutant tassel (**E**) and ear (**J**). Figures A, B, F, and G were adapted from Vollbrecht et al. (2005), Figures C, and H were adapted from Bortiri et al. (2006), Figures D, and I were adapted from Satoh-Nagasawa et al. (2006) and Figures E, and J were adapted from Gallavotti et al. (2010).

1.2.3. Control of spikelet meristem identity

In maize the determinate fate of the SM is regulated by *indeterminate spikelet1* (*ids1*) and *sister of indeterminate spikelet1* (*sid1*) (Chuck et al., 1998; Chuck et al., 2008). Both *ids1* and *sid1* encode APETALA2–ERF (AP2–ERF) family TFs, the *ids1* and *sid1* show development of extra florets compromising SM determinacy. In rice *SUPERNUMERARY BRACT* (*SNB*) and *OsIDS1*

have similar functions (Lee et al., 2007; Lee and An, 2012), the *snb* mutants show repeated development of rudimentary glumes, extra lemma/palea and floral meristems (Lee et al., 2007). The SM identity in rice is also regulated by *LEAFY HULL STERILE1* (*LHS1*), which encodes OsMADS1. The *lhs1* mutants show reiterative formation of lemma, palea, and FMs (Jeon et al., 2000), the *lhs1* mutant phenotypes are further enhanced by mutation in *MOSAIC FLORAL ORGANS*, which encodes OsMADS6 (Ohmori et al., 2009; Li et al., 2010). In rice *APO1* and *APO2* positively regulate spikelet meristem identity and number by suppressing precocious conversion of IM to SM (Ikeda-Kawakatsu et al., 2007). Thus, APO1–APO2 interaction at appropriate time point is required for SM formation in rice (Yoshida and Nagato, 2011). In maize, *INDETRMINATE FLORAL APEX1* (*IFA1*) and *REVERSED GERM ORIENTATION* (*RGO1*) are also important for SM determinacy. In mutants of *ifa1* and *rgo1* the SPMs and SMs initiate additional SMs and FMs (Laudencia-Chingcuanco and Hake, 2002; Kaplinsky and Freeling, 2003). Thus, *IDS1*, *IFA1*, and *RGO1* redundantly regulate the fate of SMs in maize (Tanaka et al., 2013) (**Figure 1.2.1**). The *BD1*/*FZP* also functions as positive regulator of SM identity by suppressing BM formation after SM initiation (Komatsu et al., 2003b; Yoshida and Nagato, 2011).

1.2.4. Control of floral meristem identity

A large number of floral homeotic genes that are important for development of floral organs including sepals, petals, stamens, and carpel (ABCDE model of flower development) have been identified in Arabidopsis and all of them encode MADS box transcription factors except the A–class gene which is an *AP2* transcription factor. The maize and rice genomes encode sets of genes with significant similarities to Arabidopsis ABCDE genes, suggesting that a similar

mechanism regulates floral development in these two grass species (Yoshida and Nagato, 2011; Sreenivasulu and Schnurbusch, 2012 and the references therein.)

1.3. Genetic regulation of inflorescence development in barley

The spike inflorescence architecture of barley is commonly seen in other species of tribe Triticeae. However, the presence of TSM that gives rise to three spikelets at each rachis internode in barley makes it unique in terms of reproductive meristem differentiation and organization. Unlike maize and rice, the barley IM does not produce BMs resulting in a comparatively simple meristem organization. Based on this fact, one may assume a simpler genetic regulation involved in barley inflorescence development. However, relatively little is known about the genetic regulation involved in barley IM initiation, development, differentiation, and organization of different meristem types during barley spike development. A comprehensive overview on different genes characterized responsible for inflorescence development in barley so far is described in the following sections.

1.3.1. Control of lateral spikelet fertility and row–type

As described previously the barley spike carries a TSM that differentiates into three spikelets at each rachis internode comprising one central spikelet (CS) and two lateral spikelets (LS). In two–rowed barleys, the CS is fully fertile, but the two LSs are either staminate or completely sterile. However, in six–rowed barleys all three spikelets are fully fertile and proceed to produce grains (Komatsuda et al., 2007). A major partition in barley germplasm is based on two– and six–rowed cultivars, which partly reflects breeding history in the past (Cockram et al., 2010). It has been hypothesized that barley was domesticated from two–rowed types found in wild barley (*H. vulgare* subsp. *spontaneum*) (Sakuma et al., 2011). The oldest known archeological barley

kernels date from 19,000 years ago derived from two–rowed types (Komatsuda et al., 2007), six–rowed barleys first appeared 8800 - 8000 years ago indicative of the earlier domestication of two–rowed barley.

The barley row–type is regulated by five known genetic loci that include Six–rowed spike 1 (*vrs1*), *vrs2*, *vrs3*, *vrs4*, and *intermedium–c* (*int–c*) (**Table 1-1**). All of the five loci display clearly distinguishable spike phenotypes (**Figure 1.3.1**). In cultivated barleys, the six–rowed spike types arose by loss–of–function mutations in *Vrs1* (2HL). *Vrs1* encodes a Class I homeodomain–leucine zipper (HD–Zip) transcription factor (HvHOX1) that functions as a negative regulator of LS development (Komatsuda et al., 2007). The loss–of–function, mutant *vrs1.a* allele, promotes LS fertility resulting in a complete six–rowed phenotype, the wild type, *Vrs1.b*, functions as a negative regulator of LS fertility and produces a two–rowed phenotype. Consistent with this, *Vrs1* is highly expressed in the two LSs. It had been proposed that *Vrs1* gene arose after duplication of a closely related HD–Zip I paralog, *HvHOX2* (2HS) which has a global expression pattern. Followed by gene duplication, the *HvHOX1* (*Vrs1*) has acquired unique expression pattern in LSs and neofunctionalized to suppress LS fertility in barley (Sakuma et al., 2010).

Table 1-1. Barley *vrs* loci, their occurrence and chromosomal location.

Locus	Occurrence	Location	Study
vrs1	Natural alleles; Induced mutants	2HL	Komatsuda *et al.*, 2007
vrs2	Induced mutant; Natural alleles	5HL	Youssef *et al.*, unpublished
vrs3	Induced mutants; Natural alleles	1HS	Bull *et al.*, unpublished
vrs4	Induced mutants	3HS	Koppolu *et al.*, 2013
int–c (*vrs5*)	Natural alleles; Induced mutants	4HS	Ramsay *et al.*, 2011

Mutation research revealed that the LS fertility in two–rowed barleys (*Vrs1.b* allele) can be modified by up to ten independent *intermedium* genes distributed across the barley genome, which when homozygous, generate either partial or complete six–rowed phenotype (Lundqvist and Lundqvist, 1988). One such locus includes *int–c* (4HS), which has been associated with natural quantitative variation for row–type (Lundqvist et al., 1997). The gene underlying *int–c* encodes a barley ortholog of maize TEOSINTE BRANCHED1, HvTB1 (Ramsay et al., 2011). Alleles at the *int–c* locus modify the LS fertility with respect to allelic constitution at *Vrs1*. The *int–c.b* allele is generally found in two–rowed barleys (*Vrs1.b*), where it inhibits floral organ development in LSs, while its presence in six–rowed barleys (*vrs1.a*) results in reduced LSs. The *Int–c.a* allele, however, is present in six–rowed barleys (*vrs1*), but *Int-c.a* in two-rowed barley produces partially fertile LSs, resulting in an intermediate phenotype between two– and six–rowed barleys termed *intermedium* spike phenotype (Ramsay et al., 2012). The other barley row–type loci, are currently being investigated; *vrs2* (Youssef et al., unpublished), *vrs3* (Bull et al., unpublished) for the underlying genes and their interaction with known row–type loci. The genetic and molecular characterization of *vrs4* is the subject of present thesis.

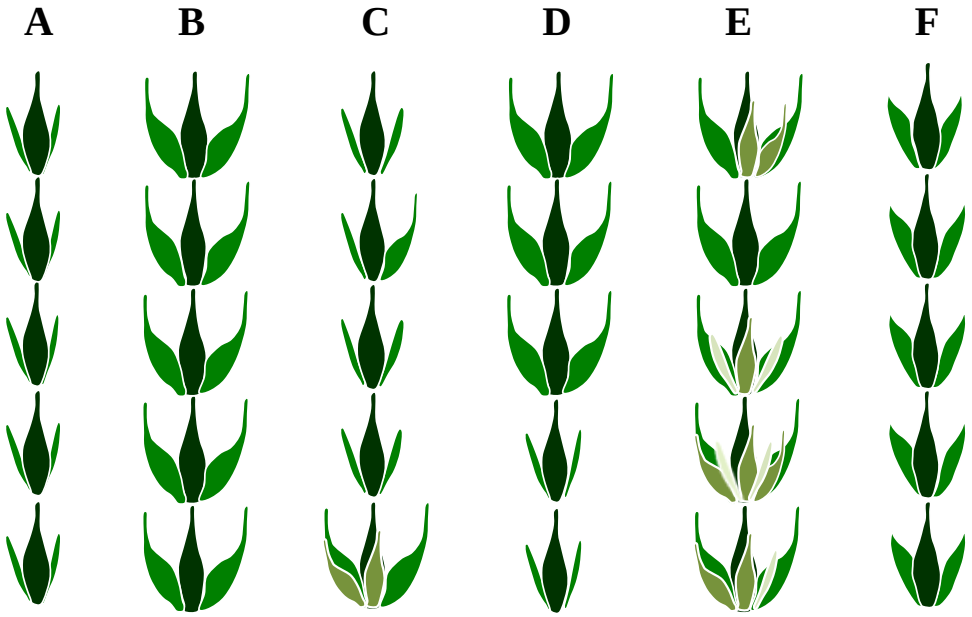

Figure 1.3.1. Spike morphology of different *vrs* loci.

(**A**) Two-rowed spike (*Vrs1*) with fertile central spikelets (CS) and sterile lateral spikelets (LSs), (**B**) Six-rowed spike 1 (*vrs1*) with completely fertile CS and LSs, (**C**) Six-rowed spike 2 (*vrs2*): LS fertility observed at the spike base with occasional additional spikelets (AS, may be fertile or sterile, AS are presented in light green color); along the spike, LS are occasionally enlarged and set seed, (**D**) Six-rowed spike 3 (*vrs3*): spike base appears two-rowed, and the remaining portion appears six-rowed, (**E**) Six-rowed spike 4 (*vrs4*): spikelet fertility is similar to *vrs1*, with frequent awn bearing ASs (light green colored), (**F**) *intermedium-c* (*int-c*): LSs are enlarged, set seed, which are usually smaller than the LSs of *vrs1*, LSs do not bear awns.

1.3.2. Control of spikelet meristem identity and spike branching

Unlike the inflorescences of rice, sorghum, and maize, where the spikelets are produced after multiple rounds of branching, the spikelets in barley are produced directly on the branchless inflorescence axis (rachis), (**Figure 1.3.2.A**). Inflorescence branching in barley is thus genetically suppressed; one prominent feature characteristic of barley and other Triticeae species. In barley a group of mutants called *compositum* (*com*) show non–canonical inflorescence branching (**Figure 1.3.2.B, and C**) and have been identified after induced mutagenesis (Franckowiak and Lundqvist, 2011). The mutant loci in this group include at least *com1* (5HL) and *com2* (2HS) (Bossinger et al., 1992). Thus, the wild type alleles at these two loci appear to actively suppress branching and may specify SM identity and determinacy. Even though the underlying candidate gene for *com2* has not been cloned yet, linkage mapping and comparative genomic analyses indicated maize *BD1*/rice *FZP* as the most likely candidate underlying *com2* (Rossini et al., 2006). The other branching regulator *com1* is currently being positionally cloned on 5HL (Poursarebani et al., unpublished). Spike branching is also evident in *vrs4* mutants, which show proliferation of additional spikelets and florets from both central and lateral spikelets (Forster et al., 2007; Koppolu et al., 2013). The other spike mutant showing ramified inflorescence features is lethal *rattail* (*rtt*) mutant (**Figure 1.3.2.D and E**). Spike ramifications

along the whole spike result in a more severe branching in *rtt* mutants with no seeds being set causing complete sterility (Robertson, 1967).

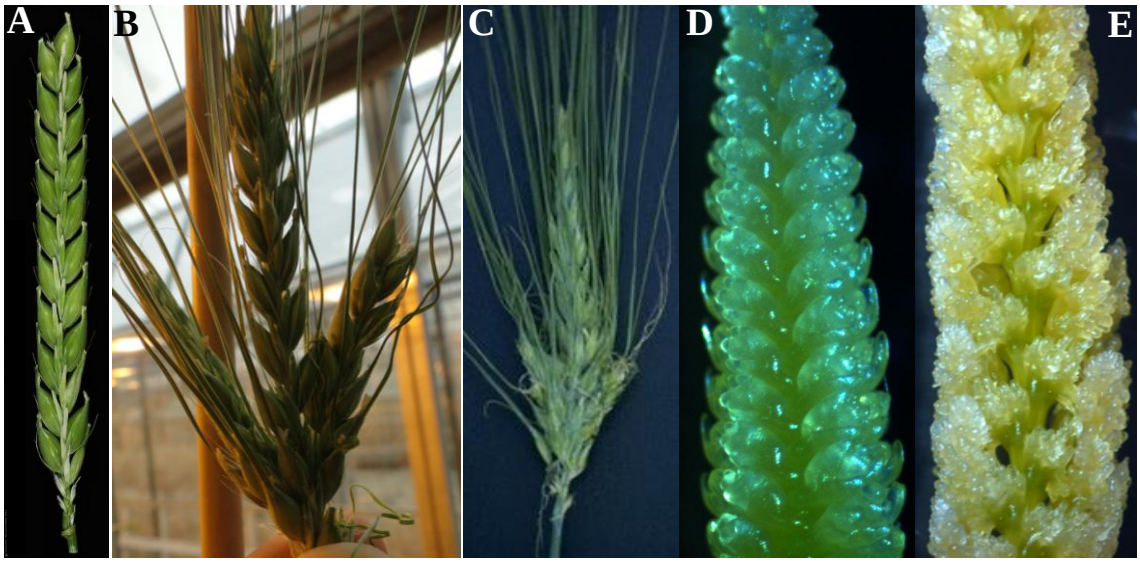

Figure 1.3.2. Spike phenotypes of *compositum* and *rattail* mutants.
(**A**) Wild-type spike without spike branching. (**B**) *compositum1* mutant (*int-h.42*) showing spike branching at the base of the spike. Picture kindly provided by Dr. Helmy Youssef (**C**) *compositum2* mutant (*com2.g*) showing spike branching. Picture kindly provided by Dr. Udda Lundqvist. (**D**) Immature wild-type spike (six-rowed) at awn primordium stage without branching. (**E**) Immature spike of barley *rattail* mutant showing highly branched spike. The individual spikelets in *rattail* mutants are transformed into a large number of inflorescence meristems, which fail to differentiate into next order meristems.

1.3.3. Control of rachis internode elongation and spike density

Length of the rachis internode between two spikelet ridges dictates spike density. Based on rachis internode length spikes were classified into two groups: compact spikes with shortened rachis internodes and lax spikes with longer rachis internodes (**Figure 1.3.3.A, B, and C**). The compact spike phenotype is evident in several induced mutants, which include *erectoides* (*ert*), *dense spike* (*dsp*), *brachytic* (*brh*), *uzu1* (*semi–brachytic*), *pyramidatum1* (*pyr1*) and *Zeocriton* (*Zeo*) loci (Forster et al., 2007; Shahinnia et al., 2012), all of them show defects in rachis internode elongation (**Figure 1.3.3.B**). Despite the abundance of mutants affecting this trait very

few loci have been isolated, which include *uzu1* and *Zeo1*. The *uzu1* gene, encodes HvBRI1, a putative brassinosteroid receptor, reflecting the link between spike density and hormonal signaling (Chono et al., 2003). Recently, Houston et al. (2013) elucidated that the highly compact spike phenotype of *Zeo1* is governed by mRNA turnover of *HvAP2*, which is targeted by *miR172 microRNA*. The mutations in *HvAP2* binding sites of *miR172* perturb the miRNA directed cleavage, resulting in high turnover of *HvAP2 mRNA* leading to a compact spike phenotype. The *dsp.ar* mutation was recently fine–mapped to a 0.37 cM interval in the centromeric region of chromosome 7H and may represent an allele of the *dps1* locus (Taketa et al., 2011; Shahinnia et al., 2012).

The extreme *lax* phenotype known as *accordion rachis* in barley is characterized by lax spikes with elongated rachis internodes (**Figure 1.3.3.C**) and is controlled by three interacting loci, the recessive *accordion rachis1* (*acr1*–2HL) and two incompletely dominant loci, *Acr2* (4HL) and *Acr3* (1HL). The *acr* phenotype can also be induced ectopically by expressing two barley MADS1 SVP–like (Short Vegetative Phase) genes BM1 and BM10 (Trevaskis et al., 2007).

1.3.4. Control of glume development

In barley spikelets are subtended by two empty bracts known as glumes. In a special class of glume mutants, which includes *third outer glume1* (*trd1* - 1HL), bract development is derepressed and an additional leaf-like glume is seen subtending the central spikelets in the basal region of the spike [(Houston et al., 2012), (**Figure 1.3.4.A and B**)]. The *Trd1* gene encodes a GATA–zinc finger transcription factor required for bract suppression. Orthologous rice *neckleaf1* (*nec1*) and maize *tassel sheath1* (*tsh1*) show analogous bract derepression phenotypes,

suggesting the existence of a conserved mechanism for bract repression in the grass family (Whipple et al., 2010).

Figure 1.3.3. Phenotypes of *dense spike* (*dsp*) and laxatum (*lax*) mutants.
(**A**) Wild type spike. (**B**) *dense spike* with reduced rachis internode length between spikelets compared to WT. (**C**) *lax* spike with increased rachis internode length between spikelets.

Figure 1.3.4. Barley *third outer glume* (*trd*) phenotype.
Figure adapted from Whipple et al. (2010). (**A**) Wild-type barley spike. (**B**) *trd1* mutant showing development of enlarged additional glume apart from the basic set of two glumes.

1.3.5. Control of lodicule and stamen development

Lodicule development in barley is under the control of *Cleistogamous1* (*Cly1*) gene. The *Cly1* gene underlies *HvAP2*, regulated by *miR172* (Nair et al., 2010). The *mRNA* turnover of *HvAP2* is inversely proportional to lodicule development. In cleistogamous spikes [(recessive *cly1* – closed spikelets with concealed anthers), (**Figure 1.3.5.B**)] the *miR172* binding site of *HvAP2* is perturbed resulting in abundant *HvAP2 mRNA*, which subsequently represses lodicule development (**Figure 1.3.5.D**). In contrast, the *miR172* down-regulates *mRNA* turnover of *HvAP2* in chasmogamous spikes (**Figure 1.3.5.A**), [(dominant *Cly1* – open spikelets with anthers

exerted out)] promoting lodicule development (**Figure 1.3.5.C**), lemma and palea are pushed apart opening the spikelets. In *lax–a* mutant the lodicule is converted into two stamens totaling to five stamens per spikelet. The phenotype indicates that the gene underlying *lax–a* mutation controls both lodicule and stamen development. The genetic elucidation of *lax–a* currently is an ongoing study (Jost et al., unpublished).

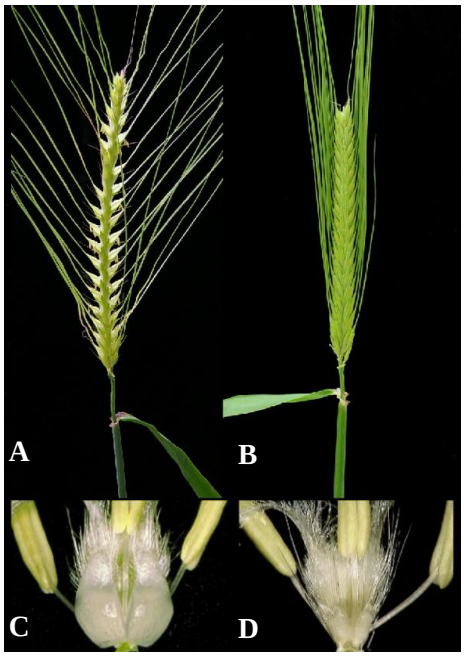

Figure 1.3.5. Phenotypes of cleistogamous and chasmogamous barley spikes.
Figure adapted from Nair et al. (2010). (**A**) Chasmogamous spike with open spikelets and anthers exerted out. (**B**) Cleistogamous spike with closed spikelets. (**C**) Swollen lodicules of a chasmogamous spikelet. (**D**) Shrunken lodicules of a cleistogamous spikelet.

1.3.6. Control of lemma and awn development

In barley and other cereals awns play an important role in seed dispersal (Elbaum et al., 2007) and contribute significantly to grain filling and yield (Taketa et al., 2011). Several mutants that show defects in lemma and awn development are available, including *Awnless1* (*Lks1*), which does not produce awns, short awn (*lks2*, *lks5*) and alleles of *breviaristatum* (*ari*), which show reduced awn length. Other loci affecting lemma–awn development include *Hooded* (*Kap1*), and *calcaroides* (*cal–b, cal–c, cal–d, cal–e*), *subjacent hood 1* (*sbk1*), *leafy lemma1* (*lel1*) and *triple awned lemma* (*trp1*) (Pozzi et al., 2000; Druka et al., 2011; Franckowiak and Lundqvist, 2011).

Among all these only two of the loci have been isolated − *Hooded* and *lks2*. In *Hooded* mutants the distal end of the lemma is converted into an ectopic FM and consequently an epiphyllous floret ("hood") develops instead of the awn. *Hooded* phenotype is seen because of a dominant mutation in barley *KNOTTED-LIKE* homeobox gene (*KNOX*), *BKN3* (Muller et al., 1995). A 305 bp duplication in intron IV of *BKN3* is responsible for the hooded phenotype. The *lks2* has been positionally cloned and identified as a *SHORT INTERNODES* (*SHI*) family transcription factor (Yuo et al., 2012).

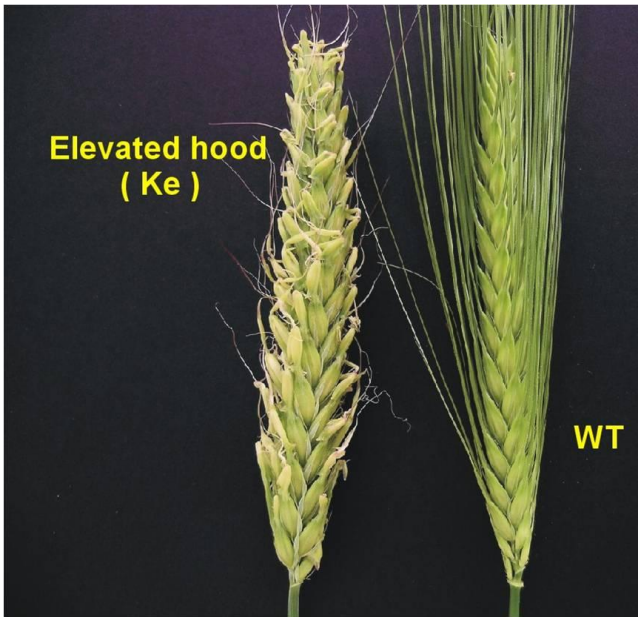

Figure 1.3.6. Spike phenotype of *Hooded* (*Kap*) barley.
The *Hooded* spike (elevated hood, allele *Ke*, left) showing transformation of lemma awn into an epiphyllous floret, compared with the wild type spike (right) showing normal development of awns. Picture was kindly provided by Prof. Antonio Micheles Stanca.

1.3.7. Control of caryopsis type

In grasses, the grain bearing spikelets are termed caryopses at physiological maturity. The lemma and palea adhere to the seed pericarp firmly and forms the seed hull. The typical caryopses with adhering hulls are known as covered/hulled barley. However, a variant with non–adhering hulls is available in natural variation known as naked/hull less barley. The covered/naked caryopsis in barley is controlled by a single locus *naked caryopsis* (*nud*) on 7HL. *Nud* encodes an ERF

transcription factor which regulates lipid deposition on the epidermis of pericarp in covered barleys (*Nud*); whereas in naked barleys (*nud*) the lipid deposition is impaired resulting in free threshing habit (Taketa et al., 2008).

Figure 1.3.7. Kernel and spike phenotypes of hulled and hull less barley.
Figure adapted from Taketa et al. 2008. Morphology of covered (*Nud*) and naked (*nud*) barley. (**A**) Mature caryopses of covered (left two kernels) and naked (right two kernels) barley. In each pair of kernels, dorsal (Left) and ventral (Right) sides are shown. (**B**) Part of a mature spike of covered (Left) and naked (Right) barley.

1.4. Genomics resources for gene cloning in barley

The genetic determinants (genes) underlying various plant developmental processes, biotic and abiotic stress responses are of high agronomic importance. Usage of such novel genes in breeding programmes to improve crop yields is necessary to mitigate the ever increasing demand for the food supplies arising from population growth and erratic nature of climate change. For the precise gene identification and functional characterization in a species like barley with large genome [(5.1 gigabases, (Gb)], availability of adequate genetic and genomic resources is highly essential. Among all of the Triticeae species, barley encompasses a very rich collection of genetic and genomic resources which aid in gene isolation by approaches like conventional map–based cloning (Stein et al., 2005; Komatsuda et al., 2007; Sutton et al., 2007; Taketa et al., 2008;

Nair et al., 2010; Yuo et al., 2012) and modern day Genome–Wide Association Studies (GWAS) (Ramsay et al., 2011; Comadran et al., 2012; Houston et al., 2013). In the recent past, a multitude of genomics resources became available to the barley research community, the details of which are briefly described in the following sections.

1.4.1. Structural genomics tools

1.4.1.1. ESTs and FLcDNAs

Expressed Sequence Tags (EST) and Full Length cDNA (FLcDNA) sequences represent a valuable source to identify spatial expression pattern of genes and also to derive gene based markers. A large number of ESTs derived from different plant tissues are available for barley. As of November 2013, 537,449 ESTs are available in GenBank (http://www.ncbi.nlm.nih.gov/). FLcDNAs which represent the entire mRNA including 5' and 3' UTRs (UnTranslated Regions) are more informative over short EST reads. A comprehensive set of 25,000 FLcDNAs (http://www.schigen.nig.sc.jp/barley/) were developed and anchored to the already mapped ESTs on seven barley chromosomes (Sato et al., 2009). These FLcDNAs are useful for gene prediction and estimation of Open Reading Frames (ORFs).

1.4.1.2. BAC libraries

Large insert genomic DNA libraries form the basis for gene discovery in map–based gene isolation projects (Schulte et al., 2011). Until today nine large insert Bacterial Artificial Chromosome (BAC) libraries are publicly available for barley research community, six of them were derived from Morex (Schulte et al., 2011; Yu et al., 2000), one from Haruna Nijo (Saisho et al., 2007), one from Cebada Capa (Isidore et al., 2005) and the other from a double haploid line CS134 (Clipper × Sahara 3771) (Shi et al., 2010). The Morex (Yu et al., 2000), Haruna Nijo,

Cebada Capa, and CS134 BAC libraries constitute 6.3, 6.6, 6.0, and 4.9 fold genome coverage, respectively, with an average insert size ranging from 106 kb to 140 kb. The five Morex BAC libraries reported in Schulte et al. (2011) cover 25 fold genome coverage with an average insert size ranging from 92 kb to 143 kb among different libraries.

1.4.1.3. Genetic and physical maps

A robust genetic map is the starting point for a good physical map (Poursarebani, 2012), which in turn is crucial for identification of physical contigs harboring genes of interest in positional cloning studies. Over the past two decades many genetic linkage maps became available based on different marker systems, including RFLPs (Graner et al., 1991; Kleinhofs et al., 1993), SSRs (Varshney et al., 2006), DArTs (Wenzl et al., 2006), ESTs (Stein et al., 2007; Potokina et al., 2008), SNPs (Rostoks et al., 2005; Close et al., 2009; Sato et al., 2009), SFPs (Luo et al., 2007) and a combination of different marker systems (Hearnden et al., 2007; Marcel et al., 2007). Recently, barley genome zippers were developed by positioning the gene-based barley 454 sequence reads which are in synteny with the genes of rice, *Brachypodium*, and Sorghum (Mayer et al., 2011). The syntenic 454 reads were positioned in between the gene-based SNP markers reported in the consensus map developed by Close et al. (2009). By this a total of 27,581 syntenic barley genes with rice, *Brachypodium* and Sorghum were positioned onto this genetic map representing a putative linear gene order on seven barley chromosomes. This served as an excellent genomic resource especially for the identification of syntenic genes and subsequent marker development in the *vrs4* genetic interval (barley physical map was not available during this study). A whole genome shot gun assembly and barley physical map of 4.98 Gb with more than 3.9 Gb anchored to the high resolution genetic map was available at the end of 2012 (IBSC,

2012). The strictly ordered BAC-based physical contigs along the seven chromosomes will simplify future map–based cloning procedures.

1.4.1.4. Gene expression arrays

The global gene expression evaluation is possible with the advent of microarray technology, where thousands of genes can be spotted on a single chip and evaluated simultaneously in one experiment. Microarrays have been proven to be useful for gene expression profiling, identification of gene regulatory networks, comparative genomic hybridization, SNP detection and many other applications (Hoheisel, 2006; Miller and Tang, 2009). Utilizing publicly available EST sequences, a 22 K barley microarray, which is well known as Barley 1 Genechip (Affymetrics), was developed (Close et al., 2004). This was developed using sequence information available from 350,000 ESTs from a range of tissues and genotypes representing 21,439 barley genes. Later on this chip was used for providing barley reference gene expression data set (Druka et al., 2006), mRNA expression profiling of tissues subjected to biotic (Caldo et al., 2004; Boddu et al., 2006; Caldo et al., 2006; Zhang et al., 2008) and abiotic stresses (Walia et al., 2007; Tommasini et al., 2008). The applicability of Barley 1 Gene chip in gene cloning was proven with the identification of *Rpr1*, a suppressor of barley stem rust resistance gene *Rpg1* (Zhang et al., 2006). Later Agilent technologies introduced custom microarray platform which allowed studying 240,000 genes in one experiment. Currently two 44K (Druka et al., 2010) and one 60 K (Sreenivasulu et al., unpublished) custom Agilent microarrays have been designed for barley.

1.4.1.5. Barley whole exome capture

Based on predicted genes from the genome assembly of barley cultivar Morex and publicly available FLcDNAs, an in–solution hybridization–based sequence capture platform that is selectively enriched for a 61.6 Mb of barley coding sequence was developed recently (Mascher et al., 2013). This platform provides a highly specific capture of targeted exonic sequences of barley genome, reducing the complexity of 5.1 Gb barley genome by several folds. This resource is particularly useful for applications including gene cloning and expression profiling.

1.4.2. Functional genomics tools

1.4.2.1. Forward genetic tools

Barley has been the subject of mutation research starting from 1928 which provided the raw material for forward genetic approaches (Lundqvist, 2009). Over the decades many researchers have collected and characterized a large number of spontaneous and chemical/ionizing radiation induced mutants. The major categories of mutant phenotypes generated include: altered spikelet morphology, altered culm length, changes in growth type, leaf development, awn development, pigmentation, and resistance to powdery mildew, differences in chlorophyll development and many other physiological mutants (Scholz and Lehmann, 1961; Lundqvist, 2009). These mutants have been systematically maintained in geneticist and breeder collections at the National Small Grain Collection, Aberdeen, ID (http://www.ars.usda.gov/Main/docs.htm?docid=2922), IPK Genebank (not publicly available) and the Nordic Genetic Resource Center, Alnarp, Sweden (http://ace.untamo.net/) (Lundqvist and Franckowiak, 2003). Several of these mutants have been backcrossed to (BW001 to BW979) a near-isogenic background in the genotype Bowman (Franckowiak et al., 1985) making their functional evaluation less cumbersome. In a recent

effort, SNP genotyping of all Bowman backcrossed mutants using genic SNP markers was conducted, which delimited the genomic introgression responsible for the mutant phenotype (Druka et al., 2011). The historical mutant resources together with SNP introgression data would be a wonderful starting point for the functional studies and positional isolation of responsible gene/s in these mutants.

1.4.2.2. Reverse genetic tools

Once a candidate gene responsible for a particular phenotype is established, the functional validation of such gene is essential. Most of the historical barley developmental mutants identified in the past have more than one mutant allele by which the underlying gene function can be validated. However, for genes being isolated by conventional bi–parental genetic analyses or GWAS, and for those mutants lacking enough number of mutant alleles, it is necessary to validate identified gene candidates using reverse genetic approaches such as TILLING (Targeting Induced Local Lesions IN Genomes) or transgenics. As of today, four different TILLING populations are available for barley. These include (i.) TILLMore, a sodium azide induced six–rowed TILLING population from Morex (Talamè et al., 2008). This population constitutes 4906 $M_{3/4}$ families, with a mutation density of one SNP per each 374 kb. (ii.) Two–rowed EMS (Ethyl Methyl Sulfonate) induced Barke TILLING population currently represents the largest TILLING population with 10,279 M_2 lines (Gottwald et al., 2009). The mutation load is one mutation per 0.5 kb. The other two unpublished resources include EMS-induced TILLING lines from two–rowed cultivars Optic (1–5 SNPs per 1.0 Mb approximately; Waugh et al., unpublished) and Haruna Nijo (Sato et al., unpublished). Such a mutation load in these populations will enable functional evaluation of genes in mutants of interest.

Testing genes of interest by transgenics is a common functional genetics approach (Hensel et al., 2011). Several transgenic approaches were established for barley by which a preferred gene can be complemented, down-regulated, knocked–out or over-expressed. Complementation is a straight forward approach by which a mutated gene can be complemented by the functional wild-type form of the gene. The quantitative effect of a gene can be analyzed through approaches like RNA interference (RNAi), Virus Induced Gene Silencing (VIGS) (Holzberg et al., 2002; Hein et al., 2005), which function through homology–dependant post–transcriptional gene silencing. However, these approaches suffer from potential off–target effects (gene family members). This problem can be circumvented through a recent technology called Transcriptional Activator–Like Effector Nucleases (TALENs), which allows sequence specific *in planta* gene targeting with typically no off–target effects in the genetic background of the host genome (Boch et al., 2009; Joung and Sander, 2013; Zhang et al., 2013b). This technology has already been proven successful in barley (Gurushidze et al.; Wendt et al., 2013).

The comprehensive set of available genetic and genomic resources discussed will be useful to isolate and characterize genetic determinants underlying various developmental processes in barley. A list of such genes identified responsible for plant development, pathogen resistance and physiological responses in barley with the help of available genetic and genomic resources is given in **Table 1-2**.

Table 1-2. Gene cloning and characterization in barley.

Locus name	Chromosome	Gene	Function	References	Approach
lks2	7HL	*SHI* TF	Awn length	(Yuo et al., 2012)	Map–based cloning
Kap	4HS	*BKN3*	Awn & lemma development	(Muller et al., 1995)	Homology based on maize
trd1	1HL	*GATA* TF	Bract growth	(Whipple et al., 2010)	Map–based cloning
eam8	1HL	*HvELF3*	Flowering time	(Faure et al., 2012; Zakhrabekova et al., 2012)	Map–based cloning
eam10	3HL	*HvLUX*	Flowering time	(Campoli et al., 2013; Gawroński et al., 2014)	Mutant analysis
eps2	2H	*HvCEN*	Flowering time	(Comadran et al., 2012)	Genome wide association
zeo1	2HL	*HvAP2* TF – *miR172*	Rachis internode elongation	(Houston et al., 2013)	Genome wide association
uzu	3HL	*HvBRI1*	Plant height	(Chono et al., 2003)	Homology approaches with rice
ncl1	1H	*CNGC4*	Programmed cell death	(Rostoks et al., 2006)	Homology based on Arabidopsis
Bot1	4HL	*Boron efflux transporter*	Boron toxicity tolerance	(Sutton et al., 2007)	Map–based cloning
HvNIP2	6HL	*HvNIP2;1 aquaporin*	Boron toxicity tolerance	(Schnurbusch et al., 2010)	Map–based cloning
HvAACT1	4H	*Citrate transporter*	Aluminium toxicity tolerance	(Furukawa et al., 2007)	Map–based cloning
Rpg4	4H	*NBS–LRR, ST kinase*	Stem rust resistance	(Brueggeman et al., 2008)	Map–based cloning
Rpg5	4H	Transmembrane protein	Stem rust resistance	(Brueggeman et al., 2008)	Map–based cloning
Vrn–H1	5HL	*MADS box* TF	Growth habit	(Yan et al., 2003)	Homology based on wheat
Vrn–H2	5H	*ZCCT* TF	Growth habit	(Yan et al., 2004)	Homology based on wheat
Vrn–H3	7HS	*HvFT1*	Growth habit	(Yan et al., 2006)	Homology based on wheat
Ppd–H1	2HS	*Pseudo response regulator*	Day length & flowering	(Turner et al., 2005)	Map–based cloning
vrs1	2HL	*HvHOX1* TF	Row–type	(Komatsuda et al., 2007)	Map–based cloning
vrs4	3HS	*HvRA2* TF	Row–type	(Koppolu et al., 2013)	Map–based cloning
int–c	4HS	*HvTB1* TF	Row–type	(Ramsay et al., 2011)	Genome wide association
cly1	2HL	*HvAP2*, miR172	Lodicule development	(Nair et al., 2010)	Map–based cloning
nud	7HL	*ERF* TF	Hull adhesion to grain	(Taketa et al., 2008)	Map–based cloning
Mla	1H	*CC–NBS–LRR*	Powdery mildew resistance	(Wei et al., 1999)	Map–based cloning
mlo	4HL	Trans membrane protein	Powdery mildew resistance	(Buschges et al., 1997)	Map–based cloning
Rpg1	1HL	*Receptor kinase–like*	Stem rust resistance	(Brueggeman et al., 2002)	Map–based cloning
rym4/rym5	3HL	*HvelF–4E*	BYMV & BMMV resistance	(Stein et al., 2005)	Map–based cloning
Ror2	5HL	*Syntaxin*	Powdery mildew resistance	(Collins et al., 2003)	Map–based cloning
Rar1	2H	Zinc binding protein	Powdery mildew resistance	(Shirasu et al., 1999)	Map–based cloning

Locus symbols: *lks*: *short awn*; *Kap*: *Hooded lemma*; *trd*: *third outer glume*: *eam*: *early maturatum*; *eps*: *earliness perse*; *zeo*: *zeochriton*; *uzu*: *semi brachytic*; *Bot*: *boron toxicity tolerance*; *Rpg*: *resistance to Puccinia graminis*; *Vrn*: *vernalization response*; *Ppd-H1*: *Photoperiod-H1*; *vrs*: Six-rowed spike; *int*: *intermedium*; *cly*: *cleistogamous*; *nud*: *naked caryopsis*; *Mla*: *Mildew resistance locus a* ; *mlo*: *mildew resistance locus o* ; *rym*: *resistance to yello mosaic virus*; *ror*: *required for mlo-specified resistance*; *rar*: *required for mla-specified resistance*.

Gene names: *SHI: SHORT INTERNODES; BKN3: BARLEY KNOTTED3; ELF3: ELONGATION FACTOR3; LUX: LUX ARHYTHMO; CEN: CENTRORADIALIS; AP2:APETALA2; BRI1: BRASSINISTEROID INSENSITIVE1; CNGC4: CYCLIC NUCLEOTIDE-GATED ION CHANNEL4; NIP2: NODULIN-26-LIKE INTRINSIC PROTEIN ; AACT1: ACETOACETYL-COA THIOLASE1*; *NBS-LRR: NUCLEOTIDE-BINDING SITE LEUCINE-RICH REPEAT; MADS: MCM1, AG, DEFA, and SERUM RESPONSE FACTOR* [(*SRF*)]*; ZCCT1: CO, CO-LIKE, and TOC1; FT1: FLOWERING TIME LOCUS1; HOX1: HOMEOBOX; RA2: RAMOSA2; TB1: TEOSINTE BRANCHED1; ERF: ETHELENE RESPONSE FACTOR; ELF-4E: ELONGATION FACTOR 4E.*

1.5. Aims of the present thesis

Compared to the model grass species rice and maize, the genetic regulation of inflorescence development in barley is poorly understood, especially the knowledge on early developmental changes that shape the inflorescence architecture is very limited. This is clearly evident from the gene cloning studies undertaken in the past, which mainly focused on spikelet fertility, flowering habit, lodicule, and awn development (Muller et al., 1995; Turner et al., 2005; Komatsuda et al., 2007; Taketa et al., 2008; Nair et al., 2010; Ramsay et al., 2011; Comadran et al., 2012; Faure et al., 2012; Yuo et al., 2012; Zakhrabekova et al., 2012; Campoli et al., 2013; Houston et al., 2013; Gawroński et al., 2014). Interestingly the barley row-type mutant Six-rowed spike 4 (*vrs4*) shows visible aberrations in spikelet/floret development along with lateral spikelet fertility as seen in mutants of other row-type loci. Hence, the present study was undertaken with a broader aim of identifying the genetic regulator that shapes the spikelet development and lateral spikelet fertility in *vrs4*. The major objectives of the present study include,

1. Detailed phenotypic analysis of spikelet/floret meristem identity and development at different pre–anthesis (microscopic) and post–anthesis (macroscopic) spike developmental phases in *vrs4* mutants in comparison to their progenitors.
2. Molecular marker mapping of *vrs4* introgression in F_2 mapping populations (initial rough scale mapping to localize the *vrs4* introgression on 3H chromosome followed by fine scale high resolution mapping using a larger mapping population.)
3. Establishment of barley physical BAC contig harboring the *vrs4* candidate gene.
4. Validation of *vrs4* candidate gene in allelic mutants. Quantification of *vrs4* express*ion* using qRT–PCR and global transcript expression profiling of *vrs4* mutants and wild types using microarray to identify potential down–stream gene targets of *vrs4*.

2.0. Materials and Methods

2.1. Plant materials and growing conditions

2.1.1. Spike phenotype analysis

Three *vrs4* mutant genotypes that include two Bowman backcross derived lines BW–NIL(*vrs.4k*) [BW903], and BW–NIL(*mul1.a*) [BW606], the WTs Bowman were studied to characterize early inflorescence development (pre–anthesis developmental stages). The genotypes BW–NIL(*vrs.4k*), BW–NIL(*mul1.a*) and Bowman were grown in pots (14 cm diameter) under green house conditions (16 hours light, 18 °C and 8 hours dark, 14 °C.)

2.1.2. F_2 mapping populations

Two F_2 mapping populations were generated by crossing mutant parent BW–NIL(*vrs.4k*) with two–rowed parents Golden Promise [BW–NIL(*vrs4.k*) × Golden Promise] and Barke [Barke × BW–NIL(*vrs4.k*)]. For mapping the *vrs4* locus, initially 94 segregating F_2 plants from each mapping population were evaluated, and for further high resolution mapping recombinant plants from 1000 segregating F_2 plants from the BW–NIL(*vrs4.k*) × Golden Promise mapping population were utilized. The F_2 plants were grown in pots (14 cm diameter) under green house conditions (16 hours light, 18 °C and 8 hours dark, 14 °C.)

2.1.3. Allelic *vrs4* mutants

Fifteen allelic *vrs4* mutants were obtained from Dr. Udda Lundqvist, Nordic Genetic Resources Center, Sweden, and three other allelic *vrs4* mutants were obtained from United States Department of Agriculture (USDA–ARS), USA. Two additional *vrs4* mutants were obtained from the Scholz mutant collection, IPK Genebank, Germany. Three *vrs4* mutants (*int-e.23*, *int-e.128*, and *vrs4.l* were grown under field conditions at NIAS, Tsukuba, Japan by our collaborator

Dr. Takao Komatsuda). The remaining mutant genotypes were grown in pots (14 cm diameter) under greenhouse conditions (16 hours light, 18 °C and 8 hours dark, 14 °C). A detailed description for these mutants is given in **Table 2-1**.

Table 2-1. *vrs4* mutant allele descriptions.

#	Mutant allele	Progenitor	Background/ corresponding *Vrs1* allele	Mutagen	Mapping study
1	*int-e.4*	Bonus	Bonus/*Vrs1.b3*	Neutrons	Lundqvist, 1991
2	*int-e.20*	Foma	Foma/*Vrs1.b3*	Neutrons	Lundqvist, 1991
3	*int-e.23*	Foma	Foma/*Vrs1.b3*	Propyl Methane Sulfonate	Lundqvist, 1991
4	*int-e.26*	Foma	Foma/*Vrs1.b3*	Neutrons + Ethyl Methane Sulfonate	Lundqvist, 1991
5	BW-NIL(*int-e.58*)	Kristina	Bowman/*Vrs1.b3*	Ethyl Methane Sulfonate	Lundqvist, 1991 Druka et al., 2011
6	*int-e.65*	Bonus	Bonus/*Vrs1.b3*	Sodium Azide	Lundqvist, 1991
7	*int-e.66*	Kristina	Kristina/*Vrs1.b3*	Ethyl Methane Sulfonate	Lundqvist, 1991
8	*int-e.72*	Bonus	Bonus/*Vrs1.b3*	X-rays	Unpublished
9	*int-e.87*	Bonus	Bonus/*Vrs1.b3*	Sodium Azide	Unpublished
10	*int-e.89*	Hege	Hege/*Vrs1.b*	Sodium Azide	Unpublished
11	*int-e.90*	Hege	Hege/*Vrs1.b*	Sodium Azide	Unpublished
12	*int-e.91*	Hege	Hege/*Vrs1.b*	Sodium Azide	Unpublished
13	*int-e.92*	Hege	Hege/*Vrs1.b*	Sodium Azide	Unpublished
14	*int-e.101*	Hege	Hege/*Vrs1.b*	Sodium Azide	Unpublished
15	*int-e.128*	Foma	Foma/*Vrs1.b3*	X-rays	Unpublished
16	BW-NIL(*vrs4.k*)	MFB104	Bowman/*Vrs1.b3*	Gamma rays	Fukuyama et al.; Druka et al., 2011
17	BW-NIL(*mul1.a*)	Montcalm	Bowman/*Vrs1.b3*	Gamma rays	Kasha & Walker; Druka et al., 2011
18	*vrs4.l* (*syn. Xc 41.5*)	Piroline	Piroline/*Vrs1.b*	X-rays	Fukuyama et al.,
19	MHOR318	Ackermann's Donaria	Ackermann's Donaria/*Vrs1.b*	X-rays	Unpublished
20	MHOR345	Heine's Haisa	Heine's Haisa/*Vrs1.b3*	X-rays	Unpublished

2.1.4. *Vrs4* candidate gene re-sequencing

For re-sequencing of *Vrs4* candidate gene and haplotype analysis 77 diverse barley genotypes were used. Of the 77 accessions, 59 represent GENOBAR collection (out of a total of 224 GENOBAR accessions), were obtained from Dr. B. Kilian, IPK whereas the remaining 18

diverse accessions were obtained from IPK Genebank, Germany. These 77 accessions represented a broader geographic range and consisted of two-rowed (38 accessions), six-rowed (34 accessions), labile (two accessions) and three unknown accessions. The genotypes used for re-sequencing were grown in pots (14 cm diameter) under green house conditions (16 hours light, 18 °C and 8 hours dark, 14 °C).

2.1.5. Microarray and qRT–PCR analyses

Two *vrs4* deletion mutants MHOR 318, MHOR 345 and their respective progenitors Ackermann's Donaria (AD) and Heine's Haisa (HH) were utilized for microarray analysis. The differentially regulated gene transcripts identified from the microarray analysis were confirmed by conducting qRT–PCR with the same samples. The relative expression of *Vrs4* candidate gene was analyzed in genotypes BW–NIL(*vrs.4k*), MHOR 318, MHOR 345 and their respective WTs Bowman, AD and HH by qRT–PCR. In case of MHOR 318, MHOR 345 and their respective progenitors Ackermann's Donaria (AD) and Heine's Haisa (HH), three plants/pot (20 cm diameter) were grown under phytochamber conditions (light conditions: 12 h/12 h day and night; temperature: 12 °C during day and 7 °C during night). The remaining genotypes [(BW–NIL(*vrs.4k*) and Bowman)] used for qRT-PCR analyses were grown under green house conditions (16 hours light, 18 °C and 8 hours dark, 14 °C) in 96-well planting trays.

2.1.6. Metabolite analysis

The *vrs4* mutant genotypes BW–NIL(*vrs.4k*), BW–NIL(*mul1.a*), MHOR 318; MHOR 345 and their respective WTs Bowman, AD and HH were analyzed to compare the metabolite concentrations. Three plants/pot (20 cm diameter) were grown under greenhouse conditions (16 hours light, 18 °C and 8 hours dark, 14 °C).

2.2. DNA preparation

For DNA preparation, leaf samples at three leaf stage were collected from the genotypes used in the present study (94, F_2 plants from each of the two mapping populations, 1000 F_2 plants used as fine mapping population from *vrs4.k* × Golden Promise, 20 *vrs4* mutant alleles, respective WTs and 77 diverse barley genotypes used for candidate gene re-sequencing and haplotype analysis). DNA was prepared using a modified Doyle and Doyle's protocol (Doyle and Doyle, 1990).

2.3. Genetic linkage and physical mapping of *vrs4* locus

2.3.1 Molecular marker development

For mapping *vrs4* locus to a precise genomic location on barley 3H chromosome, initially VeraCode Golden Gate SNP (Single Nucleotide Polymorphism) genotyping assay was carried out with a custom made SNP set of 113 BOPA (Barley Oligonucleotide Pool Assay) markers (MAF≥0.2) that are reported to map at regular intervals along the 3H chromosome (Close et al., 2009). Veracode SNP genotyping assay was carried out in a set of 94 segregating F_2 individuals from BW–NIL(*vrs4.k*) × Golden Promise and Barke × BW–NIL(*vrs4.k*) mapping populations. The raw SNP genotyping data obtained was analyzed for allele calling using the Genome studio software (Illumina). After establishing the initial mapping interval for *Vrs4* locus with VeraCode SNP assay, the 3H barley genome zipper (Mayer et al., 2011) was used for further marker development in the defined *vrs4* genomic interval. For CAPS (Cleaved Amplified Polymorphic Sequences) or INDEL (INsertion DELetion) based marker development the gene sequences from the syntenic interval in rice or *Brachypodium* were extracted from respective genome browser web servers (http://rice.plantbiology.msu.edu/cgi–bin/gbrowse/rice/ and

http://jbrowse.brachypodium.org/JBrowse.html). The obtained gene sequences were BLASTed against the IPK Barley BLAST server (http://webblast.ipk–gatersleben.de/barley/viroblast.php) to obtain orthologous barley sequences. SNP polymorphisms identified among the parents based on the primers designed from orthologous barley genes were converted to restriction enzyme based CAPS (Vincze et al., 2003) (http://tools.neb.com/NEBcutter2/) or dCAPS (Neff et al., 2002) markers (http://helix.wustl.edu/dcaps/). A complete list of polymorphic BOPA SNP markers and CAPS or INDEL based markers identified in the two mapping populations [BW–NIL(*vrs4.k*) × Golden Promise and Barke × BW–NIL(*vrs4.k*)] is given in **Supplementary Table 1a**.

2.3.2. Phenotyping of mapping populations

The F_2 plants from the two mapping populations BW–NIL(*vrs4.k*) × Golden Promise and Barke × BW–NIL(*vrs4.k*) segregating at *vrs4* locus were scored for the spike phenotype [either two–rowed (conferred by wild type *vrs4* allele from Golden promise or Barke or due to heterozygosity at *Vrs4* locus) or six–rowed spikes with indeterminate TSM [conferred by mutant *vrs4* allele derived from BW–NIL(*vrs4.k*) parent]. The parents BW–NIL(*vrs4.k*), Golden Promise, Barke, and BW–NIL(*vrs4.k*) were also grown alongside and studied for their spike phenotype

2.3.3. Linkage analysis of genotypic and phenotypic data

For the two mapping populations linkage analysis of segregation data obtained after genotyping of the polymorphic molecular markers together with phenotypic data was carried out using maximum likelihood algorithm implemented in Joinmap 3.0 (Van Ooijen and Voorrips, 2001).

The Kosambi mapping function was used to convert recombination fractions into map distances. The maps were drawn using map chart option in Joinmap 3.0.

2.3.4. High resolution mapping

For high resolution mapping within the *Vrs4* genomic region, 1000 segregating F_2 individuals from BW–NIL(*vrs4.k*) × Golden Promise population were screened with two closely linked CAPS markers Hv3717 and Hv45740 (separated by 7.5 cM interval in BW–NIL(*vrs4.k*) × Golden Promise population based on initial rough scale mapping). Only the recombinant individuals obtained from the segregating progeny within the defined marker interval were used for further marker genotyping and phenotyping studies.

2.3.5. BAC sequencing, assembly, and annotation

A single BAC (Bacterial Artificial Chromosome) contig spanning 1073 kb of the minimum tiling path (MTP) of barley chromosome 3H was obtained after screening the Morex BAC library with closely linked marker DQ327702. The 1073 kb BAC contig was shotgun sequenced using 454 sequencing technology (**Table 2-2**) (Meyer et al., 2008). The sequences were assembled as previously described (Steuernagel et al., 2009). ORFs from the BAC sequences were predicted using Genescan web server (Burge and Karlin, 1997). The predicted ORFs were annotated using BLASTx function of the National Center for Biotechnology Information (NCBI).

Table 2-2. BAC clones sequenced in *Vrs4* gene region on 3HS

BAC Clone #	BAC Clone name	BAC length (Kb)
1	HVVMRXALLeA0166J14	81
2	HVVMRXALLmA0525L04	155
3	HVVMRXALLrA0402J12	157
4	HVVMRXALLmA0524F02	116
5	HVVMRX83khA0179C14	94
6	HVVMRXALLhC0084K10	69
7	HVVMRXALLrA0075M21	49
8	HVVMRXALhLB0083N17	83
9	HVVMRX83KhA0016A06	69
10	HVVMRXALhLB0066O05	100
11	HVVMRXALLrA0390E03	120
12	HVVMRXALLeA0100K09	145
13	HVVMRXALLeA0170A17	98
14	HVVMRXALLmA0292B07	138
15	HVVMRXALLeA0349L07	111
16	HVVMRXALLeA0332L11	95
17	HVVMRXALLeA0217N06	138
18	HVVMRXALLmA0279J11	122
19	HVVMRXALLmA0260B08	105
20	HVVMRXALLmA0383N08	95
21	HVVMRXALLeA0271J13	111
22	HVVMRXALLeA0253H10	88

2.4. mRNA expression analyses

2.4.1. RNA extraction

Total RNA was extracted from immature barley spike tissues collected at double ridge, triple mound, glume primordium, lemma primordium, stamen primordium, and awn primordium stages using either PureLink® RNA Mini Kit (Ambion, life technologies) or RNAqueous®–Micro Kit (Ambion, life technologies). RNase–free DNase (Invitrogen) was used to remove genomic DNA contamination. The RNA integrity number [RIN–a scale given by Agilent technologies that ranges from zero (poor quality RNA) to 10 (high quality RNA)] values were measured using the Agilent Bioanalyzer (Agilent technologies). The RNA samples with a RIN value of 9.0 and above were used for qRT–PCR and microarray hybridizations. RNA concentrations were measured using NanoDrop UV–VIS spectrophotometer (Peqlab.)

2.4.2. Microarray hybridization and data analysis (Conducted in collaboration with the research group Abiotic Stress Genomics, AG SGN, IPK)

By utilizing 50,000 consensus EST assembly (HarvEST) the research group Abiotic Stress Genomics, at IPK, Germany developed and synthesized multiple oligos for individual sequences, generated a 244 K microarray (Agilent Technologies). A pilot study was conducted to identify and omit oligos with potential for cross hybridization across gene family members from spike meristem tissues. Upon selecting oligos with best Agilent base composition score, a custom eArray was designed to generate 56 K Agilent barley microarray (60 K × 8 plex format). All unigene sets have been annotated and functionally classified into MapMan functional categories.

RNAs isolated from spike meristems collected at glume, stamen and awn primordium stages from two *vrs4* deletion mutants (MHOR 345 and MHOR 318) and respective wild–types AD and HH were used in the microarray hybridization experiments. For each spike developmental stage three technical replicates were used for array hybridizations that resulted in 36 total hybridizations. The low input quick amp labeling kit for one–color microarray–based gene expression analysis was used for labeling of RNA samples (50ng) using Cyanine3 (Cy3) fluorescent dye (Agilent technologies). The labeled cRNA samples were subsequently purified using RNeasy mini spin columns (Qiagen). Quantity of cRNA was measured using NanoDrop, which was subsequently used to calculate the specific activity and yield of cRNA. 600 ng of Cy3–labeled, amplified cRNA with a specific activity of above six was used for subsequent hybridization following the steps of the one–color microarray–based gene expression analysis protocol (Agilent technologies). Hybridizations were carried out at 65 °C for 17 h. The slides were washed and scanned at a high resolution of 2 microns using Agilent DNA Microarray Scanner G2565CA (Agilent). The resultant 36 microarray TIF images were processed to run

batch extractions by choosing appropriate grid using Agilent's Feature Extraction Software (version 11.0). The quantified feature text file is first analysed for quality checks using Agilent QC chart tool. The qualified experiments were further processed, at first raw data (gene expression) was quantile normalized and fold changes were calculated between *vrs4* mutant and WT samples for all developmental stages analyzed. The differentially regulated gene sets (>2.0 folds), with multiple correction using Bonferroni method ($P<0.05$) were identified. Top regulated genes were subjected to the co–expression analysis using spearman correlation test and complete linkage algorithm implemented in Genespring 12.0. Only differentially regulated genes in common between both mutants (MHOR 318 and MHOR 345) were considered for further analysis and interpretation.

2.4.3. qRT–PCR

For qRT–PCR, reverse transcription and cDNA synthesis were carried out with 1 µg of RNA isolated from different spike developmental stages using the QuantiTect® Reverse Transcription Kit (Qiagen). Real–time PCR was performed using the QuantiTect® SYBR® Green PCR kit (Qiagen) and the ABI Prism® 7900HT sequence detection system (Applied Biosystems). RT–PCR results were analyzed using $2^{-\Delta\Delta CT}$ method (Livak and Schmittgen, 2001) implemented in SDS 2.2.2 software (Applied Biosystems). qRT–PCR primer sequences are listed in **Supplementary Table 1c**.

2.5. Metabolite analysis of trehalose biosynthesis intermediates and precursors (conducted in collaboration with the research group Heterosis, AG HET, IPK)

For studying the metabolite profiles of trehalose biosynthesis precursors UDP-Glucose, glucose-6-phosphate and the intermediate trehalose-6-phosphate, immature spike tissue at glume

primordium and awn primordium stages was collected from the *vrs4* mutant genotypes BW–NIL(*vrs.4k*), BW–NIL(*mul1.a*), MHOR 318; MHOR 345 and their respective WTs Bowman, AD and HH. The spike tissue was subjected to freeze drying at -30 °C for four days. Three technical replicates for each stage from each genotype were analyzed. The samples were homogenized using Retsch TissueLyser (Qiagen) for 45 s at 1800 strokes/minute. After homogenization, the samples were extracted with 270 µl of methanol/water solution (150 µl water + 120 µl methanol with 40 µl of internal standard). 1µl of sample was injected into an LC-MS/MS system [(Dionex Ulimate 3000 RSLC and API 4000 (Applied Biosystems).]

2.6. Re-sequencing and haplotype analysis of *Vrs4* in diverse barley genotypes

Three primer pairs with overlapping fragments (**Supplementary Table1b**) covering 2046 bp (987 bp of 5' region (promoter and 5'UTR), 774 bp ORF and 285 bp 3'UTR) of the *Vrs4* (*HvRA2*) gene were amplified in 77 diverse barley genotypes for direct PCR sequencing using the Sanger method (BigDye Terminator v3.1 Cycle Sequencing Kit; Applied Biosystems) in house at PGRC, IPK, Germany. Fluorescently terminated extension products were separated using a capillary–based ABI3730xl sequencing system (Applied Biosystems). The sequences were analyzed using Seqman software implemented in Laser gene software suite 9.0 (DNA STAR) Multiple sequence alignments were performed using the ClustalW method (Thompson et al., 1994). Haplotype analysis of the nucleotide sequence data was conducted using the median joining algorithm implemented in NETWORK 4.6.1.0. A default weight of 10 was applied for all substitutions and INDEL polymorphisms identified.

2.7. Phylogenetic analysis of RAMOSA2 orthologs/homologs

Nucleotide sequences for Barley LBD (LOB domain) genes were extracted from the IPK Barley BLAST server using *HvRA2* as a query sequence. The obtained nucleotide sequences were converted to protein sequences using EMBOSS Transeq (EMBL–EBI). HvRA2 protein sequence was used as NCBI BLASTp query to retrieve RA2 and RA2–LIKE proteins from monocot and eudicots species, respectively (**Supplementary Table 2**). For obtaining these sequences a cut–off E–value of 10^{-30} was applied. For phylogenetic analysis, the protein sequences were initially aligned using the MUSCLE algorithm (Edgar, 2004) implemented in MEGA 5.1 (Tamura et al., 2011). A maximum likelihood phylogenetic tree was constructed using the ML heuristic method Nearest–Neighbor–Interchange (NNI) implemented in MEGA 5.1. The bootstrap consensus tree inferred from 1000 replicates is taken to represent the evolutionary history of the sequences analyzed. Branches corresponding to partitions reproduced in less than 50 % bootstrap replicates are collapsed.

2.8. Data contributions by the author and the collaborators towards the present thesis

Majority of the data presented in this thesis has been generated in the working group PBP, IPK-Gatersleben by the author of the thesis (*Ravi Koppolu*[1]). However, some experiments such as microarray hybridization, and metabolite analyses, were performed in collaboration with other research groups Abiotic Stress Genomics (SGN, Dr. Nese Sreenivasulu), and Heterosis (HET, Prof. Dr. Thomas Altman) within IPK. The data generated with the help of our collaborators, [(where the author (*Ravi Koppolu*[1]), has significantly contributed towards the results)] has been presented in this thesis in order to make it a complete and understandable story. A detailed

overview of different tasks carried out by the author (*Ravi Koppolu*[1]) and the collaborators to achieve the objectives of the present thesis is given below.

Spike phenotype analyses

- Spike phenotyping and data analysis of the two mapping populations BW–NIL(*vrs4.k*) × Golden Promise and Barke × BW–NIL(*vrs4.k*), and 20 *vrs4* mutant alleles (except *vrs4.l*, *int-e.23* and *int-e.128*) – *Ravi Koppolu*[1].

- Sample preparation for SEMs and SEM analysis in Bowman, BW–NIL(*vrs4.k*) and BW–NIL(*mul1.a*) – *Ravi Koppolu*[1]. SEM preparation and image recordings – *Dr. Twan Rutten*[2].

Genetic and physical mapping of *vrs4*

- Marker development (VeraCode SNP oligo pool design, CAPS, dCAPS marker development), screening and initial rough scale mapping in the two *vrs4* mapping populations – *Ravi Koppolu*[1].

- High resolution fine scale mapping (recombinant screening and further marker development) – *Ravi Koppolu*[1].

- Selection of BACs for physical mapping: *Ravi Koppolu*[1]; preparation of BACs for physical mapping – *Ravi Koppolu*[1]; BAC sequencing – *Dr. Axel Himmelbach*[3]; BAC sequence assembly: *Dr. Burkhard Steuernagel*[4]; BAC sequence annotation: *Ravi Koppolu*[1].

Mutant analyses

- Resequencing of *vrs4* mutant alleles and data analyses – *Ravi Koppolu*[1].

- Allelism tests for *int-e.4* and *int-e.23* with *vrs4.m* – *Dr. Udda Lundqvist*[5].

Gene expression analyses

- Quantification of *HvHOX1*, *HvRA2*, *HvBAD1*, *HvCKX2*, *HvPIN1-LIKE*, and *HvSRA* expression in various *vrs4* mutants – *Ravi Koppolu*[1].

- Microarray experimental design – *Dr. Thorsten Schnurbusch*[1], *Dr. Nese Sreenivasulu*[6], and *Ravi Koppolu*[1]; sample collection and RNA preparation for microarray experiment: *Ravi Koppolu*[1]; microarray hybridization: *Dr. Christiane Seiler*[6]; Microarray data extraction: *Dr. Nese Sreenivasulu*[6]; Microarray data analysis and interpretation: *Ravi Koppolu*[1] with the help from *Dr. Thorsten Schnurbusc*[1]; Validation of microarray data by qRT-PCR: *Ravi Koppolu*[1].

Metabolite analysis

- Experimental setup, sample collection and preparation – *Ravi Koppolu*. Experimental procedure for metabolite analysis – *Ravi Koppolu*[1]. Data analysis and interpretation: *Ravi Koppolu*[1] with the help from *Dr. Thorsten Schnurbusch*[1].

Haplotype analysis

- Experimental set up, sample collection, preparation, resequencing and data analysis – *Ravi Koppolu*[1].

Phylogenetic analysis

- *Ravi Koppolu*[1] together with the help of an anonymous reviewer of the PNAS publication based on the present thesis.)

[1] AG PBP, IPK – Gatersleben, Germany
[2]AG SZB, IPK – Gatersleben, Germany
[3]AG GED, IPK – Gatersleben, Germany
[4]AG BIT, IPK – Gatersleben, Germany
[5]Nordic genetic resource center – Alnarp, Sweden
[6]AG SGN, IPK – Gatersleben, Germany.

3.0. Results

Identification of the key genetic determinants (genes) that regulate inflorescence architecture and a broader elucidation of their gene regulatory networks forms a very important basis to understand the floral development in grasses and other crop species. Knowledge gained through such studies can be applied to manipulate floral architecture and subsequently increase future cereal crop yields which are the staple food source to humans. The regulation of inflorescence development has been broadly elucidated in plant species, such as *Arabidopsis*, rice and maize, with the help of a wealth of mutant collection that display abnormal inflorescence development (Malcomber et al., 2006; Yoshida and Nagato, 2011; Sreenivasulu and Schnurbusch, 2012; Pautler et al., 2013; Tanaka et al., 2013). However, in barley functional knowledge of genes and genetic mechanisms involved in spike development is very limited so far. The present study identified barley *RAMOSA2* (*HvRA2*) as the gene that underlies the Six–rowed spike 4 (*vrs4*) locus, which by large regulates the determinate fate of spikelet meristems along the spike. The present study also identified *Vrs4* as a key regulator of the six–rowed pathway controlling *Vrs1* transcript expression. With the help of microarray analysis in *Vrs4/vrs4*, important putative targets of *HvRA2* in its gene regulatory network were identified. In the following sections the results obtained during the process of *vrs4* cloning and its functional evaluation are further elucidated.

3.1. Spikelet development in *Vrs4* wild type and mutant inflorescences

In WT barley, spike development starts with a first visible reproductive stage called double ridge (DR) containing upper spikelet ridge (i.e. first axillary meristem) and a lower leaf ridge (**Figure 3.1.1.A**). Unlike maize or sorghum, in which spikelets develop from SPMs, immature barley

spikes develop a TSM; the TSM arises from the upper ridge of the DR stage. The DR stage is also seen in wheat spikelet development, but unlike in barley, the upper axillary ridge of the double ridge in wheat proceeds to develop a single spikelet meristem. This makes the TSM unique to barley. The TSMs are determinate and form three distinct mounds termed as triple mound (TM), each mound producing one spikelet meristem: the central spikelet meristem (CSM) and two lateral spikelet meristems (LSMs) (**Figure 3.1.1.A**). Each spikelet meristem develops a pair of glume primordia (GP), and then differentiates into one FM (**Figure 3.1.1.A**). CSM normally develops ahead of LSMs (**Figure 3.1.1.A**). Spikelet meristems are also determinate structures producing only one FM (**Figure 3.1.1.A**), which develops floral organs (three stamen primordia (SP) and one pistil primordium) and finally result in the formation of one single-flowered CS and two single-flowered LSs. In two–rowed barleys lateral florets developmentally abort approximately after SP stage, whereas in six–rowed types lateral floral structures continue to differentiate further.

To better understand the developmental deviations in SM identity in *vrs4* mutants detailed phenotypic analyses at different stages of immature spike development that include pre–anthesis spike development (DR, TM, GP, lemma primordium (LP), SP, and awn primordium (AP) stages), and post–anthesis spike development were conducted.

3.1.1. Scanning electron microscopy showed early developmental changes in inflorescences of *vrs4* mutants leading to indeterminate spikelet development and altered axillary meristem identity

A careful comparison of scanning electron micrographs (SEM) obtained from wild type *Vrs4* (Bowman) and mutant *vrs4* [(BW-NIL(*vrs4.k*) and BW-NIL(*mul1.a*)] inflorescences revealed no visible morphological differences at DR stage, suggesting that there is no change in determinacy

of Axillary Meristem (AM) that gives rise to triple spikelet meristem (**Figure 3.1.1.B**). The *vrs4* mutants exhibited the development of the basic set of TSM (one CSM and two LSMs) as seen in the WT. The appearance of two additional mounds on either side of the LSMs was the first visible deviation observed in *vrs4* mutant inflorescences that occurred between TM and GP stages (**Figure 3.1.1.B**). These additional mounds developed into additional spikelets/florets (AS/AF) at later stages of spike development (**Figure 3.1.1.D** and **E**). The formation of the secondary additional spikelet meristem (SASM) on the additional spikelets showed that *vrs4* mutants can potentially produce more additional spikelets (**Figure 3.1.1.D** and **E**). The AS lags in development compared to their counterparts (**Figure 3.1.1.D** and **E**), suggesting that branching, rather than subdivision within the TSM, produces the ASs. Loss of determinacy in AMs became even more apparent when CSMs frequently produced branch–like inflorescence meristems (BIM) with ridges (resembling pre–double ridge stage of primary inflorescence), which later differentiated into TMs (**Figure 3.1.1.C, D,** and **E**) and eventually produced a *vrs4*–like inflorescence meristem (**Figure 3.1.1.C**). The majority of BIMs aborted as growth continued (**Figure 3.1.1.C, D,** and **E**), and only few meristems at the base developed into ASs. Apart from the ASs/AFs rarely additional pistils were also seen, suggesting that FM determinacy was also affected in *vrs4* mutants. SEM analysis revealed that *vrs4* mutants lost determinacy of the TSMs, and subsequently SMs, thus producing supernumerary spikelets and florets.

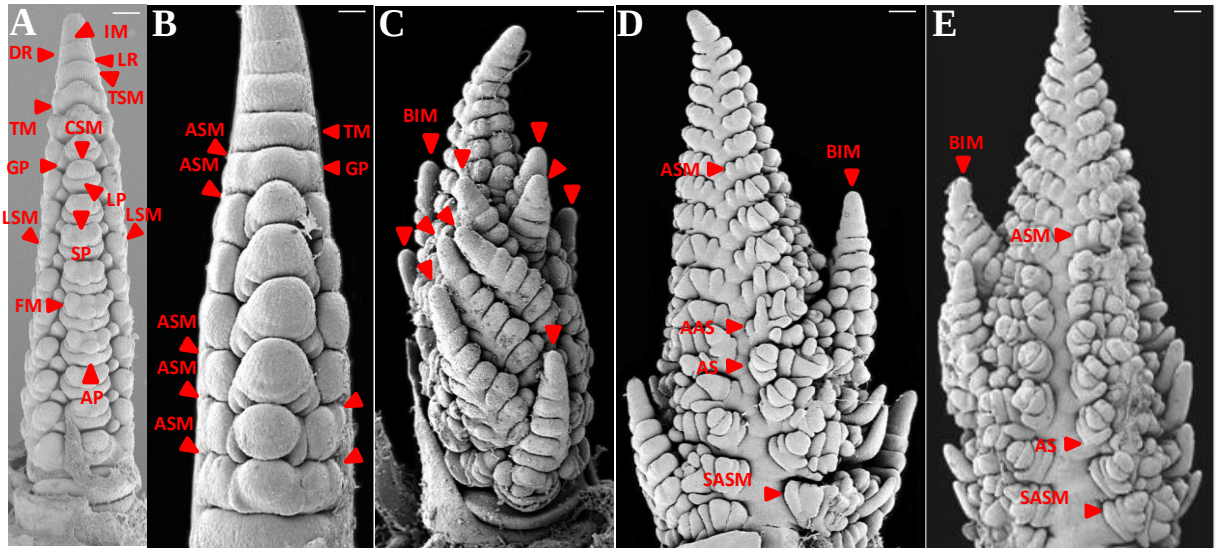

Figure 3.1.1. SEM analysis of BW-NIL(*mul1.a*) and BW-NIL(*vrs4.k*).

(**A**) Wild-type inflorescence (Bowman) at stamen primordium (SP) stage showing inflorescence meristem (IM) forming double ridge (DR), upper ridge containing triple spikelet meristem (TSM), and lower leaf ridge (LR). TSM forms a triple mound (TM), which transitions into one central spikelet meristem (CSM) and two lateral spikelet meristems (LSMs). A pair of glume primordia (GP) and a single floral meristem (FM) are produced by each SM. (**B**) BW-NIL(*mul1.a*) mutant at LP initiating additional spikelet meristems (ASMs) (red triangles). (**C**) BW-NIL(*vrs4.k*) mutant at stamen primordium (SP) stage showing BIM at TM. (**D**) BW-NIL(*vrs4.k*) at awn primordium (AP) stage showing BIM in LP. (**E**) BW-NIL(*mul1.a*) inflorescence showing LSs at an advanced stage of development, and additional spikelet meristems (ASMs) which either remain rudimentary as aborted additional spikelets (AASs) or form additional spikelets (ASs). SASM, Secondary additional spikelet meristem. Scale bars: 400 μm in **A, B,** and **E** and 700 μm in **C**, and **D**.

3.1.2. Different types of additional axillary structures produced by *vrs4* mutants

The indeterminate nature of TSM in *vrs4* mutants lead to the formation of additional spikelets/florets in the mature inflorescences. Two very obvious phenotypes observed at spike, maturity in *vrs4* mutants included well developed lateral spikelets and development of additional spikelets/florets compared with the WT *Vrs4* spikes (**Figure 3.1.2.A, B,** and **C**). The *vrs4* mutants BW-NIL(*vrs4.k*) and BW-NIL(*mul1.a*) showed completely fertile lateral spikelets compared to their two-rowed WT Bowman (**Figure 3.1.2.A, B,** and **C**). The Additional Spikelets

(ASs) and Additional Florets (AFs) in *vrs4* mutants were clearly distinguishable based on their orientation on the spike axis (rachis). ASs had the same orientation (lemma primordia on abaxial side of rachis) as in normal spikelets (**Figure 3.1.2.F**). However, AFs were oriented opposite to the normal spikelet (lemma primordia on the adaxial side of rachis showing the alternate orientation of floret formation on the rachilla) and lacked glumes (**Figure 3.1.2.F**). Unlike in WT, where each spikelet produced a single floret on the determinate rachilla, *vrs4* mutants produced additional florets on the rachilla of both the central and lateral spikelets. Thus, the restriction on the number of spikelets and florets is lost in *vrs4* mutants. The additional spikelets/florets emerging at rachis internodes were frequently fertile and developed into grains (**Figure 3.1.2.D, E,** and **G**). The apparent indeterminate nature of spikelet meristem is observed in all 20 *vrs4* mutant alleles analyzed in the present study (**Figures 3.1.2** and **3.1.3**), indicating that the *Vrs4* gene is in fact involved in a genetic pathway that mediates highly conserved determinate nature of the TSM inherent to *Hordeum* species.

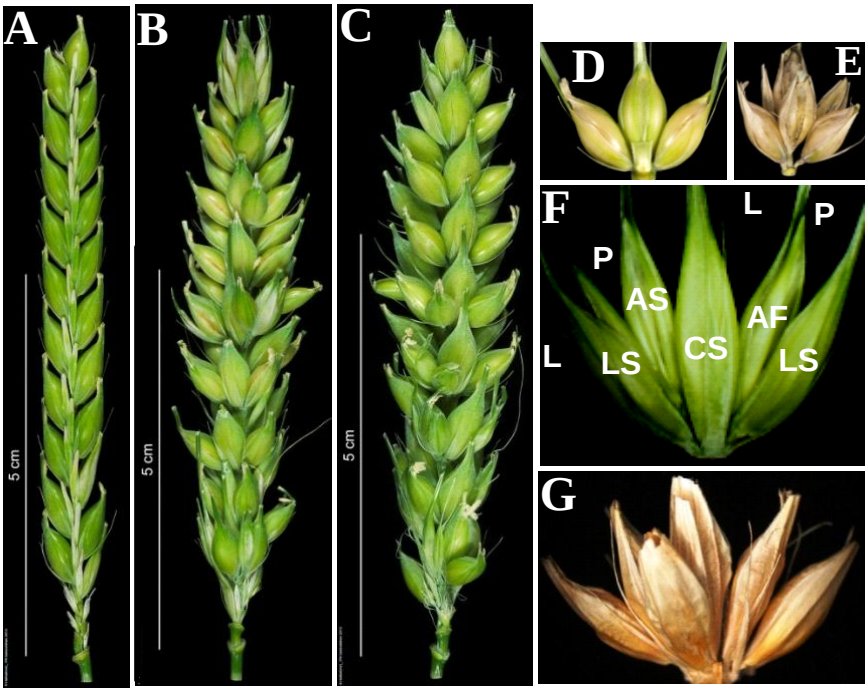

Figure 3.1.2. Spike morphology of Six-rowed spike 4 (*vrs4*) mutants.

(**A**) Two-rowed WT spike (Bowman). *vrs4* mutant spikes: (**B**) BW-NIL(*mul1.a*), (**C**) BW-NIL(*vrs4.k*): six-rowed-like appearance and formation of additional spikelets (AS) and additional florets (AF). (**D**) Spikelet triplet at one rachis internode, (**E**) BW-NIL(*vrs4.k*) and (**F**) *vrs4.l* showing AS and AF; initial triplet: CS, LS with lemma (L) and palea (P). AF developed on the rachilla of LS. (**G**) Seed formation involving AS and AF. Figures 3.1.2.F and G were kindly provided by Dr. Takao Komatsuda's group, NIAS, Japan.

Apart from these phenotypes, *vrs4* mutants also showed deviations in the lemma and glume development. In WT *Vrs4* inflorescence, each spikelet meristem (SM) produces a pair of glume primordia which later develop into inner and outer glumes. The glume developmental defects in *vrs4* mutants included occasional absence or rudimentary formation of one or both of the glumes and failure in separation of inner and outer glumes (**Figure 3.1.2-1.A**). In some cases the glumes became indeterminate with more than two per spikelet (**Figure 3.1.2-1.B**) and also the glumes were modified to produce additional spikelets/florets in some cases (**Figure 3.1.2-1.A**). Additional lemma–like structures with partially or completely developed awns were also observed in both the central and lateral spikelets/florets (**Figure 3.1.2-1.C**). In case of BW–NIL(*vrs4.k*) and BW–NIL(*mul1.a*), spikelets were pedicelled compared to sessile spikelets of their wild types (**Figure 3.1.2-1.B**). Another notable phenotype observed in BW–NIL(*vrs4.k*) and BW–NIL(*mul1.a*) was the prostrate growth of tillers compared to erect growth in wild type Bowman (**Figure 3.1.2-1.D**.)

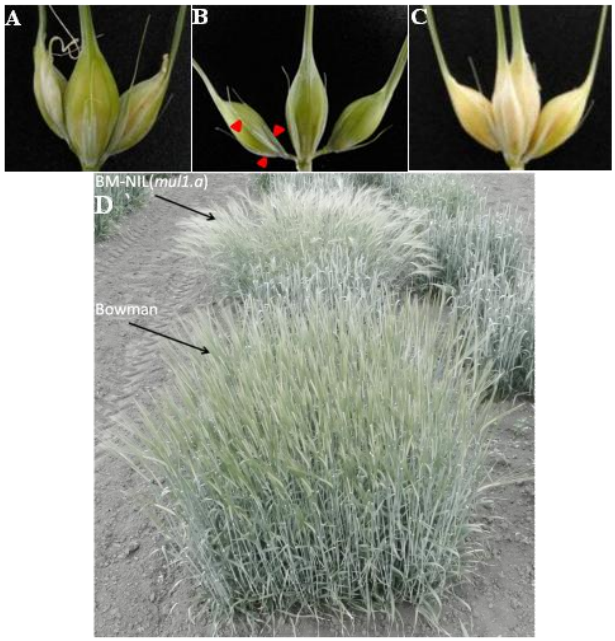

Figure 3.1.2-1. Glume, lemma and tillering defects in *vrs4* mutants.

(**A-B**) glume defects in *vrs4* mutants including conversion of glumes into additional florets, failure in separation of inner and outer glumes (**A**), formation of more than two glumes and pedicelled spikelets (**B**). (**C**) Formation of additional lemma with awn. (**D**) Prostrate tiller growth in BW-NIL(*mul1.a*) compared with Bowman.

3.1.3. Lateral spikelet fertility is completely restored in *vrs4* mutant inflorescences

Most of the *vrs4* mutants analyzed in the present study displayed yet another important and notable feature of restoration of LS fertility with a complete or partial six–rowed phenotype (**Figure 3.1.3**). All of the *vrs4* mutant alleles used in the present study were derived from their respective two–rowed progenitors with a dominant *Vrs1.b* allele at *Vrs1* which usually promotes floral abortion in LSs (**Table 2-1**). The six–rowed phenotype observed in *vrs4* mutants was analogous to that of *vrs1* mutants. Three out of the 20 *vrs4* mutant alleles in the present study did not show a six–rowed phenotype, which included *int–e.4*, *int–e.20*, and *int–e.72*. Notably the spikelets were clearly enlarged in these three *vrs4* mutants (analogous to *intermedium* barleys) compared to their progenitors indicating a probable leaky nature of the *vrs4* mutation in these

alleles. Thus, the promotion of LS fertility in *vrs4* mutants in a genotypic background having the functional form of *Vrs1.b* gave us an indication that the gene underlying *Vrs4* functions as a positive upstream transcriptional regulator of *Vrs1*.

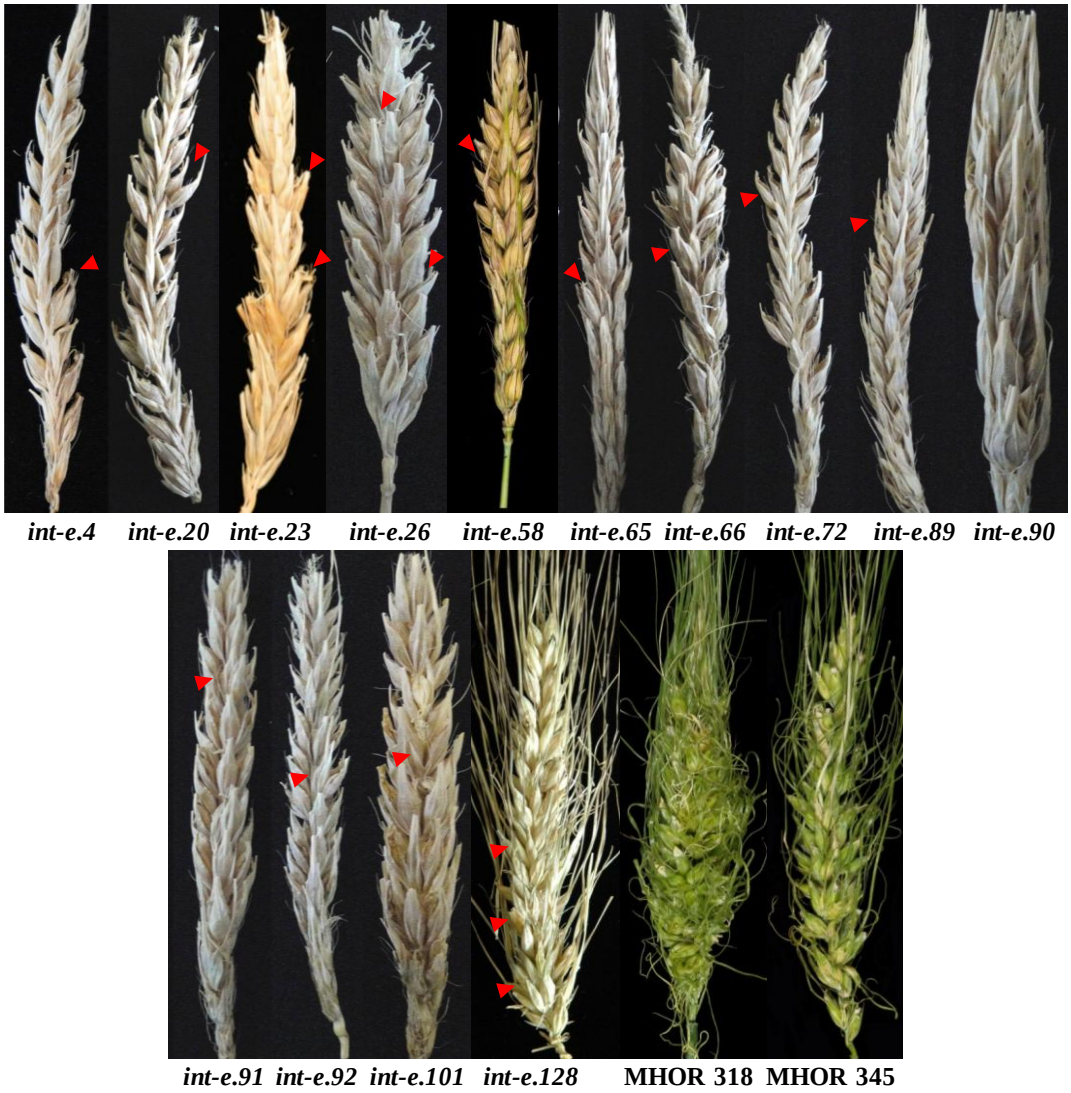

Figure 3.1.3. Spike phenotypes of *vrs4* mutant alleles.

Different *vrs4* mutant alleles showing lateral spikelet fertility and loss of spikelet determinacy (Red triangles mark the presence of additional spikelets due to the indeterminate nature of the TSM). The MHOR mutants (MHOR 318 and MHOR 345 show a high degree of indeterminacy of the TSM compared to other *vrs4* mutants. Spike images for *int-e.23* and *int-e.128* were kindly provided by Dr. Takao Komatsuda's group, NIAS, Japan.

3.2. Genetic and physical mapping of *vrs4* locus

3.2.1. Low resolution mapping in F_2 populations localizes *vrs4* to chromosome 3HS

For initial rough scale mapping the BW–NIL(*vrs4.k*) × Golden Promise and Barke × BW–NIL(*vrs4.k*) mapping populations comprising of 94 segregating (for spike row–type at *vrs4* locus) F_2 individuals (188 gametes) from each population, were phenotyped. The two populations used for mapping showed unambiguous spike phenotypes in segregating F_2 progenies and did not differ in their suitability for mapping. In each of the two mapping populations, six–rowed and two–rowed phenotypes segregated according to the expected Mendelian inheritance pattern typical for a monogenic recessive gene (3:1 segregation ratio) (**Table 3-1**), indicating that the *vrs4* phenotype is controlled by a single recessive nuclear mutation.

Table 3-1. *vrs4/Vrs4* segregation analysis in the two F_2 mapping populations.

Cross	# of F_2 individuals (gametes)	Wild-type	Mutant	$\chi 2$/P value for 3:1
BW-NIL(*vrs4.k*) × Golden Promise	94 (188)	71	23	0.014/0.905
Barke × BW-NIL(*vrs4.k*)	94 (188)	71	23	0.014/0.905

The *vrs4* locus was initially reported on chromosome 3H long arm, 27.5 cM distal to the *uzu* locus (Fukuyama et al., 1982). The recent genotyping of *vrs4* Bowman introgression lines with BOPA markers showed SNP polymorphisms spanning from 3H short arm until extreme long arm (Druka et al., 2011). BW–NIL(*int–e.58*) is shown to be associated with BOPA SNPs 1_0672 to 2_1083 (consensus map positions 38.56 to 156.06 cM), BW–NIL(*mul1.a*) with 1_0762 and 2_0115 (consensus map positions 38.56 and 126.83 cM), BW–NIL(*vrs4.k*) with 1_0863 to

1_0926 (consensus map positions 64.85 to 85.26 cM) and with 2_1493 to 1_1330 (positions 161.43 to 178.12 cM) (Franckowiak and Lundqvist, 2011).

In an effort to map *vrs4* to a particular chromosomal region on 3H, a VeraCode SNP Golden Gate genotyping assay with 113 BOPA SNPs mapping at regular intervals on 3H was developed. Of the 113 BOPA SNPs analyzed in the two mapping populations 39 and 33 SNPs were polymorphic in *vrs4.k* × Golden Promise and Barke × BW-NIL(*vrs4.k*) populations. Three and seven SNP markers displayed a distorted segregation pattern in BW-NIL(*vrs4.k*) × Golden Promise and Barke × BW-NIL(*vrs4.k*) populations respectively; hence they were not mapped in the respective populations. Mapping of 36 and 26 polymorphic markers (**Supplementary Table 1a**) with good quality segregation data in BW-NIL(*vrs4.k*) × Golden Promise and Barke × BW-NIL(*vrs4.k*) populations together with the phenotypic data localized *vrs4* locus between markers 3_0571 (32.83 cM) and 2_0276 (58.64 cM) in Barke × BW-NIL(*vrs4.k*) and between 3_0953 (40.0 cM), 1_1401 (58.01 cM) in BW-NIL(*vrs4.k*) × Golden Promise populations, indicating its presence either on the short arm or close to the centromere (**Figure 3.2.1**). Further, SNP-based CAPS markers were developed within the *vrs4* genetic interval (established based on VeraCode assay) using synteny with rice (chromosome 1) and Brachypodium (chromosome 2) as reported in barley genome zipper. Mapping of these markers within the defined *vrs4* genetic interval showed a strict co–segregation (due to lack of recombination) of *vrs4* phenotype with a cluster of tightly linked markers (Hv03717, DQ327702, Hv04360, and Hv04380) derived from the short arm of barley 3H chromosome. With this result it became clear that *vrs4* is localized on the short arm of chromosome 3H in between 37.17 cM and 41.68 cM (based on marker positions in barley 3H genome zipper).

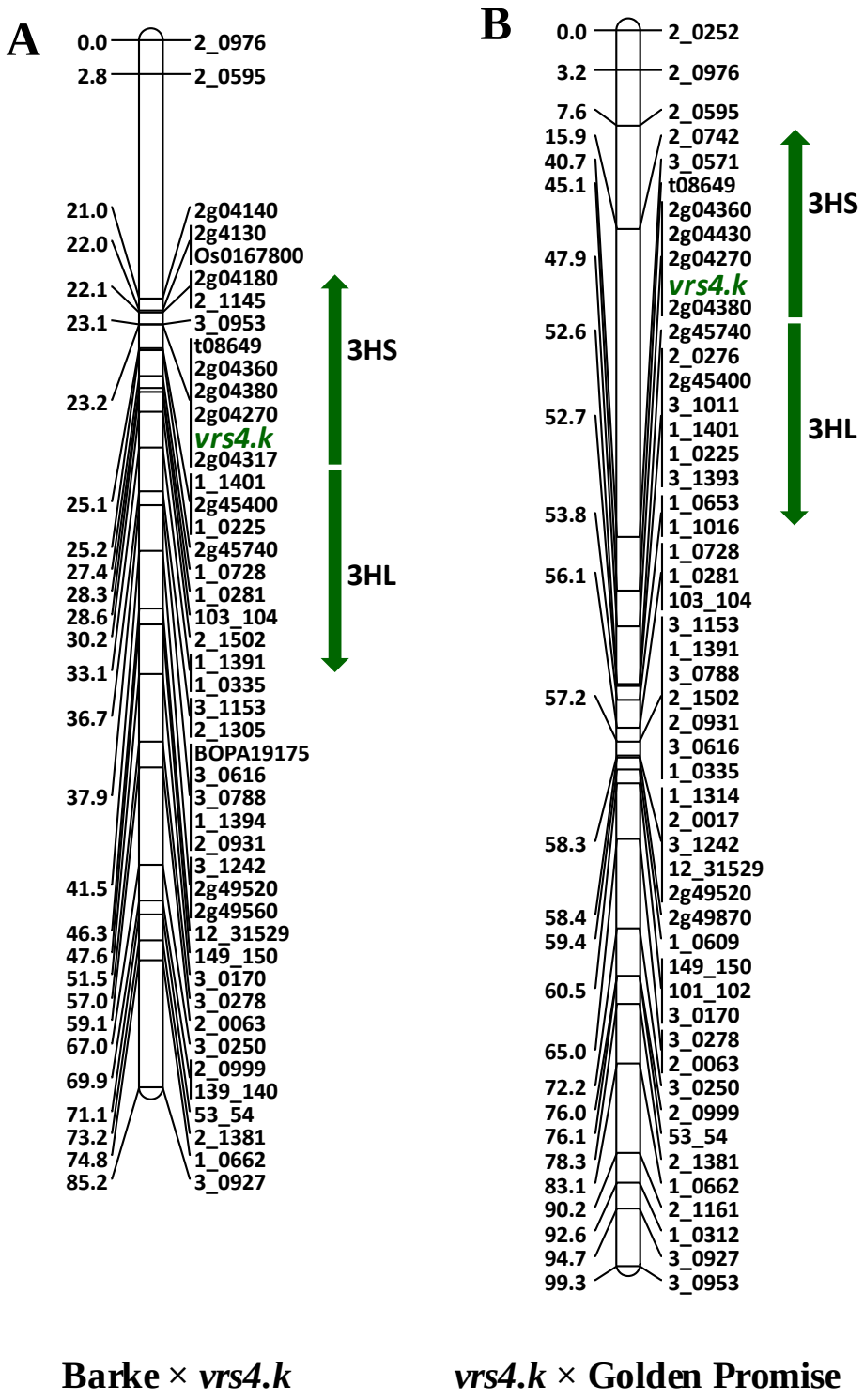

Figure 3.2.1. Linkage maps for the *vrs4* locus on barley chromosome 3H.

(**A, B**) Linkage maps were developed based on two F_2 mapping populations. Upward and down ward arrows indicate the short arm and long arm of chromosome 3H. Map distances are shown in centiMorgans (cM). Scale: 1cM = 2.7 mm.

3.2.2. High resolution and fine scale mapping of *vrs4* locus on 3HS

After localizing the *vrs4* locus on 3HS, the high resolution mapping in the *vrs4* interval was conducted by analyzing a segregating progeny equivalent to 2000 gametes (1000 F_2 individuals) from BW–NIL(*vrs4.k*) × Golden Promise mapping population. By screening two linked CAPS markers Hv03717 and Hv45470 (**Supplementary Table 1a**) within the previously established *vrs4* interval (separated by 7.5 cM genetic interval), 140 recombinant individuals were identified with in this region [(71 recombinants had mutant, heterozygous allele constellation (allele scores A (mutant) with one marker, H (heterozygote) with the other, whereas 66 recombinants had wild type, heterozygous allele constellations (allele scores B (wild type) with one marker, H (heterozygote) with the other), and the remaining three recombinants had mutant, wild type allele constellations (allele scores A, B) at Hv03717 and Hv45470)]. The higher number of recombinants identified in this region indicated it as highly recombinogenic despite its proximity to the centromere. By further marker development in this region, the *vrs4* interval was narrowed down to 0.8 cM between closely linked flanking markers DQ327702 (no recombination with *vrs4* phenotype) and Hv4360 (two recombinants) (**Figure 3.2.3.C**). A comparison of gene colinearity (micro synteny) between barley, *Brachypodium*, and rice revealed highly conserved gene colinearity among these three grass species within the *vrs4* genomic region (**Figure 3.2.3.A, B, and C**.)

3.2.3. Establishment of barley physical BAC contig around *vrs4* locus

To establish a physical BAC contig across the *vrs4* locus, the two closely linked markers DQ327702 and Hv4360 were screened in the Morex BAC library with a 25 fold genome representation, developed at IPK, Gatersleben (Schulte et al., 2011). The two flanking markers

were localized to a 1073 kb BAC contig, which was sequenced using a MTP containing 22 BAC clones. Analysis of the corresponding sequence data in Genescan web server (based on maize protein sequences) resulted in six potential protein coding ORFs. Annotation of these ORFs by BLASTx analysis revealed six protein coding genes that included *RAMOSA2* (*HvRA2*), *RESURRECTION1* (*RST1*), *TRYPTOPHAN AMINO TRANSFERASE* (*TPA*), *EMBRYO SAC/BASAL ENDOSPERM TRANSFER LAYER/EMBRYO SURROUNDING REGION* (*EBE*), *STACHYOSE SYNTHASE*, and *RECEPTOR LIKE PROTEIN KINASE* (*INRPK1*) (**Figure 3.2.3.D**). A marker derived from the gene *TPA* (Hv04290) further narrowed down the candidate *vrs4* genomic region to zero recombinants between DQ327702 (*HvRA2*) and Hv04290 (**Figure 3.2.2.D**) indicating either of these two as the candidate genes for *vrs4*.

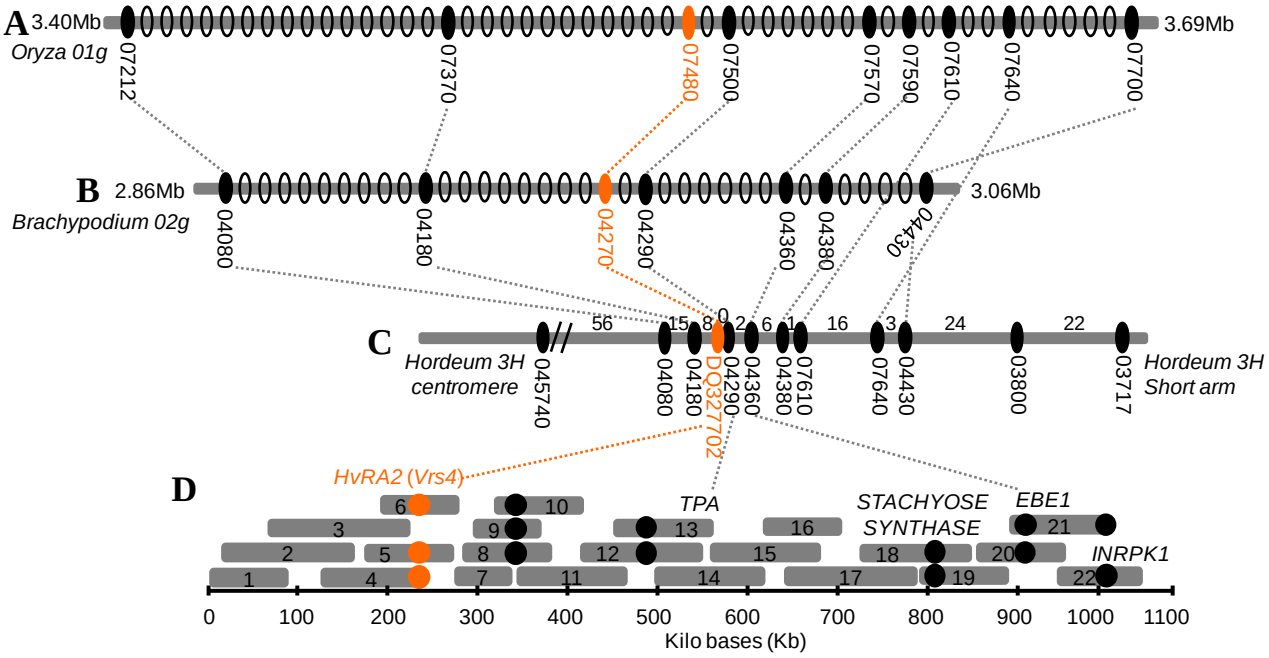

Figure 3.2.3. High resolution linkage and physical map of *vrs4*.

Rice (**A**) and *Brachypodium* (**B**) chromosomal regions syntenic with barley chromosome 3H (**C**) in the *vrs4* region. Predicted genes in rice, *Brachypodium* and barley chromosomes are indicated by ovals [(Gene names start with *Os01g* (rice) or *Bradi2g* (*Brachypodium*) followed by five digit number)]. Solid black ovals mark the genes from which markers were derived for mapping in the *vrs4* region. Numbers of

recombinants are indicated between mapped markers on the barley chromosome. (**D**) Single BAC contig sequenced in the *vrs4* region (22 overlapping BAC clones covering 1,073 kb) (see **Table 2-2** for corresponding BAC names). Predicted genes identified from the BAC sequences are indicated as circles.

3.3. Identification of candidate gene responsible for *vrs4* phenotype and its validation

3.3.1. *Vrs4* underlies a barley ortholog of maize inflorescence architecture gene *RAMOSA2* (*HvRA2*)

Among the two potential candidates *HvRA2* and *TPA*, *HvRA2* appeared to be a more convincing candidate gene for *vrs4* because the function of the orthologous maize *RA2* had already been implicated in maize inflorescence development. In maize, mutants of *RA2* produce inflorescence branches (both tassel and cob) with increased indeterminacy or meristematic potential (Bortiri et al., 2006). The barley, *vrs4* mutants similarly display a highly disorganized spikelet development due to the indeterminate nature of TSM with increased meristematic activity. The analogy in the inflorescence development pattern between the maize *ra2* mutants and barley *vrs4* mutants prompted to resequence *HvRA2* in the *vrs4* mutants. Subsequently re-sequencing of *HvRA2* in the BW–NIL(*vrs4.k*), its progenitor MFB 104 and isogenic Bowman resulted in a unique single nucleotide deletion that caused a frame shift within the ORF of *HvRA2*. The frame shift resulted in a premature stop codon quite early in the ORF (Amino acid 68 of 257). This re-sequencing result convinced that the *vrs4* phenotype underlies *HvRA2*.

3.3.2. Validation of *HvRA2* gene candidate in allelic *vrs4* mutants by re-sequencing

Because all *vrs4* mutants in the present study showed loss of TSM determinacy with enhanced meristematic activity in general (**Figure 3.1.3**), *HvRA2* gene was sequenced in 19 other *vrs4* mutants available from different sources (**Table 2-1**). In line with the initial sequencing result obtained from BW–NIL(*vrs4.k*), 17 out of the 19 *vrs4* mutants showed molecular lesions that are

directly located to *HvRA2* ORF (**Figure 3.3.2a** and **3.3.2b**). In barley generally three spikelet meristems develop at each rachis internode giving rise to three spikelets. However, in *vrs4 mutants* the number of spikelet/floral meristems is partially unrestricted, two additional spikelet/floral meristems develop in pairs near the base and on opposite sides of the previous meristems, giving a bud number series of 1, 3, 7, and possibly 15 (Forster et al., 2007). From the mutant re-sequencing and phenotyping analyses, it was clearly evident that irrespective of the type of lesion in various mutant alleles of *vrs4*, all of them showed indeterminacy of the TSM to a certain degree giving rise to additional spikelets/florets (**Figures 3.1.1, 3.1.2,** and **3.1.3**). The molecular nature of the lesions in mutants clearly correlated with the severity of *vrs4* phenotype. Five mutants with the strongest *vrs4* phenotype (increased indeterminacy of TSM, and complete lateral spikelet development) had either a premature stop codon [BW–NIL(*vrs4.k*), BW–NIL(*mul1.a*), *vrs4.l* (*syn*. *Xc 41.5*), *int–e.26* and *int–e.128* (*syn. hex–v.48*)] or a putative gene deletion (**Figures 3.1.1, 3.1.2,** and **3.1.3, Table 3-2**). Weaker alleles with a less severe phenotype, (moderate indeterminacy of TSM, slightly enlarged lateral spikelets) possessed amino acid (AA) substitutions either within the DNA binding domain (*int–e.23,* BW–NIL(*int–e.58*), *int–e.72*) or in other conserved regions (see the following section) of the protein indicating the leaky nature of the *RA2* mutation in these alleles (*int–e.65, int–e.66, int–e.87, int–e.89, int–e.90, int–e.91, int–e.92, int–e.101*) (**Figure 3.1.3**, and **3.3.2a**). The two *vrs4* mutants *int–e.4* and *int–e.20* did not show any molecular lesions, suggesting possible transcriptional or post–transcriptional regulation in these alleles (**Table 3-2**). The two *vrs4* mutant alleles *int–e.4* and *int–e.20*, which did not harbor any lesion, have been tested previously for their allelism with *vrs4* by Dr. Udda Lundqvist and confirmed that they are allelic (**Supplementary Text**). Thus the collection of 18 ORF mutants strongly indicated that *HvRA2* underlies the *Vrs4* locus.

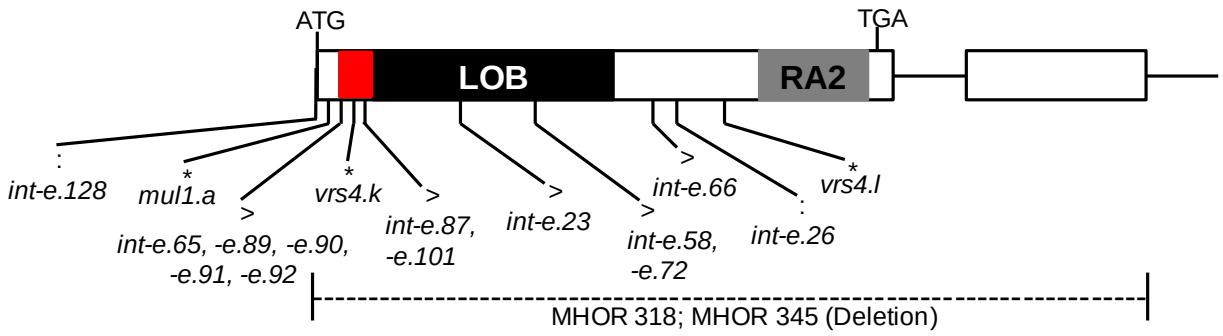

Figure 3.3.2a. *HvRA2* gene model localized with lesions in *vrs4* mutant alleles.

Lesions in 18 ORF-mutant alleles are indicated below the gene structure. LOB domain is represented with a black box, the grass specific domains at 5' and 3' regions of the ORF are indicated by red and grey boxes respectively. ':' Nucleotide substitution leading to premature stop codon, '*' INDELS leading to frame shift, '>' non-synonymous SNP in the coding region. ATG and TGA represent start and stop codons. The bar between the two exons represents intronic sequence within the 3'UTR. *HvRA2* resequencing data for *int-e.23*, *int-e.128*, and *vrs4.l* was kindly provided by Dr. Takao Komatsuda's group, NIAS, Japan.

```
     G                                                          -- ---   (int-e.128-SNP-Nonsense mutation)
1    ATG GCA TCC CCG TCG AGC ACC GGC AAC TCC ATC GTC TCC GTG GTG GTT   48
1     M   A   S   P   S   S   T   G   N   S   I   V   S   V   V   V    16
                                                                      (mul1.a-11bp deletion-Nonsense mutation)
                                                                      (int-e.65, .89, .90, .91, .92- Missense)
                                                                      (vrs4.k-1bp deletion-Nonsense mutation)
     --- ---                   A   -   A                            (int-e.87/int-e.101-Missense mutation)
49   GCA GCG GCC ACG ACA CCG GGG GCC GGG GCG CCG TGC GCT GCG TGC AAG   96
17    A   A   A   T   T   P   G   A   G   A   P   C   A   A   C   K    32
                             E       E

97   TTC CTG CGG CGC AAG TGC CTC CCC GGC TGC GTG TTC GCG CCC TAC TTC   144
33    F   L   R   R   K   C   L   P   G   C   V   F   A   P   Y   F    48

145  CCG CCG GAG GAG CCG CAG AAG TTC GCC AAC GTG CAC AAG GTG TTC GGC   192
49    P   P   E   E   P   Q   K   F   A   N   V   H   K   V   F   G    64

      T                                                               (int-e.23-SNP-Missense mutation)
193  GCC AGC AAC GTG ACC AAG CTG CTC AAC GAG CTG CCG CCG CAC CAG CGG   240
65    A   S   N   V   T   K   L   L   N   E   L   P   P   H   Q   R    80
      V
                T                                                     (int-e.58/int.e-72-SNP-Missense mutation)
241  GAA GAC GCC GTG AGC TCG CTG GCC TAC GAG GCG GAG GCG CGG GTC AAG   288
81    E   D   A   V   S   S   L   A   Y   E   A   E   A   R   V   K    96
                V
289  GAC CCC GTC TAC GGC TGC GTC GGC GCC ATC TCC GTG CTC CAG CGC CAG   336
97    D   P   V   Y   G   C   V   G   A   I   S   V   L   Q   R   Q    112

337  GTC CAC CGC CTC CAG AAG GAG CTC GAC GCC GCG CAC ACC GAG CTC CTC   384
      V   H   R   L   Q   K   E   L   D   A   A   H   T   E   L   L    128

                                                            T         (int-e.66-SNP-Missense mutation)
385  CGG TAC GCC TGC GGC GAG CTC GGC AGC ATC CCC ACC GCG CTC CCC GTT   432
129   R   Y   A   C   G   E   L   G   S   I   P   T   A   L   P   V    144
                                                            L
433  GTC ACG GCC GGC GTC CCC AGC GGC AGG CTC TCA TCC GCC GTA ATG CCC   480
145   V   T   A   G   V   P   S   G   R   L   S   S   A   V   M   P    160

                T                                               -     (int-e.26-SNP-Nonsense mutation)
481  TGC CCC GGC CAG CTC GCC GGC GGC ATG TAC AGC GGT GGC GGT GGC GGT   528
161   C   P   G   Q   L   A   G   G   M   Y   S   G   G   G   G   G    176

     --- --- --- --- --- ---                                          (vrs4.1-19bp deletion-Nonsence mutation)
529  GGC TTC CGG AGG CTC GGG CTT GTG GAC GCG ATA GTA CCA CAG CCC CCT   576
177   G   F   R   R   L   G   L   V   D   A   I   V   P   Q   P   P    192

577  CTT TCC GCC GGC TGC TAC TAC AAT ATG CGG AGC AAC AAC AAC GCT GGA   624
193   L   S   A   G   C   Y   Y   N   M   R   S   N   N   N   A   G    208

625  GGC AGC GTC GCT GCC GAC GTG GCG CCC GTT CAG ATC CCC TAC GCC TCC   672
209   G   S   V   A   A   D   V   A   P   V   Q   I   P   Y   A   S    224

673  ATG GCG AAT TGG GCC GTG AAC GCC ATT AGC ACC ATT ACC ACC ACC TCA   720
225   M   A   N   W   A   V   N   A   I   S   T   I   T   T   T   S    240

721  GGA TCA GAG AGC ATT GGG ATG GAT CAC AAG GAA GGA GGC GAC AGC AGC   768
241   G   S   E   S   I   G   M   D   H   K   E   G   G   D   S   S    256

769  ATG TGA ACTGACGCGCCCAACCAACAgtgagtggcccgtttgagtaaatcgttgcactgta   829
257   M   *
830  atcatgcgtgtatatatgctagcttcatgagttatctaatgctgcattcttgccttgtgcag   891
892  TGAATGTGGATTACCTCTCCTACTCTCAAGATTTATGGATGTGGAGAATGATATGCGCTTTGG   954
955  CCGGCCTTGACGCTCAAGGAAGGAAGCTTCGGGGAGACTGATGGGATCGAGCTAGCTCATTCC  1017
1018 CAGGATAATTAAGCTAAGAAGCAATCTATCTATGAATCTATCTATATATAGCCAACATGAATT  1080
1081 ATATATGTCAGTGTCTCCCTTTTTGCATGTTGTGCAAGCCATACTTTGTGTCGACTTTGGAGT  1143
1144 TCTATATGTAATCGAATCGAGATCTAGCTTGATCTCTCTTCTTT                     1187
```

Figure 3.3.2b. *HvRA2* (*Vrs4*) nucleotide and protein sequences showing mutated positions in sixteen *Vrs4* mutant alleles. Small deletions and SNPs in the *vrs4* mutant alleles leading to frame shifts, non-synonymous changes and premature stop codons have been indicated in respective colors with that of mutant alleles. The sequence in the boxed area represents the LOB domain. The blue highlighted sequence at the 3' end marks the 3'-UTR, the underlined region within the 3'-UTR indicates the intron.

Table 3-2. *vrs4* mutant alleles with type of molecular lesion in *HvRA2* and their position within ORF.

#	Mutant allele	Type of mutation	Polymorphism/Position*
1	*int-e.4*	No mutation	—
2	*int-e.20*	No mutation	—
3	*int-e.23*	Mis-sense	Transition (C to T) 194bp
4	*int-e.26*	Non-sense	Transition (C to T)/490bp
5	BW-NIL(*int-e.58*)	Mis-sense	Transition (C to T) 248bp
6	*int-e.65*	Mis-sense	Transition (G to A)/68bp
7	*int-e.66*	Mis-sense	Transition (C to T)/428bp
8	*int-e.72*	Mis-sense	Transition (C to T) 248bp
9	*int-e.87*	Mis-sense	Transition (G to A)/74bp
10	*int-e.89*	Mis-sense	Transition (G to A)/68bp
11	*int-e.90*	Mis-sense	Transition (G to A)/68bp
12	*int-e.91*	Mis-sense	Transition (G to A)/68bp
13	*int-e.92*	Mis-sense	Transition (G to A)/68bp
14	*int-e.101*	Mis-sense	Transition (G to A)/74bp
15	*int-e.128*	Non-sense	Transition (A to G)/1bp
16	BW-NIL(*vrs4.k*)	Non-sense	Deletion (1bp)/72-72bp
17	BW-NIL (*mul1.a*)	Non-sense	Deletion (11bp)/44-54bp
18	*vrs4.l* (*syn. Xc 41.5*)	Non-sense	Deletion (14bp)/528-546bp
19	MHOR318	Gene deletion	—
20	MHOR345	Gene deletion	—

*Nucleotide positions of lesions in different *vrs4* mutant alleles with respect to reference sequence of *HvRA2*. GenBank accession number for *HvRA2* reference sequence is KC854554.

3.3.3. Validation of *HvRA2* gene candidate by qRT–PCR

To test whether the molecular lesions observed in *vrs4* mutant alleles affected the regulation of mRNA transcript levels in *HvRA2*, the *HvRA2* expression in *vrs4* mutants and the respective wild types was quantified. The relative quantification analysis in BW–NIL(*vrs4.k*) (lesion – INDEL causing a pre–mature stop codon), MHOR 318 (lesion – complete gene deletion), MHOR 345 (lesion – complete gene deletion) and their respective wild type progenitors MFB104, AD, HH at various spike developmental stages (TM, GP, LP, SP, and AP) showed a clear down-regulation of *HvRA2* transcripts in all of the *vrs4* mutants analyzed. As expected the expression of *HvRA2*

in the two deletion mutants MHOR 318 and MHOR 345 could not be detected because the complete gene is deleted in these two mutants (**Figure 3.3.3**.)

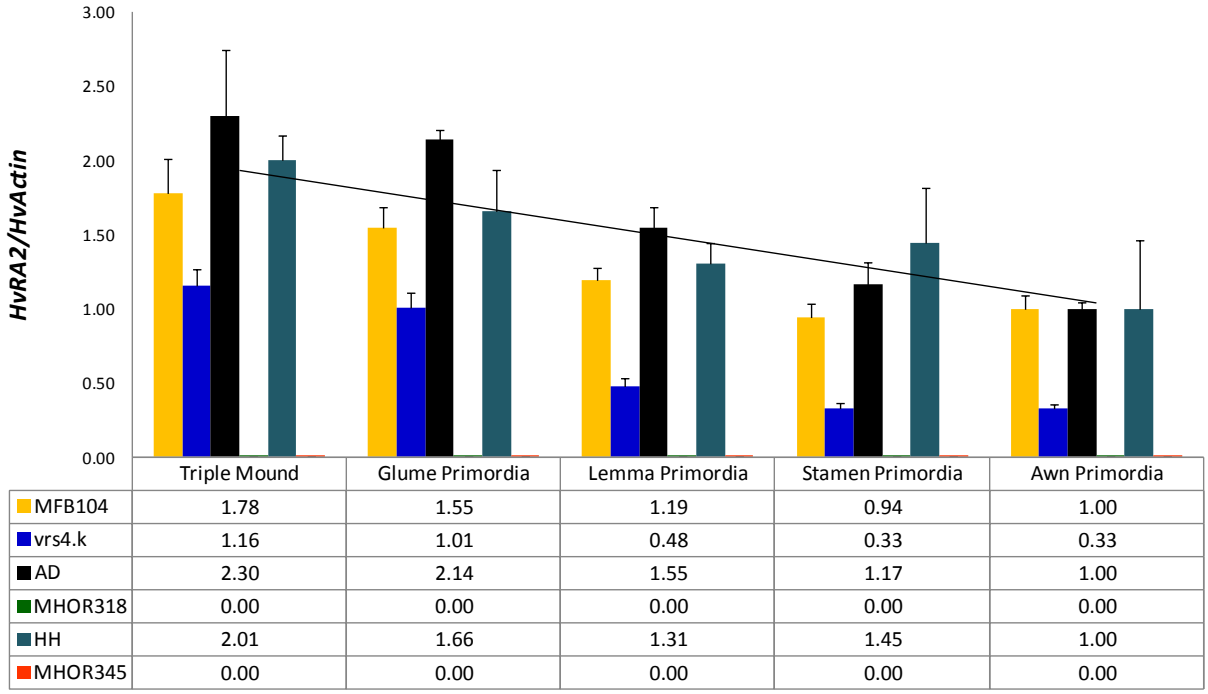

Figure 3.3.3. Relative expression of *HvRA2* in BW-NIL(*vrs4.k*), MHOR 318 and MHOR 345 compared to their progenitors. Values in the table below the graph indicate expression of *HvRA2* in wild-types and respective *vrs4* mutants. Error bars indicate mean±S.E. of three replicates. Trend line depicts the relative expression at different stages of immature spike development.

3.3.4. *HvRA2* encodes a LOB domain transcription factor with grass specific domains

The genes encoding LOB domain proteins are specifically found in plants and are expressed at the boundaries of lateral organs during vegetative and reproductive plant development (Shuai et al., 2002). The LOB domain proteins function as TFs (Shuai et al., 2002; Husbands et al., 2007)**.** The BLASTp analysis against non-redunt protein sequence database of NCBI, showed HvRA2 as a class I LOB domain protein. LOB domain proteins typically possess three important features, which include a cysteine–rich repeat (CX2CX6CX3C), a highly conserved GAS residue

block, and a Leucine–zipper coiled–coil motif (LX6LX3LX6L) (**Figure 3.3.4**), the signature features conserved in HvRA2 and all other class I LOB domain proteins (Shuai et al., 2002). Apart from the canonical LOB domain, HvRA2 and its orthologs from various grass species (monocots) posses a unique C–terminal putative activation domain (44AA) that is not present in *Arabidopsis* and other eudicots (Bortiri et al., 2006) (**Figure 3.3.2a** and **3.3.4**). However, in the current study apart from the unique C–terminal domain, another important and conserved grass specific N–terminal region was identified based on multiple sequence alignments generated from orthologous/homologous RA2 proteins from a range of monocot and dicot species. The novel N–terminal domain identified is of 16AA long preceding the LOB domain (**Figure 3.3.2a** and **3.3.4**). The last four AA of the N–terminal domain (PGAG) are strictly conserved across the RA2 orthologs from different monocot species analyzed (**Figure 3.3.4**). Interestingly, seven of the *vrs4* mutant alleles possessed AA substitutions in the last four AA of the conserved N–terminal region (*int–e.65*, *int–e.87*, *int–e.89*, *int–e.90*, *int–e.91*, *int–e.92*, and *int–e.101*). These seven *vrs4* mutants carrying AA substitutions in the conserved N–terminal region showed indeterminate TSM and six–rowed phenotype (**Figure 3.1.3**). The data from these analyses signifies the putative functional role of this novel N–terminal region, which might be an activation domain similar to the C–terminal activation domain found in grass species.

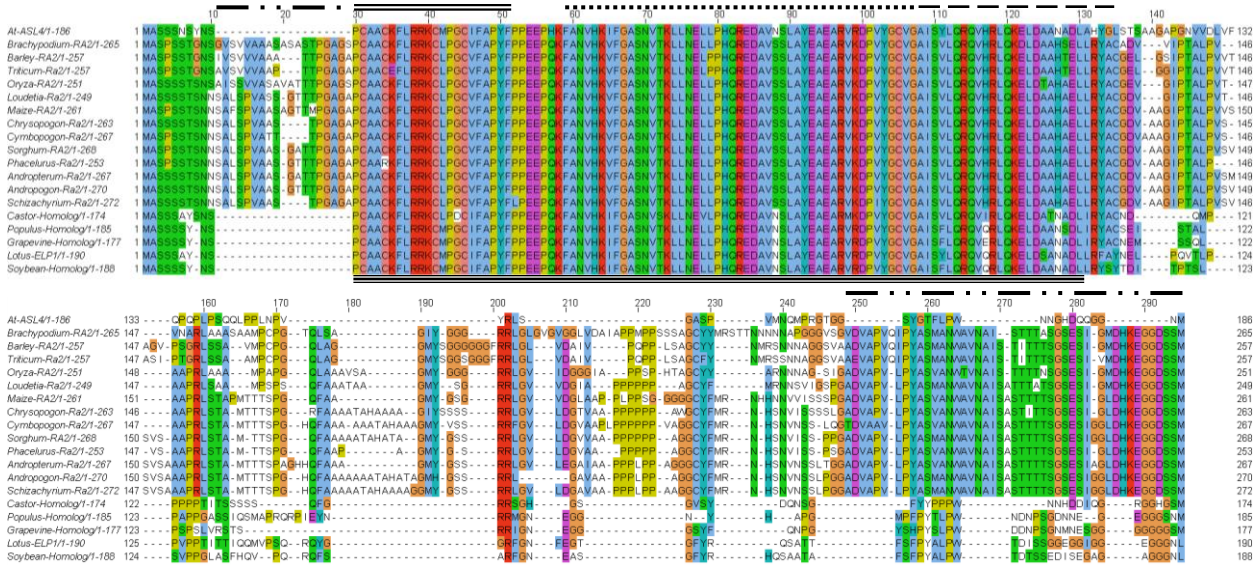

Figure 3.3.4. RA2 and RA2-like proteins in grasses and eudicots.

Multiple sequence alignment of RA2 proteins in monocotyledonous and dicotyledonous species. The unique grass specific domains at N-terminal and C-terminal are indicated with a combination of dashed and dotted lines; LOB domain is marked with a triple line (The components of LOB domain such as Cysteine rich region, GAS block and Leucine Zipper coiled coil motif are marked with double, dotted and dashed lines respectively. GenBank accession numbers for RA2 & RA2-like proteins are given in **Supplementary Table 2**.

3.4. Phylogenetic analysis of RAMOSA2 orthologs/homologs from grasses and eudicots groups them into two distinct and respective clades

RAMOSA2 orthologs posses the conserved N– and C– terminal regions, which make them unique to monocot species. A true ortholog of RA2 is not present in the eudicot species (Bortiri et al., 2006). With the aim of revealing the phylogenetic relationships among the orthologs of RA2 from various grass species and their relationship with RA2-LIKE proteins from eudicot species, phylogenetic analysis was conducted with available RAMOSA2 orthologs from grass species and RA2-LIKE proteins from eudicot species. Sixty seven class I LOB domain (LBD) protein sequences (monocot and dicot proteins) were extracted from NCBI using BLASTp (e–value cut-off: 10^{-30}). LOB domain (LBD) encoding barley genes were extracted from the IPK barley

BLAST server (26 calss I and four class II proteins). For the analysis 17 full length barley protein (13 class I and four class II) were included (**Table 3-3**). A maximum likelihood phylogenetic tree generated based on these 84 LBD proteins grouped them into three distinct phylogenetic clades that include, (i) clade I – containing RA2 orthologs from different grass species (16 proteins) and RA2–LIKE sequences (RA2 homologs) from eudicot species (32 proteins), (ii) clade II containing LBD proteins that are different from RA2/RA2–LIKE proteins (32 proteins), and (iii) clade III containing class II LBD proteins from barley (4 proteins) (**Figure 3.4.0**).

The clade I carrying the RA2 orthologs/homologs clearly separated the RA2 orthologs and homologs into monocot and eudicot sub-clades. Within the monocot sub-clade, distinct groups and branches at the level of grass subfamilies and tribes could be recognized (**Figure 3.4.0**). For example the RA2 orthologs from different wheat species and the barley RA2 (tribe Triticeae) grouped together. The RA2 orthologs from nine different species from tribe Andropogoneae clustered together (**Figure 3.4.0**) indicating tribe specific sequence signatures within these orthologs. The grouping of RA2 orthologs clearly reflected the evolutionary history of grasses (Gaut, 2002). The conserved N– and C–terminal regions in grasses, which are unique to monocot species, would have been lost during evolution of eudicots, indicating that a different mechanism might be responsible to regulate inflorescence branching in eudicots. The mutant of the closest *Arabidopsis* homolog of RA2, *ASSYMETRIC LEAVES–2 LIKE4* (BAH10548.1) does not show a detectable alteration in inflorescence structure (Shuai et al., 2002). Another close homolog from legume species is *ELONGATED PETIOLULE1* (AFK81066.1, AFK81064.1, AFK81063.1, and AFK81065.1), which regulates the leaf motor organ (pulvinus) responsible for nastic leaf movements (Chen et al., 2012).

The second phylogenetic clade (clade II) consisted of LBD proteins that are distantly related to RA2/RA2–LIKE sequences which included LBD PROTEIN1–LIKE (Ctg135924_5HL and Ctg62778_4HL), LBD PROTEIN6–LIKE (XP_004152887.1, XP_003545810.1, Ctg61827_3HL, Ctg45166_1H, Ctg51474_4HS), LBD7–LIKE (Ctg98873_3HL), LBD PROTEIN11–LIKE (Ctg54974_1H), LBD PROTEIN16–LIKE (Ctg46032_6HL), LBD PROTEIN24 (Ctg47723_4HL), LBD PROTEIN36 (XP_004148465.1), LBD PROTEIN38 (Ctg36895), LBD PROTEIN39 (Ctg1561909), and LBD PROTEIN41 (Ctg42541_2HL and Ctg50476_4HL). These proteins are involved in various organ developmental processes like leaf formation (Ori et al., 2000; Semiarti et al., 2001), root formation, auxin response (Okushima et al., 2007; Okushima et al., 2005), and flower development (Chalfun et al., 2005). The clade III, which contained class II LOB domain proteins, formed into an out group. The out grouping of these proteins is because the class II LOB domain proteins significantly differ from class I proteins in the cysteine-rich region of the LOB domain (9–13 Cysteine residues in class II proteins against to four–seven in class I). Apart from this, the leucine zipper coiled coil motif is completely absent in all class II LBD proteins (Shuai et al., 2002). The class II LBD proteins are reported to be involved in plant metabolism (Scheible et al., 2004; Rubin et al., 2009; Albinsky et al., 2010.)

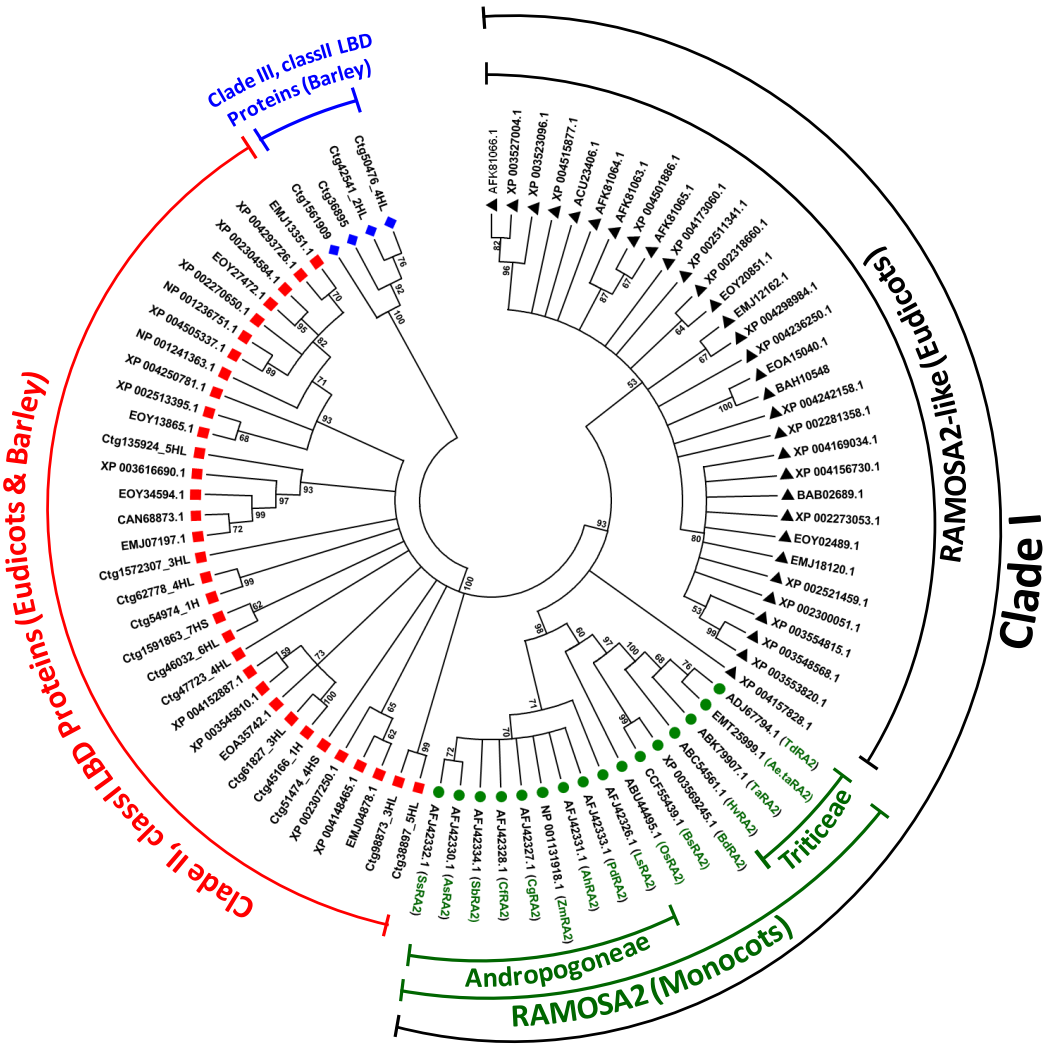

Figure 3.4.0. Phylogenetic analysis of RAMOSA2 orthologs/homologs and other LBD proteins.

A maximum likelihood based condensed phylogenetic tree of RAMOSA2 orthologs (RAMOSA2 proteins from grasses) and homologs (RA2-LIKE proteins from eudicot species) together with other LBD proteins from barley and eudicots. From the phylogenetic tree three separate clades are evident; clade I carrying RAMOSA2 orthologs and homologs, clade II carrying the LBD proteins other than RAMOSA2 orthologs/homologs (red squares), and clade III carrying barley class II LBD proteins (blue squares). The clade I carrying RAMOSA2 orthologs/homologs has two sub clades, one with the RAMOSA2 orthologs from grasses (green circles) and the other with RAMOSA2 homologs from eudicots (black triangles). Td: *Triticum durum*; Ae.ta: *Aegilops tauschi*; Ta: *Triticum aestivum*; Hv: *Hordeum vulgare*; Bd: *Brachypodium distachyon*; Bs: *Brachypodium sylvaticum*; Os: *Oryza sativa*; Ls: *Loudetia spp.*; Pd: *Phacelurus digitatus*; Ah: *Andropogon hallii*; Zm: *Zea mays*; Cg: *Chrysopogon gryllus*; Cf: *Cymbopogon flexosus*; Sb: *Sorghum bicolor*; As: *Andropterum stolzii*; Ss: *Schizachyrium sanguineum*. (Please refer to **Supplementary Table 2** for the details of remaining protein accessions used in phylogenetic analysis).

3.4.1. *HvRA2* is unique among the barley LBD gene family members

A BLASTN analysis using nucleotide sequence encoding the LOB domain of *HvRA2* against Morex contigs (50X survey sequences) and high confidence genes in barley viroBLAST web server resulted in 29 other LBD encoding genes apart from HvRA2 indicating it as a relatively large gene family (30 members) in barley (**Table 3-3**). In *Arabidopsis*, 43 LBD gene family members have been reported (Shuai et al., 2002) and in monocot species like rice and maize 35 and 43 members have been reported, respectively (Yang et al., 2006; Schnable et al., 2009). Of the 30 genes identified in barley 24 genes were full length and six were partially available. A careful comparison of HvRA2 protein sequence against the remaining 29 LBD gene family members revealed that HvRA2 is unique with its putative functional N– and C–terminal domains, whereby none of the 29 other members shared identity in these two regions (Data not shown). The phylogenetic analysis of LBD gene family members grouped HvRA2 (ABC54561.1/ Ctg2547112_3HS) in the sub-clade carrying RA2 orthologs from grasses (clade I). The remaining LBD gene family members were grouped into a different clade carrying LBD proteins that are different from RA2/RA2–LIKE proteins (clade II) (**Figure 3.4.0**). These results clearly suggest that HvRA2 has a unique function in regulating inflorescence branch architecture, which may not be accomplished by any of the other barley LBD gene family members.

Table 3-3. List of barley LOB domain (LBD) encoding genes.

LBD gene contig	LBD Class	Partial/Complete	FLcDNA ID
Ctg2547112_3HS	Class I	Complete	-
Ctg45166_1H	Class I	Complete	MLOC_61156.1
Ctg51474_4HS	Class I	Complete	MLOC_66372.1
Ctg135924_5HL	Class I	Complete	MLOC_5148.1
Ctg54974_1H	Class I	Complete	MLOC_68570.1
Ctg46032_6HL	Class I	Complete	AK368515
Ctg1572307_3HL	Class I	Complete	MLOC_16076.3
Ctg62778_4HL	Class I	Complete	MLOC_73009.1
Ctg47723_4HL	Class I	Complete	-
Ctg1591863_7HS	Class I	Complete	MLOC_20803.1
Ctg38897_5HL	Class I	Complete	-
Ctg61827_3HL	Class I	Complete	AK373607
Ctg98873_3HL	Class I	Complete	MLOC_81908.1
Ctg42541_2HL	Class II	Complete	-
Ctg50476_4HL	Class II	Complete	AK373051
Ctg1561909	Class II	Complete	-
Ctg36895	Class II	Complete	MLOC_51325.1
Ctg39781_4HL	Class I	Partial	-
Ctg63283_3HL	Class I	Partial	-
Ctg1559770_4HL	Class I	Partial	-
Ctg39524_1H	Class I	Partial	-
Ctg41408_4HS	Class I	Partial	-
Ctg40527_1H	Class I	Partial	-
-	-	Complete	MLOC_57082.1
-	-	Complete	MLOC_54949.1
-	-	Complete	MLOC_56075.1
-	-	Complete	MLOC_10784.1
-	-	Complete	MLOC_10783.1
-	-	Complete	AK373051
-	-	Complete	MLOC_78342.2

Note: Contig IDs represent morex contigs from survey sequencing, corresponding FLcDNA is indicated when ever is present.

3.5. Re-sequencing of *HvRA2* shows reduced nucleotide diversity

The already characterized row–type genes *Vrs1* and *Int–c* posses row–type specific alleles in two–rowed (*Vrs1.b*, *int–c*) and six–rowed barleys (*vrs1.a*, *Int–c*) (Komatsuda et al., 2007; Ramsay et al., 2011). In an attempt to identify row–type specific alleles at *Vrs4* locus in natural variation, nucleotide sequence analysis of the *HvRA2* ORF and parts of the 5' and 3' regulatory regions (promoter, UTRs) in a set of 77 diverse two–rowed and six–rowed barley genotypes was conducted (**Table 3-4**). Interestingly, the nucleotide diversity observed in these 77 accessions was quite limited. Unlike *Vrs1* and *Int–c*, which showed row–type specific alleles in natural variation, *Vrs4* appeared to be conserved across diverse two–rowed and six–rowed germplasm revealing very low natural nucleotide variation in the coding region (**Figure 3.5.0.A**). Haplotype analysis of the nucleotide sequence data resulted in one major and seven minor nucleotide haplotypes derived from the major haplotype (**Figure 3.5.0.B**). GenBank accession numbers for the eight haplotypes are from KC854546 to KC854553. The present set of accessions used in this study did not show sequence haplotypes that are specific to a particular geographic region, all haplotypes contained both two–and six–rowed accessions. These results clearly indicated that HvRA2 is mainly involved in regulating the determinate fate of spikelet meristems in two–rowed, six–rowed and all other spike forms (*intermedium*, *labile*) in barley; the six–rowed phenotype observed in *vrs4* mutants could be a secondary effect mediated by *vrs4*. Among the eight nucleotide haplotypes identified, only one haplotype comprising of the two–rowed genotype, Palmella Blue, coded for an AA substitution (Glycine → Aspargine, at 163rd AA of 257 AAs) in an unconserved region of the protein outside LOB domain (**Figure 3.5.0.**C). Phenotypic evaluation of this genotype neither showed indeterminate nature of spikelet meristems nor a six–rowed phenotype, indicating the AA substitution as silent (Data not shown).

The 3' UTR analyzed is completely conserved, suggesting that it may be a target site for *cis* regulatory elements (miRNA) or may be involved in mRNA metabolism.

Table 3-4. Barley accessions used for *Vrs4* haplotype analysis with their haplotypes.

Genotype	Origin	Row-type	Haplotype #
Foma	Sweden	2	Hap1
Song bong Gaekori	Korea	6	Hap1
HOR4727	Turkey	6	Hap1
Rabbat	Morocco	6	Hap1
Trabut Barley	Australia	6	Hap1
Golden Promise	Great Britain	2	Hap1
Haruna Nijo	Japan	2	Hap1
Kristina	Sweden	2	Hap1
Betzes	Germany	2	Hap1
MFB104	Hungary	2	Hap1
Bigo	Netherlands	6	Hap1
Olli	Finland	6	Hap1
CarlsbergII	Denmark	2	Hap1
MR3/51	Israel	2	Hap1
Goldfoil	Austria	2	Hap1
Spartan	CzechRepublic	2	Hap1
ORGE AUSTRALIE	Tunisia	2	Hap1
Haya Omugi	Japan	-	Hap1
Blenheim	Great Britain	2	Hap1
Ingrid	Ingrid	2	Hap1
Viking	Russia	2	Hap1
Odesskij36	Ukrain	2	Hap1
Belogorskij	Russia	6	Hap1
Valetta	NewZealand	2	Hap1
HOR12830	Syria	6	Hap1
Pumper	Austria	6	Hap1
FNC6-1	Uruguay	2	Hap1
Klepeninskij	Ukrain	6	Hap1
FNC1	Uruguay	2	Hap1
FAO3443	Iran	2	Hap1
Optic	-	2	Hap1
Nancy	Sweden	2	Hap1
EDong85-1	China	2	Hap1
Apex	Germany	2	Hap1

Arupo	Mexico	2	Hap1
Granal	Kazakhstan	2	Hap1
Ancap2	Uruguay	6	Hap1
FAO3444	Iran	2	Hap1
Sacasco1	Peru	6	Hap1
Morex	USA	6	Hap1
Libra	Chile	2	Hap1
IG31444	Syria	2	Hap1
Peatland	USA	6	Hap1
ShayirIG32973	Oman	6	Hap1
Clipper	Australia	-	Hap1
Iki Kiran	Turkey	6	Hap1
HOR2455	China	6	Hap1
Tammi	Finland	6	Hap1
Vladivostok	China	6	Hap1
Harrington	Canada	2	Hap1
Bonus	Sweeden	2	Hap1
Palmella Blue	Argentina	2	Hap2
HOR5281	Ethiopia	labile	Hap3
Agneta	Finland	6	Hap4
Beka	France	2	Hap5
IG31424	Syria	2	Hap6
ACOxbow	Canada	2	Hap6
Compana	USA	2	Hap6
HOR750	Albania	6	Hap7
CM67	USA	6	Hap7
IG128216	Libya	6	Hap7
HOR9340	Ethiopia	labile	Hap7
IG128162	Pakistan	6	Hap7
IG31903	Morocco	6	Hap7
Psaknon	NewZealand	6	Hap7
SHEKI	Ethiopia	2	Hap7
Aliso	Mexico	6	Hap8
IG128089	Afghanistan	2	Hap8
Gang Tuo Qing Ke1hao	China	6	Hap8
Kwanchike1	Korea	6	Hap8
Karubori	Korea	6	Hap8
Erythraea	Ethiopia	-	Hap8
Bowman	USA	2	Hap8
Dairokkaku	Japan	6	Hap8
FAO3413	Iran	6	Hap8

BalliaLocal	India	6	Hap8
Shimabara	Japan	6	Hap8

A

Haplotype#	891bp(-)	816bp(-)	743bp(-)	148bp(-)	147bp(-)	146bp(-)	145bp(-)	144bp(-)	143bp(-)	142bp(-)	141bp(-)	140bp(-)	139bp(-)	47bp(-)	18bp(-)	17bp(-)	102bp(+)	141bp(+)	488bp(+)
Hap1	T	C	C	T	T	C	C	C	A	G	A	A	C	A	—	—	G	C	G
Hap2	T	C	C	T	T	C	C	C	A	G	A	A	C	A	—	—	G	C	A
Hap3	T	C	C	T	T	C	C	C	A	G	A	A	C	A	—	—	A	T	G
Hap4	—	T	T	T	T	C	C	C	A	G	A	A	C	G	—	—	G	C	G
Hap5	—	T	T	T	T	C	C	C	A	G	A	A	C	G	—	—	G	C	G
Hap6	—	T	T	—	—	—	—	—	—	—	—	—	—	A	—	—	G	T	G
Hap7	—	T	T	—	—	—	—	—	—	—	—	—	—	A	—	—	A	T	G
Hap8	—	T	T	—	—	—	—	—	—	—	—	—	—	A	A	T	A	T	G

B

C

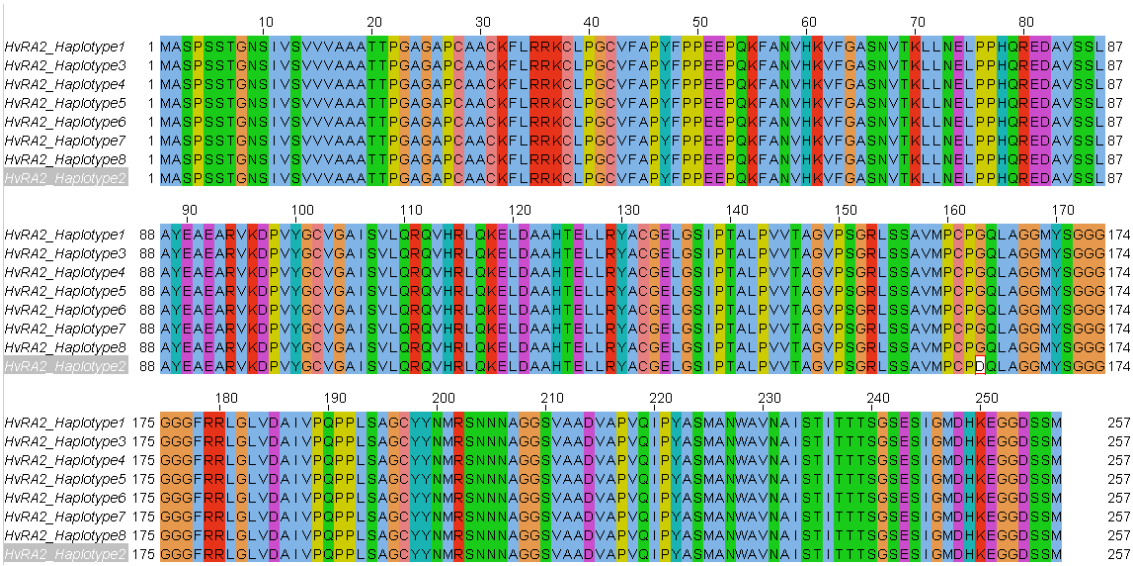

Figure 3.5.0. Re-sequencing of *HvRA2* in diverse barley genotypes.

(**A**) Haplotype structure of eight haplotypes observed at *HvRA2*. Symbols "- ,+" next to fragment size indicate the upstream and downstream nucleotide positions respectively of the start codon and "—" indicates single nucleotide deletion. (**B**) Haplotype analysis of nucleotide sequence data. Circles denote the relative number of samples represented in each *Vrs4* haplotype. Number of accessions within a

particular haplotype is indicated in brackets. Pie slices within the circles indicate geographic distribution of haplotypes. Lines connecting haplotypes denote number of mutations (SNPs or deletions) between haplotypes. (**C**) Multiple sequence alignment of protein sequences generated from eight haplotypes identified after re-sequencing of *HvRA2* in 77 diverse barley genotypes. Only Haplotype2 coded for a non-synonymous nucleotide substitution leading to amino acid change (488 bp, G to A; 163 AA, gly to asp). Haplotype2 is highlighted in grey color and the AA substitution is marked with a red box.

3.6. Identification of downstream target genes of *Vrs4* by mRNA expression analysis

Because *vrs4* encodes a transcription factor HvRA2, a genome wide expression profiling in immature spikes of *vrs4* mutants and WTs was conducted using barley 60 K microarray to better understand the underlying *HvRA2* gene regulatory network. Apart from this, a more targeted qRT–PCR-approach was also used to understand the expression profiles of genes that are known to show analogous inflorescence phenotypes in related species (rice and maize). The microarray analysis was conducted in two deletion mutants MHOR 318, MHOR 345 (*X*–ray induced mutants) and respective WTs AD, HH at Glume Primordium (GP), Stamen Primordium (SP), and Awn Primordium (AP) stages. Because *X*–ray induced mutants have been known to cause larger deletions in the genome, the extent of deletion in and around the *HvRA2* region was characterized in these two mutants (**Table 3-5**). The 60 K microarray analysis in the two *vrs4* mutants, identified a total of 752 genes that showed robust expression differences with a fold change of >2 at an adjusted *P*-value of <0.05. Among these, 337 genes were down–regulated and 415 genes were up–regulated in the *vrs4* mutants at two or more developmental stages analyzed (**Supplementary Table 3** and **Supplementary Figure 1**). Interestingly, more than 70 % of the differentially regulated genes were reproduced in the two deletion mutants (**Supplementary Table 4**) and the remaining 30 % of the changes seen mainly in MHOR 318 could be related to the larger deletion in and around *HvRA2* (**Table 3-5**.)

Table 3-5. Characterization of *X*-ray induced deletion in MHOR 318 & MHOR 345.

Brachy gene	Annotation	MHOR 318	MHOR 345
Bradi2g04110.1	proactivator polypeptide-like 1-like	Intact	Intact
Bradi2g04117.1	mini-chromosome maintenance complex-binding protein-like	Intact	Intact
Bradi2g04130.1	uncharacterized membrane protein At1g06890-like	Intact	Intact
Bradi2g04140.1	hypothetical protein	Intact	Intact
Bradi2g04150.1	Putative expressed protein	Intact	Intact
Bradi2g04160.1	pentatricopeptide repeat-containing protein At5g66631-like	Intact	Intact
Bradi2g04170.1	Putative expressed protein	Intact	Intact
Bradi2g04180.3	Putative expressed protein	Intact	Intact
Bradi2g04190.1	Putative expressed protein	Intact	Intact
Bradi2g04197.1	zinc finger, C3HC4 type family protein	Deleted	Intact
Bradi2g04210.1	autophagy 18D-like protein	Deleted	Intact
Bradi2g04220.1	DUF246 domain-containing protein At1g04910-like	Deleted	Intact
Bradi2g04230.1	catalytic/ hydrolase	Deleted	Intact
Bradi2g04240.1	flavin-containing monooxygenase YUCCA10-like	-	-
Bradi2g04247.1	flavin-containing monooxygenase YUCCA10-like	-	-
Bradi2g04257.1	flavin-containing monooxygenase YUCCA10-like	-	-
Bradi2g04270.1	ramosa2	Deleted	Deleted
Bradi2g04280.1	RST1	Deleted	Deleted
Bradi2g04290.1	tryptophan aminotransferase-related protein 2-like	Intact	Intact
Bradi2g04297.1	Putative expressed protein	Intact	Intact
Bradi2g04310.1	galactinol--sucrose galactosyltransferase-like	Intact	Intact
Bradi2g04317.1	D111/G-patch domain-containing protein	Intact	Intact
Bradi2g04330.1	probable LRR receptor-like serine/threonine-protein kinase At4g26540-like	Intact	Intact

The genes encoding C3HC4 zinc finger, AUTOPHAGY18D–LIKE in MHOR 318 and RESURRECTION1 in MHOR 318 and MHOR 345 were among the top differentially regulated genes in the present study (**Supplementary Table 5**). The differential regulation observed in these genes can be attributed to their deletion in the respective MHOR mutants (**Table 3-5**) and may not be regulated by *HvRA2*. The 60 K microarray used in the present study did not contain a oligo probe for *HvRA2* detection because of which the expression differences for *HvRA2* could

not be detected between mutants and WTs. Nevertheless, qRT–PCR data from three independent mutants clearly showed that *HvRA2* is down–regulated in *vrs4* mutants (**Figure 3.3.3**). Since the two MHOR mutants used for the analysis are *X*–ray induced and they are not back–crossed to an isogenic background, only the genes that consistently showed differential regulation in both MHOR mutants were considered for data interpretation. Transcripts of 22 and 33 genes commonly showed up- and down-regulation, respectively, in wild types compared to MHOR mutants (**Supplementary Table 5**.)

3.6.1. *Vrs1* is highly down-regulated in *vrs4* mutants

In an attempt to identify the regulators of *Vrs1*, Sakuma et al. (2013) analyzed the expression of *Vrs1* in four other known six–rowed mutants, which included *vrs2*, *vrs3*, *vrs4*, and *int–c*. Among these four mutants, *Vrs1* expression was significantly lowered in *vrs4* followed by *vrs2* mutants. In the present study, expression analysis of *Vrs1* in the *vrs4* mutant BW–NIL(*vrs4.k*) and its progenitor MFB104 also showed highly reduced expression of *Vrs1* at different spike developmental stages including TM, GP, LP, SP, and AP (**Figure 3.6.1**). Independent of the qRT–PCR results microarray analysis in the two MHOR mutants showed yet another compelling evidence for *Vrs4* mediated *Vrs1* regulation. Transcripts of *Vrs1* (AB259783, 35_34639) were among the top significantly down-regulated in the two MHOR mutants at all stages analyzed in the present study (FC: –748.50, [AD] vs. [MHOR 318] & FC: –390, [HH] vs. [MHOR 345], (**Figure 3.6.2.A**, and **Supplementary Table 5**). In accordance with the observed transcript regulation, all *vrs4* mutants showed a six–rowed-like phenotype (**Figures 3.1.2** and **3.1.3**). This kind of data clearly indicated *Vrs4* as the positive upstream transcriptional regulator of *Vrs1*.

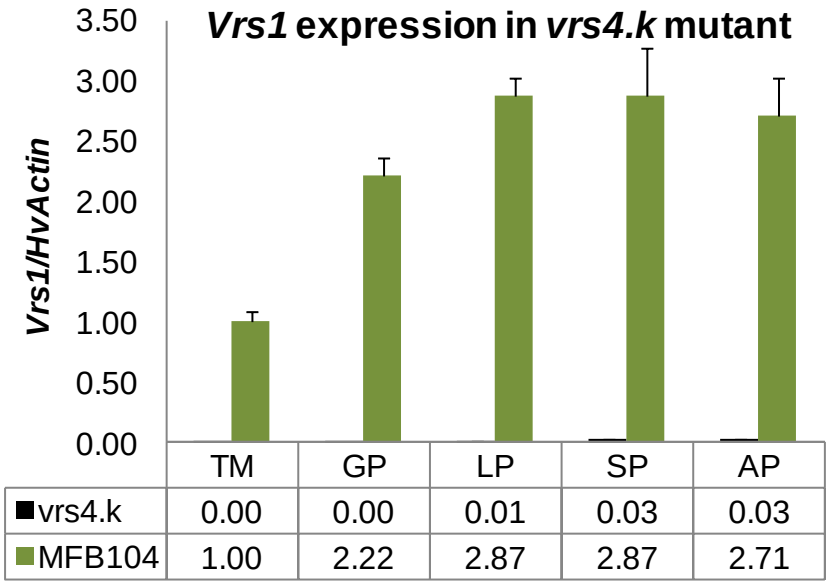

Figure 3.6.1. Relative mRNA expression of *Vrs1* in *vrs4.k* mutant.

Vrs1 expression in BW-NIL(*vrs4.k*) and progenitor MFB104. Mean ± S.E. of three biological replicates is shown. Expression values are given at the bottom of the graph.

3.6.2. *vrs4* mutants showed down-regulation of genes involved in trehalose biosynthesis

The microarray data showed differential regulation for two trehalose biosynthetic pathway genes encoding trehalose-6-phosphate synthase (TPS) and trehalose-6-phosphate phosphatase (TPP) genes in both MHOR mutants and respective WTs. The maize *RA3* gene encoding TPP has already been implicated in control of inflorescence branch architecture (Satoh-Nagasawa et al., 2006). The transcripts of *TPP* (*syn. HvSRA*), [(catalyse conversion of trehalose-6-phosphate (T6P) into trehalose)], were down-regulated in *vrs4* mutants (FC: 4.26 [AD] vs. [MHOR318] & FC: 3.89 [HH] vs. [MHOR345]). Transcripts of another trehalose biosynthetic gene *TPS* (involved in T6P biosynthesis) were also down-regulated in the two MHOR mutants (FC: 13.6 [AD] vs. [MHOR318] & FC: 10.5 [HH] vs. [MHOR345]) (**Figure 3.6.2.A**, and **Supplementary Table 5**). The down-regulation of the two trehalose biosynthetic pathway genes in two *vrs4*

mutants (MHOR 318 and MHOR 345) compared to their two-rowed progenitors (AD and HH) implicate that the maintenance of T6P homeostasis might be important for determinate inflorescence development in barley.

3.6.3. *EGG APPARUS1–LIKE* is highly up-regulated in *vrs4* mutants

EGG APPARUS1 (*EA1*) encodes a secretary protein involved in pollen tube attraction towards female gametophyte in maize (Marton et al., 2005). Mutants of *EA1* in maize show a highly reduced seed set. Interestingly, transcripts of *EA1–LIKE* were significantly up-regulated in MHOR 318 and MHOR 345 mutants compared to WT counterparts at all stages analyzed (FC: 33.5 [AD] vs [MHOR318] & FC: 32.0 [HH] vs [MHOR345], (**Figure 3.6.2.B**, and **Supplementary Table 5**). Most likely implications for such a regulation of *EA1* in *vrs4* mutants are discussed in section **4.3.2**.

3.6.4. *vrs4* mutants showed differential regulation of transcripts involved in cytokinin biosynthesis and auxin transport

The microarray analysis revealed differential regulation for transcripts of *LONELYGUY–LIKE* (*LOG–LIKE*) genes which are involved in cytokinin biosynthesis (Kurakawa et al., 2007). The *LOG* genes that were up-regulated in both MHOR mutants included *LOG1–LIKE* (35_10423) and *LOG8–LIKE* (35_30795, 35_9810, and 35_9790), (**Figure 3.6.2.B**, and **Supplementary Table 5**). Up–regulation of *LOG–LIKE* genes in *vrs4* mutants indicated that higher amount of *LOG–LIKE* transcripts may promote meristematic activity in *vrs4* mutants. It has been shown that *LOG1* is required for the accumulation of *KNOTTED1*–type homeobox (*KNOX*) transcripts in rice (Kurakawa et al., 2007). Rupp et al. (1999) showed that overproduction of cytokinin resulted in increased steady state levels of *KNOTTED* gene transcripts. Conversely, KNOTTED

proteins are shown to activate cytokinin biosynthesis in the shoot apical meristem (SAM) through the induction of *ISOPENTENYL TRANSFERASE* (*IPT*) genes in Arabidopsis and rice (Yanai et al., 2005; Sakamoto et al., 2006). Thus, *KNOTTED* and cytokinin may act in a positive feedback loop with *KNOTTED* genes promoting cytokinin biosynthesis and in turn cytokinins up–regulate *KNOTTED* biosynthesis. The microarray data based on two *vrs4* mutants showed that *KNAT3* (*KNOTTED1-LIKE3* - Contig25238_at, and 35_10104), (**Figure 3.6.2.B**, and **Supplementary Table 5**) is up–regulated in both MHOR mutants, suggesting a possible co–regulation of *LOG–LIKE* and *KNOTTED1–LIKE* genes in *vrs4* mutants. The differential regulation observed for different genes described above in the two *vrs4* mutants (MHOR 318 and MHOR 345) based on microarray experiments was further validated by qRT-PCR analyses (**Figure 3.6.4**.)

Transcript levels of genes, glutathione S–transferase (GSTF1–like), vacuolar sorting receptor7–like, GTP binding protein Rab1–like, protease Do–like14 probably involved in protein degradation and cell death were up–regulated in both MHOR mutants in comparison to wild type (**Figure 3.6.2.B**). The up–regulation of these genes might play a critical role in abortion of BIMs and ASs/AFs at early spike developmental stages in *vrs4* mutants (**Figure 3.1.1**.)

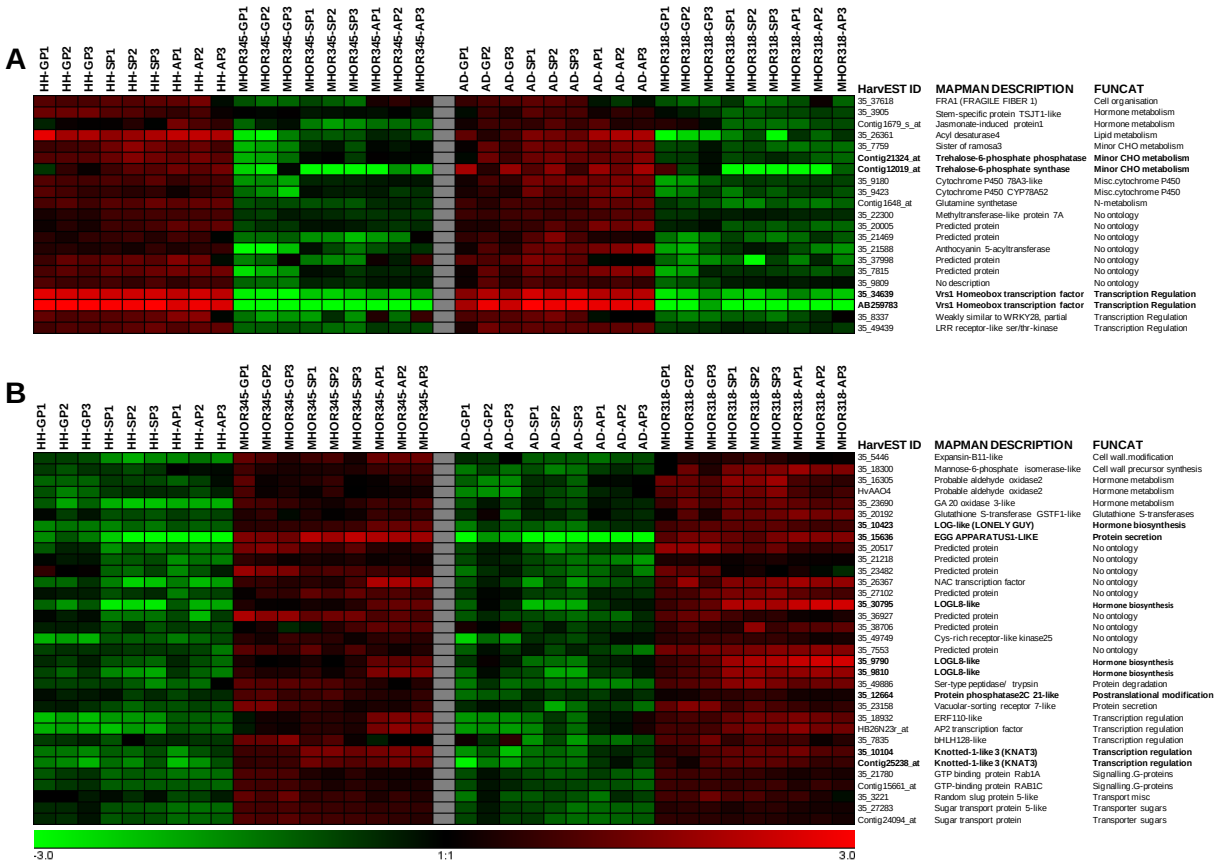

Figure 3.6.2. Gene expression analysis in *vrs4* using microarray.

(**A-B**) Microarray heat maps show genes conjointly down-regulated (**A**), and up-regulated (**B**) in two *vrs4* deletion mutants (MHOR 318 and MHOR 345) and their respective wild types (Ackermann's Donaria and Heine's Haisa). GP: glume primordium, SP: stamen primordium, AP: awn primordium. The scale at the bottom of the heat maps indicates the level of differential regulation observed for different genes between WTs and mutants (green color indicates down-regulation and red color indicates up-regulation).

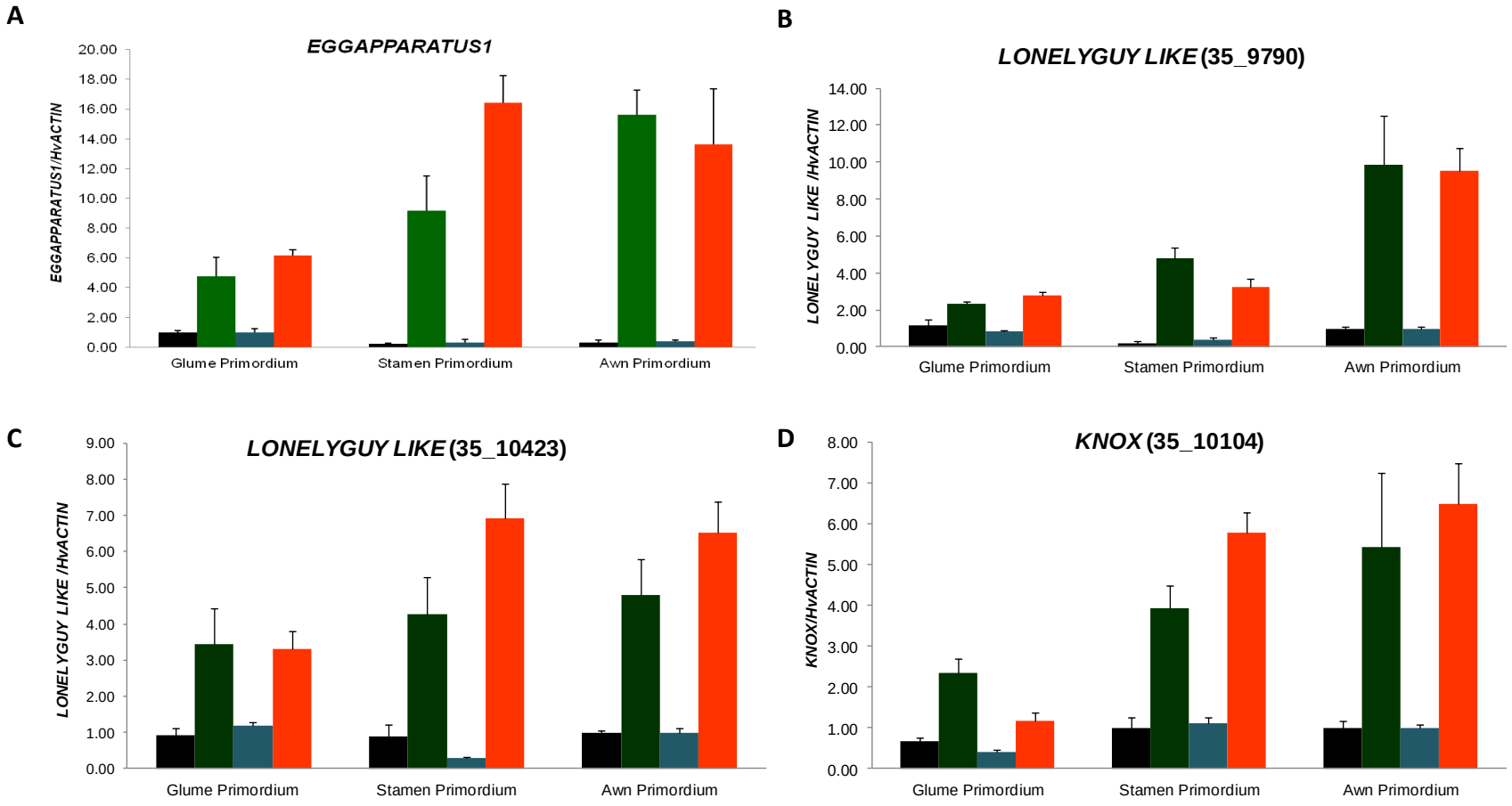
A
EGGAPPARATUS1
EGGAPPARATUS1/HvACTIN
20.00
18.00
16.00
14.00
12.00
10.00
8.00
6.00
4.00
2.00
0.00
Glume Primordium
Stamen Primordium
Awn Primordium
B
LONELYGUY LIKE (35_9790)
LONELYGUY LIKE /HvACTIN
14.00
12.00
10.00
8.00
6.00
4.00
2.00
0.00
Glume Primordium
Stamen Primordium
Awn Primordium
C
LONELYGUY LIKE (35_10423)
LONELYGUY LIKE /HvACTIN
9.00
8.00
7.00
6.00
5.00
4.00
3.00
2.00
1.00
0.00
Glume Primordium
Stamen Primordium
Awn Primordium
D
KNOX (35_10104)
KNOX/HvACTIN
8.00
7.00
6.00
5.00
4.00
3.00
2.00
1.00
0.00
Glume Primordium
Stamen Primordium
Awn Primordium

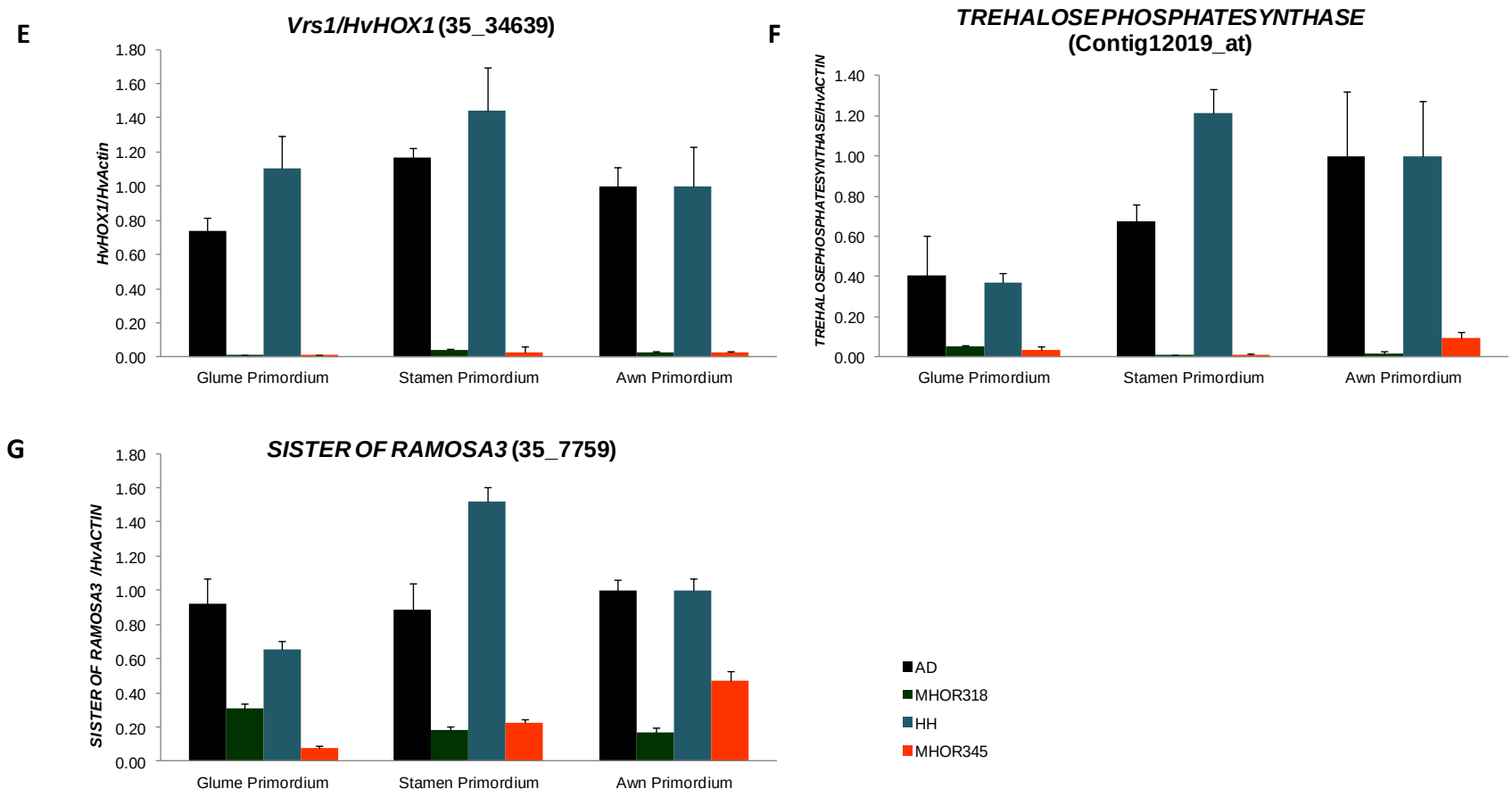

Figure 3.6.4. qPCR validation of differentially regulated genes identified in the *vrs4* microarray experiment.

(**A-D**) qPCR validation of genes up-regulated in MHOR 318, MHOR 345 (*vrs4* mutants) in comparison to their respective wild types Ackermann's Donaria (AD) and Heine's Haisa (HH). The validated genes include *EGGAPPARTUS1* (**A**), *LONELYGUY-LIKE* (*B-C*) and *KNOX* (**D**). (**E-G**) qRT-PCR validation of genes down-regulated in *vrs4* mutants in comparison to their respective wild types, include *Vrs1* (**E**) *TREHALOSE PHOSPHATE SYNTHASE* (*F*), *SISTER OF RAMOSA3* (*syn. TREHLOSE-6-PHOSPHATE PHOSPHATASE*) (**G**). RNA samples from three spike developmental stages (glume primordium, stamen primordium and awn primordium) were analyzed. Mean ± S.E of three biological replicates is shown.

Independent qRT–PCR analyses of few important genes (not present on the microarray and identified based on extrapolation of *vrs4* mutant phenotype with known mutant inflorescence architecture genes characterized in rice or maize), revealed differential regulation for *CYTOKININ OXIDASE/DEHYDROGENASE* (*HvCKX2*) (**Figure 3.6.5**), which is involved in cytokinin degradation and meristem size (Ashikari et al., 2005). *HvCKX2* transcript levels in BW–NIL(*vrs4.k*) and MHOR 318 were lowered (**Figure 3.6.5**), consistent with higher meristematic activity observed in the mutant inflorescences. Transcripts of another gene, *PINFORMED1–LIKE* (*PIN1–LIKE*) (Galweiler et al., 1998), were also up–regulated in BW–NIL(*vrs4.k*) and MHOR 318, suggesting that altered auxin transport affected lateral organ development in *vrs4* mutants (**Figure 3.6.5**.)

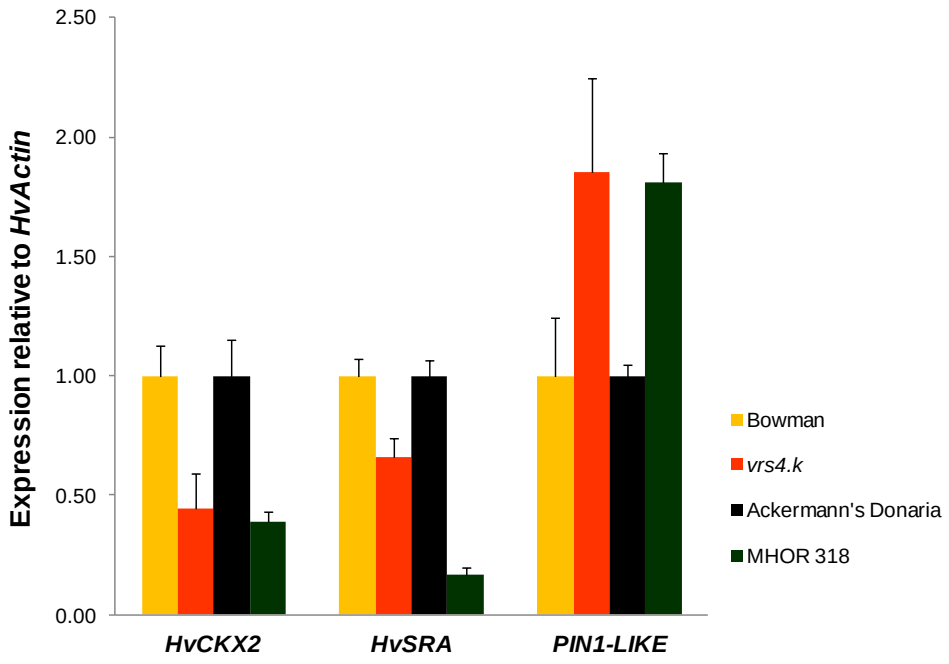

Figure 3.6.5. Expression of *HvCKX2*, *HvSRA* and *HvPIN1-LIKE* in *vrs4* mutants.
vrs4 mutants BW-NIL(*vrs4.k*), MHOR 318 and their respective wild types Bowman and Ackermann's Donaria were analyzed. RNAs sampled at awn primordium were used to quantify the expression. *HvActin* was used to normalize target gene expression. Mean ± S.E. of three replicates.

3.7. Metabolite analysis in *vrs4* mutants showed unaltered pools of Trehalose–6–Phoshate, Glucose–6–Phosphate and UDP–glucose

In higher plants trehalose biosynthesis starts with the condensation of UDP–Glucose (UDP–G) and Glucose–6–phosphate (G6P) catalyzed by trehalose–6–phosphate synthase (TPS) leading to the formation of trehalose–6–phosphate (T6P) (Cabib and Leloir, 1958). T6P is further metabolized to trehalose by trehalose–6–phosphate phosphatase (TPP). Trehalose itself is eventually hydrolyzed by trehalase into two molecules of glucose (Elbein et al., 2003) (**Figure 3.7.0**.)

$$\begin{array}{c}\text{UDP-Glucose}\\ +\\ \text{Glucose-6-phosphate}\end{array} \xrightarrow{1} \text{Trehalose-6-phosphate} \xrightarrow{2} \text{Trehalose} \xrightarrow{3} \text{Glucose (2)}$$

Figure 3.7.0. Trehalose biosynthesis in higher plants.

Figure adapted from O'Hara et al., (2012). The condensation reaction of UDP-glucose and glucose-6-phosphate, catalyzed by trhalose-6-phosphate synthase (1) leads to formation of trehalose-6-phosphate. The T6P is acted upon by trehalose-6phosphate phosphatase (2), cleaves phosphate group from T6P , releases trehalose. The trehalose is eventually hydrolyzed to two molecules of glucose by trehalase (3).

Because the *vrs4* mutants showed elevated transcript levels for genes encoding TPS and TPP, the concentrations of the trehalose biosynthesis precursors UDP-G, G6P and the intermediate T6P, were measured in *vrs4* mutants MHOR 318, MHOR 345, BW-NIL(*vrs4.k*), BW-NIL(*mul1.a*), and their respective WTs - AD, HH, and Bowman. Even though the transcript levels of TPS (involved in condensation reaction of UDP-G and G6P into T6P), were lowered in the two *vrs4* mutants (MHOR 318 and MHOR 345) in comparison to their respective WTs (AD and HH), the metabolite analysis of these two precursors (UDP-G and G6P) did not show significant differences in the concentrations between these two mutants, respective WTs. Like-wise no

differences for UDP-G and G6P were observed between Bowman and the Bowman backcross derived mutants BW-NIL(*vrs4.k*), BW-NIL(*mul1.a*) (**Figure 3.7.1.A, and B**). Concentration of UDP-G showed slight elevation in MHOR 318 in comparison to AD at GP and AP stages; however, the concentration of G6P remained similar in MHOR 318 and AD at both developmental stages. In a similar manner the concentration of T6P was slightly elevated in MHOR 318 at GP and AP. However, in contrast, the concentration of T6P was significantly lowered in BW-NIL(*vrs4.k*) and BW-NIL(*mul1.a*) in comparison to Bowman. (**Figure 3.7.1.C**). The T6P concentrations between MHOR 345 and its progenitor HH remained similar.

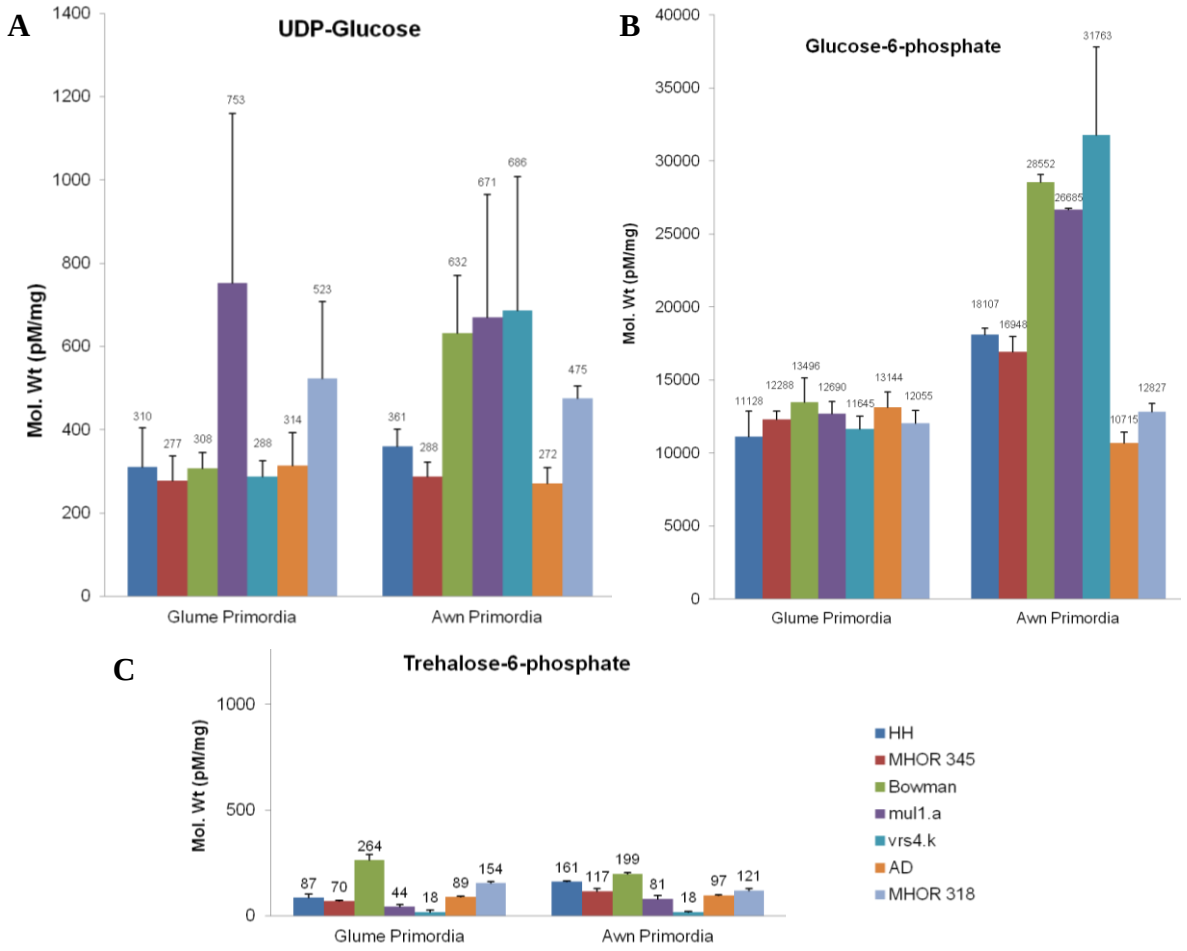

Figure 3.7.1. Metabolite analysis of trehalose biosynthesis precursors, intermediates. UDP-Glucose (**A**), Glucose-6-phosphate (**B**), and Trehalose-6-phosphate (**C**) concentrations in *vrs4* mutants and wild types.

4.0. Discussion

Understanding the genetic basis of variation in inflorescence architecture is important to know how the great diversity in plant form has been generated (Malcomber et al., 2006; Kellog, 2007). Grass species differ from one another in their arrangement of branches, spikelets and florets (Clifford, 1987). Therefore, genes that regulate their arrangement may have been involved in the evolution of the grasses (Kellogg, 2001). For example the temporal differences in the onset of *RAMOSA1* expression in maize, Miscanthus and Sorghum (Andropogoneae species) dictate the spikelet pair meristem identity which leads to varied inflorescence architectures in the respective species (Vollbrecht et al., 2005). In the tribe Triticeae the number of spikelets per rachis internode in different species vary from one to many (Sakuma et al., 2011). However the triple spikelet meristem (TSM) is one of the unique and important characteristics of barley inflorescence (spike), that gives rise to one central spikelet (CS) and two lateral spikelets (LSs). In two-rowed barley (with functional *Vrs1*) the CS is fertile and the LSs are sterile, whereas the six-rowed barleys (with non-functional *vrs1*) possess fertile central as well as lateral spikelets. In barley *vrs4* mutants (with intact *Vrs1*) the characteristic TSM is disrupted leading to more than three spikelets per rachis internode and completely fertile lateral spikelets. Thus the wild type *Vrs4* appears to be important for regulating the inflorescence architecture in barley. The present study attempted to identify the genetic determinant underlying *vrs4* and the putative targets in its gene regulatory network.

4.1. *Vrs4* (*HvRA2*) regulates two distinct genetic pathways in barley inflorescence development

The phenotypic and genetic evaluation of *vrs4* mutants and the respective WTs clearly indicated that *Vrs4* is important for regulating two distinct genetic pathways, such as (i) regulation of spikelet determinacy, and (ii) regulation of spike row–type.

4.1.1. *HvRA2* regulates spikelet determinacy of barley's TSM

The number of spikelets at each rachis internode in barley is generally confined to three in both two– and six–rowed types. However, in *vrs4* mutants this confinement is relaxed to a large extent displaying more than six additional spikelets/florets at maturity apart from the basic triplet of spikelets arising from the TSM (**Figure 3.1.2.E, F,** and **G**). The proliferation of additional spikelets/florets is in fact much more at early stages of spike development than what is observed at spike maturity (**Figure 3.1.1.C, D,** and **E**). Such a phenotype is consistently observed in all 20 *vrs4* mutants analyzed in the present study (**Figure 3.1.3**); however, their immediate progenitors displayed unaffected spikelet determinacy (determinate TSM with three spikelets per rachis internode). Analogous inflorescence indeterminacy phenotypes are also evident in orthologous maize *ra2* (*ZmRA2*) mutants. *ZmRA2* regulates SPM identity by temporal suppression of indeterminate LBM in tassel and confers determinacy to SPMs in both tassel, and cob. In mutants of *ZmRA2* the SPM identity is delayed due to the derepression of LBM outgrowth in tassel. The determinacy of SPMs is also compromised in maize resulting in formation of mixed branches in tassel with more than two spikelets arising from the SPM (Bortiri et al. 2006). A similar phenotype is also seen in ear inflorescence of *ZmRA2* mutants, where the otherwise branchless cob is transformed into a branched cob. Interestingly, the gamma-ray induced *vrs4* mutant MC(*mul1.a*) shows a severe branch outgrowth from the basal to middle portion of spike,

a phenotype consistently seen in all spikes on a plant. Such branching phenotype is not seen in its progenitor Montcalm (**Figure 4.1.1**). The branching phenotype in MC(*mul1.a*) suggests that the functional *HvRA2* is also important for negative regulation of branch development in barley. The spike branching phenotype is also evident from all severe alleles of *vrs4* at pre-anthesis development; however, these branches are aborted at later stages of spike development (**Figures 3.1.1**). Thus the compendium of indeterminate spikelet phenotypes observed in *vrs4* mutants (*HvRA2*) and *maize ra2* (*ZmRA2*) mutants clearly indicated that the *RA2* orthologs in both species (maize, barley) and probably other grass species are important for regulation of spikelet determinacy and branch out growth. However, the barley ortholog plays yet another interesting role of regulation of row–type identity apart from mediating spikelet determinacy.

Figure 4.1.1. Branching phenotype in *vrs4* mutant, MC(*mul1.a*).

(**A**) Mature spike of cultivar Montcalm with determinate triple spikelet at each rachis internode. (**B-D**) Mature spikes of *vrs4* mutant, MC(*mul1.a*) showing various levels of branch proliferation from spike base to middle portion of the spike. Scale bar, 5 cm.

4.1.2. *HvRA2* regulates barley row–type pathway

The row–type identity is specific to the genus *Hordeum*, and is not seen in any other grass species, including the genera from tribe Triticeae. In barley, the row–type identity is conferred by lateral spikelet/floret development (six–rowed spike) or abortion (two–rowed spike). Komatsuda et al. (2007) showed that *Vrs1*, an HD–Zip I transcription factor preferentially expressed in lateral spikelets, is sufficient to confer the row–type identity. Functional *Vrs1* alleles (*Vrs1.b*) result in two–rowed spikes; whereas non–functional *vrs1.a* produces six–rowed spikes. However, all of the induced *vrs4* mutants analyzed in the present study showed either a complete or partial six–rowed phenotype, suggesting that *HvRA2* is also important for regulation of row–type. Most importantly, the experimental results obtained from the present study showed *Vrs4* as an important regulator of *Vrs1* in the row–type pathway.

4.1.2.1. Converging evidence for transcriptional regulation of *Vrs1* by *Vrs4*

One of the most important findings from the present study is the evidence for the transcriptional regulation of *Vrs1* by *HvRA2* (*Vrs4*). The qRT–PCR and microarray analyses clearly showed that the *Vrs1* transcripts are significantly down–regulated in *vrs4* mutants at different spike developmental stages (**Figure 3.6.1**). Thus, a clear reduction of *Vrs1* transcripts in *vrs4* mutants indicated that *HvRA2* directly controls *Vrs1* transcripts, and thus the row–type pathway (**Figure 4.1.2.A,** and **B**).

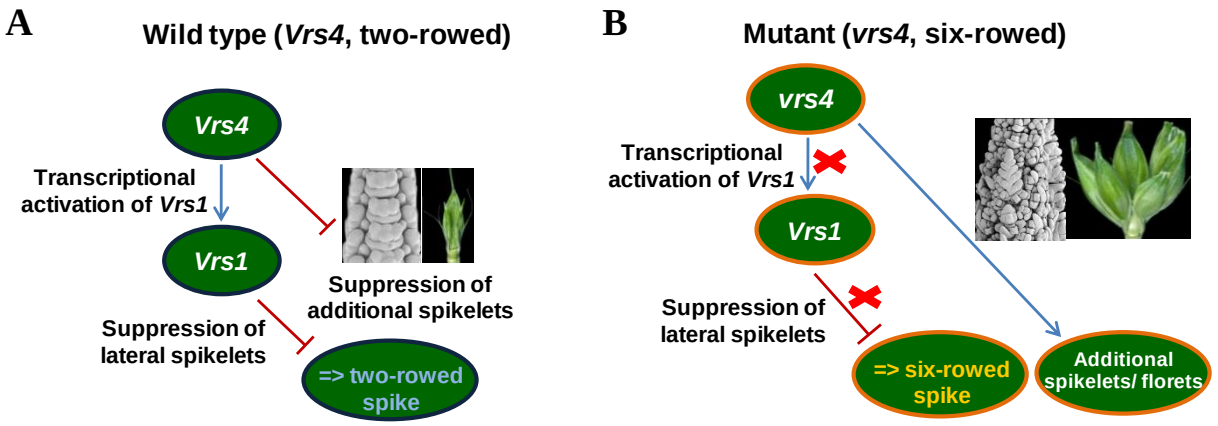

Figure 4.1.2. Model of *Vrs4* interaction with *Vrs1*.

(**A**) Functional *Vrs4* suppresses additional spikelet formation and activates *Vrs1* transcription which results in aborted lateral spikelets and two-rowed condition. (**B**) Mutant *vrs4* cannot control determinacy of the TSM; thus additional spikelets are formed. Transcriptional activation of *Vrs1* expression is omitted (red cross) resulting in lateral spikelet fertility and a six-rowed phenotype.

It is well known that functional DNA domains of transcription factor proteins modulate the expression of their target genes by binding to the *cis*–regulatory elements (promoter, 5'UTR, introns and 3'UTR) of corresponding genes. Circumstantial evidence supporting this view came from the HvRA2 LOB domain consensus DNA recognition motif 5'–CCGGCG–3' (Husbands et al., 2007) present in the *Vrs1* promoter region close to the transcriptional start site (–60 to –65 bp) and also within the 5'UTR (117 bp upstream of start codon 'ATG'). It is expected that the LOB domain of HvRA2 binds to such *cis*–regulatory elements owing to their close proximity to the transcriptional start site of the *Vrs1* (**Figure 4.1.2-1.A**). Previous *in vitro* protein binding assays in Arabidopsis showed strong binding affinity of LOB domain proteins to this consensus motif (Husbands et al., 2007). However, the physical interaction between HvRA2 and *Vrs1 cis*–regulatory elements needs to be established using methods such as yeast one hybrid assays or promoter binding and gel mobility shift assays.

The temporal changes in the expression patterns of *Vrs1* and *HvRA2* within the lateral spikelet meristems also suggested a putative interaction among these two genes. The transcripts of *Vrs1* start to accumulate in the lateral spikelets at a stage when the TSM starts to differentiate into three spikelet meristems (triple mound) (**Figure 4.1.2-1.D**), with no detectable expression during double ridge stage (DR - first reproductive stage) (**Figure 4.1.2-1.B;** Komatsuda et al., 2007). However, the transcripts of *Vrs4* start to accumulate at DR stage, in contrast to *Vrs1* (**Figure 4.1.2-1.C**). Thus, *Vrs4* expresses temporally ahead of *Vrs1*. The temporal advancement of *Vrs4* expression most probably ensures a sufficient overlap between transcripts of *Vrs1* and *HvRA2* for the proposed transcriptional regulation to occur. An overlay of *Vrs1* and *HvRA2* expression patterns based on mRNA *in situ* hybridization results clearly showed that transcripts of these two genes are expressed in a highly overlapping region within the meristems of lateral spikelets, suggesting a putative interaction among them (**Figure 4.1.2-1.F**). In addition to this phenomenon, the *HvRA2* transcripts show maximum localization in the lateral spikelet meristems with a reduced expression in central spikelet meristems at TM stage at which the *Vrs1* transcripts start to accumulate in the lateral spikelet meristems (**Figure 4.1.2-1.E;** Koppolu et al., 2013). This further indicates that at TM stage the *Vrs4* transcripts are prioritized for their localization in lateral spikelets than the central spikelets because *Vrs1* expression is concentrated in lateral spikelets.

Consistent with the above mentioned findings, the SEM analysis at early spike developmental stages in *vrs4* mutants BW–NIL(*vrs4.k*), BW–NIL(*mul1.a*), and respective WTs also suggested a putative interaction between HvRA2 and *Vrs1*. In *Vrs4* WT plants (i.e. two-rowed type; functional *Vrs1*), the growth of lateral floral organs ceases approximately between SP and AP stages due to the activity of VRS1 protein, which negatively regulates development in lateral

spikelets. However, in *vrs4* mutants the lateral floral organs continue to develop normally after AP stage and proceed to produce fertile spikelets/florets (**Figure 3.1.1.D,** and **E**). This precisely indicated that the *Vrs1* transcriptional activation activity of *Vrs4* is lost in *vrs4* mutants, resulting in the development of fertile lateral spikelets in *vrs4* mutants. Subsequently the majority of *vrs4* mutants analyzed in the current study showed a complete six–rowed phenotype at maturity, which is analogous to the six–rowed phenotype of *vrs1* mutants (**Figures 3.1.2**, and **3.1.3**). Thus, *vrs4* mutant spike phenotypes from several independent mutants support the idea that the transcriptional regulation of *Vrs1* is under the control of HvRA2.

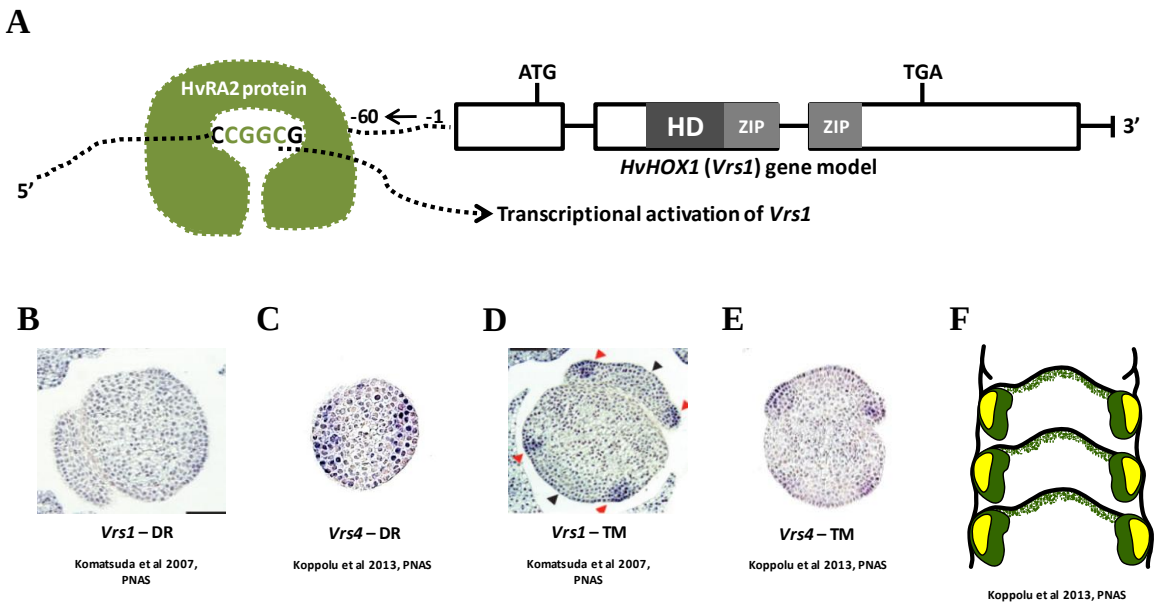

Figure 4.1.2-1. HvRA2 functions as a transcriptional regulator of *Vrs1*.

(A) Hypothetical interaction between HvRA2 and *Vrs1*. HvRA2 protein binds to the LOB domain *cis*-recognition element 5'-CCGGCG-3' present upstream of *Vrs1* gene and activates its transcription. -1 bp to -60 bp represents the bases upstream of transcriptional start cite of *Vrs1*. (**B-E**) *In situ* localization of mRNA expression in *Vrs1* and *Vrs4*. *Vrs1* (**B**) and *Vrs4* (**C**) expression at double ridge, *Vrs1* (D) and *Vrs4* (**E**) expression at triple mound. (**F**) Overlay of *Vrs1* (yellow) and *Vrs4* (green) expression pattern at triple mound stage. The figures **4.1.2-1.B, D** were adopted from Komatsuda et al., (2007) and the figures **4.1.2-1.C, E, F** were adopted from Koppolu et al., (2013.)

Yet another interesting evidence for regulation of *Vrs1* by *Vrs4* was observed from spike phenotype of *vrs1/vrs4* double mutants. The *vrs4* mutant allele MC(*mul1.a*), was isolated in a six–rowed background Montcalm (*vrs1.a*), and has recessive genetic status at both *vrs1* and *vrs4* loci, consequently the spikes of the MC(*mul1.a*) mutant showed a synergistic spike phenotype displaying the six–rowed spike with complete lateral spikelet fertility, as observed in Montcalm, and also indeterminate nature of the TSM, diagnostic of *vrs4* mutants (**Figure 4.1.1**). The enhanced phenotype observed in MC(*mul1.a*) mutant suggests that *vrs4* functions in regulation of the determinate nature of barley's TSM and also row–type pathway.

4.2. Genetic regulation of *RAMOSA* pathway in barley may differ from that of maize and other Andropogoneae species.

In maize the functional *RAMOSA* pathway is required for the shift from indeterminate long branch identity to short branch identity (spikelet pairs) in tassel and repression of branch outgrowth in cob inflorescences. The *RAMOSA* pathway in maize is under the coordinated regulation of four genes *RA1* [(C2H2 ZINC FINGER transcription factor; (Vollbrecht et al., 2005)], *RA2* [(LBD transcription factor; (Bortiri et al., 2006)], *RA3* [(TPP; (Satoh-Nagasawa et al., 2006)], and *REL2* [(WD40 and CTLH domain containing protein; (Gallavotti et al., 2010)], wherein the RA1–REL2 determinacy–providing complex is transcriptionally regulated by *RA2* and *RA3* (Gallavotti et al., 2010). Mutations in any of these four genes result in impaired SPM identity and extended tassel branching as well as de-repression of branch outgrowth in cob. Such a genetic regulation may be unique to maize and other Andropogoneae species, which produce their spikelets in pairs. *RA1* and *RA3* orthologs are specifically found in species belonging to tribe Andropogoneae; orthologs of these two genes are not reported in other grasses (Vollbrecht et al., 2005; Satoh-Nagasawa et al., 2006). We found the other two genes *RA2* and *REL2* being

present in barley and all other grass species. *ZmRA3* is expressed in a highly localized domain at the base of axillary meristem primordia (Satoh-Nagasawa et al., 2006). The maize genome has a paralog of *ZmRA3* dubbed as *SISTER OF RAMOSA3* (*ZmSRA* - physically linked to *ZmRA3* in maize) that shows 70% AA identity in TPP domain and 65% overall identity to ZmRA3 protein (Satoh-Nagasawa et al., 2006). Interestingly, several grass species including barley (*HvSRA*) possess a homolog of *SISTER OF RAMOSA3.* The homolog of rice *SRA* (*OsSRA*) like *ZmRA3* also shows a highly localized expression pattern at the base of all inflorescence BMs, indicating that *OsSRA* plays a similar regulatory role like *ZmRA3* to control inflorescence architecture in rice (Satoh-Nagasawa et al., 2006). The microarray analysis of *vrs4* mutants from the present study showed a significant down-regulation of *HvSRA* in *vrs4* mutant inflorescences, consistent with indeterminate nature of TSM in *vrs4* mutants. Such regulation suggests that *HvSRA* is under the control of *HvRA2*, which is an important genetic determinant of barley's TSM determinacy (**Figure 4.3.0**), whereas *ZmRA3* expression is independent of *ZmRA2* (Satoh-Nagasawa et al., 2006) indicating a divergent gene regulation in barley compared to maize.

Even though a true ortholog of the other *RAMOSA* pathway gene *ZmREL2* (transcriptional co-repressor) is present in barley, the microarray analysis did not reveal differential regulation for *HvREL2* transcripts in *vrs4* mutants, implying that *HvREL2* might also function differently in barley and other grasses compared to maize. Recently Yoshida et al. (2013) characterized the rice *ABERRANT SPIKELET AND PANICLE1* (*ASP1*) gene, which encodes the rice ortholog of *ZmREL2*. Mutants of *ASP1* show pleiotropic phenotypes including de–repression of vegetative axillary bud outgrowth, prolonged IM activity and precocious transition of BM to SM and reversion of SM into BM. Such phenotypes indicate that *ASP1*, like maize *ZmREL2* plays important role in rice inflorescence architecture by imposing determinate fate on different BMs

and also by preventing precocious phase transition during inflorescence development. The barley *REL2* might play a similar role to regulate the determinate spike architecture; however, *REL2* orthologs in barley, rice and other non–Andropogoneae species may bind to a different target protein (i.e. RA1 equivalent) to repress the transcription of genes promoting indeterminate inflorescence architecture; as orthologs of *RA1* are not present in these species (Vollbrecht et al., 2005.)

Bai et al., (2012) showed *ZmRA2* as an upstream positive regulator for *BRANCH ANGLE DEFECTIVE1* (*BAD1*), which controls the angle of basal long branches in maize tassel. In maize *bad1* mutants, the angle of basal long branches in the tassel is acute which results in upright tassel branches, a similar phenotype is also evident in *Zmra2* mutant tassels (Bortiri et al., 2006). The qRT–PCR analyses in three independent *vrs4* mutants in the present study showed that the transcripts of orthologous barley *BAD1* (*HvBAD1*) are down-regulated in *vrs4* mutants indicating a similar regulation in barley (*HvRA2* upstream of *HvBAD1*) (**Figure 4.2.0**). However, as the spike inflorescence of barley does not possess long branches no visible alteration of spike phenotype was observed in *vrs4* mutants, suggesting that *HvBAD1* may play a different role in barley inflorescence development.

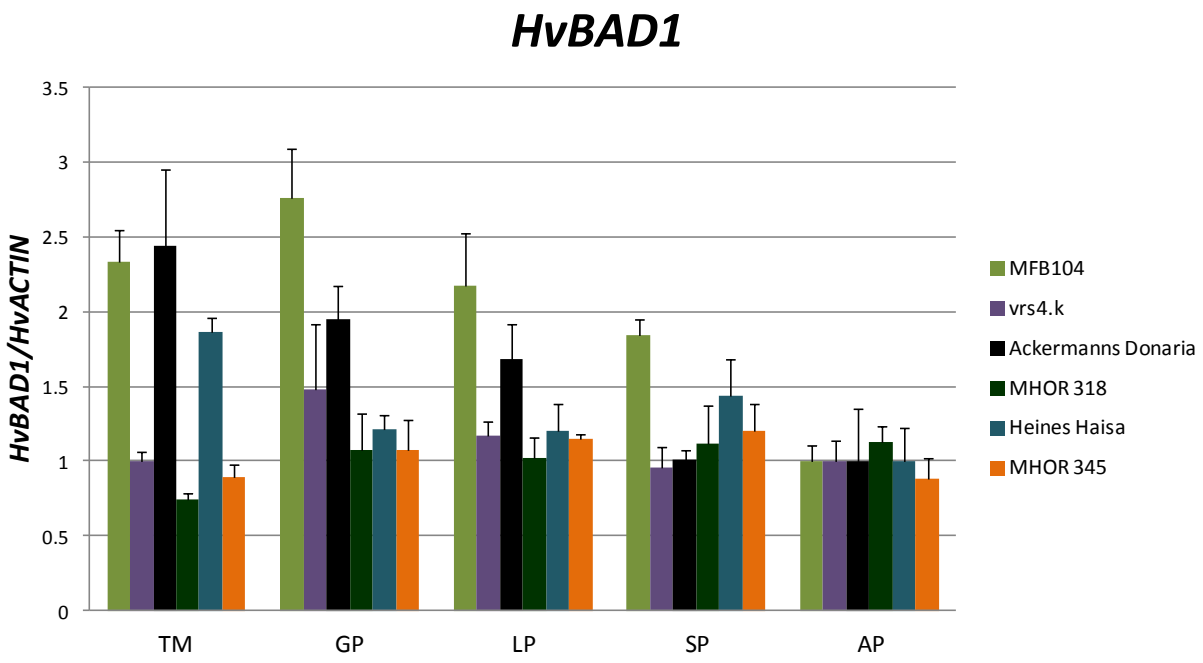

Figure 4.2.0. *HvBAD1* expression in *vrs4* mutants.

HvBAD1 expression in BW-NIL(*vrs4.k*), MHOR 318, MHOR 345 and respective wild types Bowman, Ackermann's Donaria, Heine's Haisa. Mean ± S.E of three biological replicates is shown. TM: Triple Mound; GP: Glume Primordium; LP: Lemma Primordium; SP: Stamen Primordium; AP: Awn Primordium.

4.2.1. Evolution of *RAMOSA2*

The well-understood *RAMOSA* gene network in maize appears to be specific to species of tribe Andropogoneae. Apart from the species belonging to tribe Andropogoneae (subfamily Panicoideae), orthologs of *RA3* are also seen in other species of Panicoideae [(for example *SvRA3* in foxtail millet (*Setaria italica* subsp. *viridis* L.), (tribe Paniceae)] (Satoh-Nagasawa et al., 2006). However, the presence of *RA1* orthologs outside Andropogoneae has not been documented (Vollbrecht et al., 2006). On the other hand orthologs of *RA2* and *REL2* are present in most of the grass species (Bortiri et al., 2006; Gallavotti et al., 2010). A closer look at the phylogenetic evolution of RA2 proteins from different grass species analyzed in the present

study clearly reflected the grass evolutionary history (**Figure 3.4.0**). The RA2 proteins from the species of grass subfamily Panicoideae (species belonging to tribes Andropogoneae, Paniceae) showed a clear divergence from the species belonging to other subfamilies of monophyletic BEP clade (Bambusoideae, Erhartoideae, Pooideae – includes bamboo, rice, barley, wheats and oat) probably owing to the different regulation of *RAMOSA* pathway (*RA1* and *RA3* are not seen in the subfamilies of BEP clade). The two monophyletic groups Panicoideae and BEP had a common ancestor 50 million years ago (Mya) (Gaut, 2002), the *RA3* paralogs might have originated via the duplication of *SRA* in Panicoideae grasses possibly after their divergence from other grass species (BEP clade). The unique presence of *RA1* orthologs in Andropogoneae species indicates that *RA1* could have originated from duplication in the species of tribe Andropogoneae (After the divergence of Andropogoneae from other Panicoideae grasses). However, the presence of *RA2* and *REL2* in most of the grass species suggests an ancient origin for these two genes compared to *RA1* and *RA3*. Thus, *RA2* as the central regulator of the *RAMOSA* pathway might have evolved different gene regulatory networks in species belonging to the BEP clade owing to the absence of *RA1* and *RA3* orthologs in those species.

4.2.2. *HvRA2* is co–opted for regulating row–type phenotype in barley

Co–option is the process by which an orthologous gene acquires new function in a different species, while it may or may not retain its ancient function (True and Carroll, 2002). Co–option occurs when natural selection finds new uses for existing genes during speciation (e.g duplicated genes). It has been reported that co–option of transcription factor proteins for different purposes in different tissues is a common mechanism during evolution and development (Carroll, 2005). The presence of functional *RA2* in different grass species is probably important for the regulation of determinate inflorescence architecture in various species. However, the *vrs4* mutants display

two distinct spike phenotypes, which include indeterminate nature of barley's TSM and lateral spikelet fertility conferring a six–rowed phenotype. Thus, in barley, *HvRA2* appears to be co–opted for regulating the row–type phenotype while retaining its ancient function to control determinate spike architecture. The barley row-type is majorly regulated by *Vrs1*, which arose after duplication of a closely related HD–Zip I paralog *HvHOX2* (2HS) with global expression pattern. Following gene duplication, the *Vrs1* has acquired unique expression pattern in LSs and neofunctionalized to suppress LS fertility (Sakuma et al., 2010). The row–type phenotype is only evident in species of *Hordeum* and not seen in maize and even in its close relatives wheat and *Brachypodium*. Barley and wheat have an evolutionary divergence time of approximately 13 million years. Thus, the row–type phenotype in barley might have a very recent origin. The phenotypic and gene expression analyses of *vrs4* mutants in the present study clearly showed that *HvRA2* controls the row–type pathway by transcriptionally regulating the row–type gene *Vrs1*, indicating that *HvRA2* co–opted for regulating row–type through *Vrs1*.

4.3. Gene expression analysis using microarray indicated that *HvRA2* may regulate phytohormones and trehalose-6-phosphate biosynthesis and metabolism

4.3.1. *HvRA2* may control trehalose-6-phosphate homeostasis

Trehalose-6-phosphate (T6P) has emerged as a powerful signaling molecule for plant metabolism and development in the recent past (Zhang et al., 2009; Martinez-Barajas et al., 2011; O'Hara et al., 2013), the levels of T6P are controlled by Trehalose-6-phosphate Synthase (TPS) and Trehalose-6- Phosphate Phosphatase (TPP). In plants, T6P acts as an inhibitor of sucrose non–fermenting (SNF1)–related protein kinase1 (SnRK1), which activates a cascade of degradation pathways under limiting carbon source (Zhang et al., 2009; Paul et al., 2010; Martinez-Barajas et al., 2011). When a plant's carbon energy status is low (low sucrose, glucose

and T6P) the SnRK1 inhibition by T6P is compromised and subsequently SnRK1 activates genes involved in degradation processes, photosynthesis and inhibits those involved in biosynthetic processes (Baena-Gonzalez et al., 2007). The *Arabidopsis* and rice genomes harbor 11 *TPS* genes (*AtTPS1 – AtTPS11* and *OsTPS1 – OsTPS11*). However, only AtTPS1 and OsTPS1 were shown to have T6P synthase activity (Blázquez et al., 1998). It has been shown that the other rice *TPS* genes, which do not have T6P synthase activity (especially OsTPS5 and OsTPS8) form a protein complex and regulate the activity of OsTPS1 (Zang et al., 2011). Thus all *TPS* genes appear to be involved in trehalose biosynthesis either directly (TPS1 involved in T6P biosynthesis) or indirectly (TPS5 and TPS8 regulating TPS1). The *Arabidopsis* genome contains ten *TPP* genes (*AtTPPA – AtTPPJ*); and all of these were reported to encode a functional TPP enzyme with phosphatase activity (Vandesteene et al., 2012). Whereas in rice nine *TPP* genes were identified (*OsTPP1 – OsTPP9*) and OsTPP1 and OsTPP2 were shown to have phosphatase activity (Pramanik and Imai, 2005; Shima et al., 2007). T6P is also important for sugar utilization in plants. The *Arabidopsis tps1* mutants, which fail to make T6P, are embryo lethal and super-sensitive to exogenously supplied sugar (Schluepmann et al., 2003). By contrast, the high levels of T6P promote efficient utilization of exogenously supplied sugar and show growth increase when compared with wild type plants (Schluepmann et al., 2012). The abnormal growth increase is also evident in maize *ra3* mutant inflorescences, which do not have a functional TPP (Satoh-Nagasawa et al., 2006). The absence of TPP activity in *Zmra3* mutants may lead to T6P accumulation allowing efficient sugar utilization and a corresponding growth increase.

The microarray gene expression analysis in *vrs4* mutants showed down–regulation of *HvSRA*, (encodes a Trehalose-6-Phosphate Phosphatase), implying that T6P levels might be elevated in *vrs4* inflorescences. Thus, elevated T6P pools in *vrs4* mutants may possibly promote the

abnormal growth increase and indeterminate nature of TSM. However, transcripts of the other trehalose biosynthetic pathway gene *TPS* (involved in T6P biosynthesis) were also down-regulated in *vrs4* mutant inflorescences. Such a down-regulation of transcripts of both *TPP* and *TPS* could suggest a feedback regulation (down-regulation) of *TPS* due to the abundant T6P pools arising from the lowered TPP activity in *vrs4* mutants (**Figure 4.3.0**). On the other hand, the barley *TPS* gene, which is down-regulated in *vrs4* mutants (Contig12019_at), may not possess the T6P synthase activity as is the case with the majority of rice and *Arabidopsis TPS* genes. The lack of T6P synthase transcript activity (Contig12019_at) is also evident from the metabolite data which showed no significant differences for UDP–Glucose and Glucose-6-Phosphate (G6P) concentrations, the substrates for the TPS condensation reaction (if the Contig12019_at has T6P synthase activity the pools of the substrates UDP–G and G6P might be lowered) (**Figure 3.7.1**). Surprisingly, the metabolite data did not reveal significant differences for T6P levels between *vrs4* mutants and WTs (**Figure 3.7.1**). In a recent study, Wahl et al., (2013) showed that accumulation of T6P in Arabidopsis shows diurnal rhythmicity, with maximum T6P accumulation towards the end of light phase during the day. The maximum T6P accumulation also overlapped with the expression onset of circadian regulated genes *CONSTANS* and *FT*. This phenomenon might also hold true for barley and other monocot species. The probable reason for the unaltered pools of T6P observed in metabolite analysis could be due to the lack of time course sampling of spike tissue over the day because T6P accumulation may follow diurnal rhythmicity. Moreover, Carillo et al. (2013) while analyzing the T6P pools in maize *ra3* mutant tassels, collected in a time course manner, also did not find significant differences between mutants and WTs; instead they found lowered trehalose and trehalose:T6P ratio in *ra3* mutants. Thus, in maize *ra3* mutants, altered trehalose and trehalose:T6P ratio may

promote the abnormal growth increase in tassel and ear branches. A similar mechanism might be functioning in barley *vrs4* mutants, which need to be tested in future.

4.3.2. HvRA2 may regulate active cytokinin pools and polar auxin transport

The role of cytokinins in development of plant reproductive meristems and grain yield has been well documented (Ashikari et al., 2005; Rijavec et al., 2009; Zalewski et al., 2010; Bartrina et al., 2011). In the present study, the gene expression analyses using microarray and qRT–PCR showed differential regulation for genes involved in cytokinin biosynthesis and metabolism. The transcripts of *HvCKX2*, a cytokinin oxidase/ dehydrogenase involved in cytokinin catabolism were down-regulated, indicating that higher levels of cytokinins are maintained in *vrs4* inflorescences to promote the meristematic activity (**Figure 4.3.0**). The *CKX* is a small gene family with 11 gene family members (*CKX1 – CKX11*) in most of the Poaceae species including barley, rice, maize, sorghum, foxtail millet, and Brachypodium (Mameaux et al., 2012). In a classical QTL cloning study of rice *Gn1a,* Ashikari et al., (2005) showed that mutations in *OsCKX2* lead to an increase in cytokinin levels and a corresponding increase in grain numbers by promoting meristematic activity of different branch meristems in rice inflorescence. Zalewski et al. (2012) also showed that knock out of barley *CKX2* (*HvCKX2*) resulted in elevated cytokinin levels and a corresponding yield increase. A similar yield increase due to elevated cytokinin levels was also observed in transgenic knockouts of *HvCKX1* and *TaCKX1* in barley and wheat, respectively (Zalewski et al., 2010). In contrast, constitutive over-expression of *HvCKX1* resulted in failure of transition to flowering in barley (Mrizova et al., 2013). In *vrs4* mutant spikes also the number of spikelet/floret meristems were increased probably due to the lowered activity of *HvCKX2* and a corresponding increase of cytokinin concentration. However, comparative analysis of active cytokinins in *vrs4* mutant and wild type inflorescences would

clarify whether the observed down-regulation of *HvCKX2* contributes to elevated cytokinin levels and a corresponding increase of meristematic activity in *vrs4* inflorescences.

The microarray data also revealed higher transcript abundance for the *LONELY GUY–LIKE* (*LOG*-like) genes in *vrs4* mutants (**Figure 4.3.0**). LOG catalyzes the conversion of inactive cytokinin nucleotides to active cytokinin. The rice genome has 11 *LOG*-like genes (Kurakawa et al., 2007); however, only seven of these orthologs have been reported in the barley genome (Mrizova et al., 2013). In rice, *LOG1* has been shown to be important for BM activity and grain yield. The mutants of rice *LOG1* with lowered cytokinins showed a small panicle with reduced number of primary, secondary and tertiary (spikelets) branches (Kurakawa et al., 2007). The higher *LOG–LIKE* transcripts in *vrs4* inflorescences may probably lead to high cytokinin concentrations and enhanced meristematic activity. Thus, the co–ordinated regulation of the two genes involved in cytokinin biosynthesis and catabolism (*LOG1–LIKE* and *HvCKX2*) may play an important role in *vrs4* inflorescence development. The *vrs4* mutants also showed elevated transcript levels of auxin efflux carrier, *HvPIN1-LIKE*, which may lead to elevated auxin transport which might be important for enhanced meristematic activity.

Apart from the genes involved in phytohormone biosynthesis and metabolism, *vrs4* mutants also showed regulation for *EA1-LIKE*, a secretary protein involved in pollen tube growth and ovule fertilization (Marton et al., 2005). The up–regulation of *EA1–LIKE* transcripts in *vrs4* mutants can be attributed to two important developmental changes, (i) more EA1–LIKE protein in *vrs4* mutants may be needed to fertilize ovules of lateral spikelets (six–rowed condition), whereas in two-rowed condition the ovules of lateral spikelets do not require EA1-LIKE activity because lateral florets are aborted in two-rowed types. In such a situation one can assume *Vrs1* as a

negative regulator of EA1 in two-rowed types; however, further experiments are needed to test the *EA1-LIKE* transcript levels in two- and six-rowed spikes to validate this assumption. Alternatively, (ii) elevated levels of *EA1–LIKE* transcripts may be required to promote the fertility of proliferating additional spikelets/florets formed in *vrs4* mutants (**Figure 4.3.0**.)

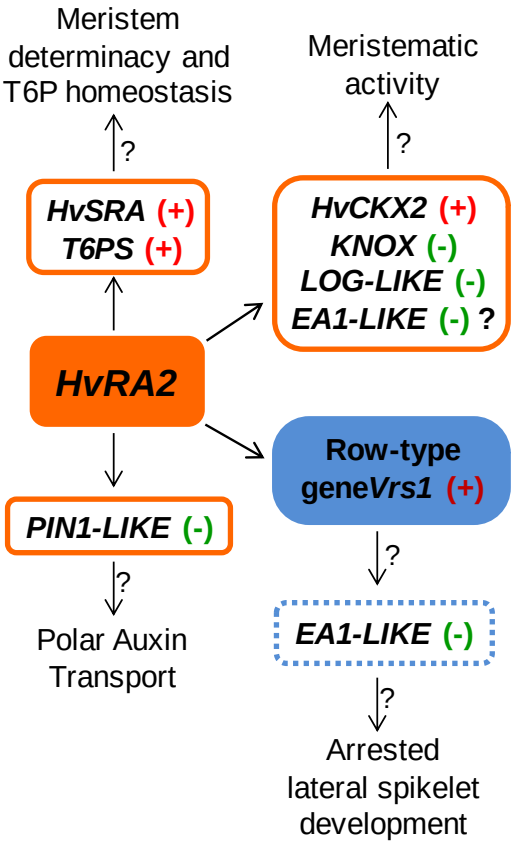

Figure 4.3.0. Models of *Vrs4* interactions showing putative targets of *HvRA2*.

HvRA2 may regulate transcripts of trehalose-6-phosphate synthase (TPS) and *HvSRA*, a putative trehalose-6-phosphate phosphatase, thereby maintaining T6P homeostasis and spikelet determinacy. In *Vrs4*, transcript levels of *PIN1-LIKE* are maintained at constant level but are up-regulated in *vrs4*. In wild type plants, *HvRA2* functions up-stream of *HvHox1* (*Vrs1*), which in turn may down-regulate transcripts of *EA1-LIKE*, resulting in abortion of lateral florets, possibly producing a two-rowed spike (hypothetical). However, up-regulation of *EA1-LIKE* in *vrs4* mutants may likely be due to enhanced meristematic activity related to the six-rowed spike phenotype and additional spikelets/florets. Transcript levels of genes involved in meristematic

activity, e.g. cytokinin oxidase (*CKX2*), *LONELY GUY-LIKE* and *KNOX* genes are also regulated by *HvRA2*. + and – signs indicate up and down-regulation respectively in the wild type (*Vrs4* – two-rowed condition).

4.4. The reduced sequence variation at *HvRA2* may represent purifying selection

The re–sequencing data of *HvRA2* (*Vrs4*) across diverse barley germplasm showed very limited and synonymous natural variation. The 3'UTR region was completely conserved across the 77 genotypes surveyed. A highly reduced level of polymorphisms in the 3' regulatory regions was also observed in maize domestication loci *RA1* (Sigmon and Vollbrecht, 2010) and *GRASSY TILLERS1* (Whipple et al., 2011). Unlike *Vrs1* and *Int–c*, *Vrs4* did not show any natural variation that contributes to differences in row–type. One possible reason for such low level of natural sequence variation may be is the result of purifying selection (negative selection) of the naturally occurred variation at *Vrs4* in two– and six–rowed barleys in the past, which otherwise would be deleterious and disrupts determinate nature of the TSM, leading to disordered spike formation. In case of strong purifying selection, purging of deleterious mutations results in occasional removal of linked variation producing a decrease in the level of variation surrounding the locus under negative selection. A sequence polymorphism survey around the *Vrs4* locus in two of the mapping parents BW–NIL(*vrs4.k*) and Golden Promise used in the present study revealed very much reduced variation (2 SNPs in approximately 60 kb of sequence surveyed). This could be the effect of naturally occurred purifying selection in the *Vrs4* genomic region. However, a more detailed sequence analysis in and around the *Vrs4* locus is required in order to make such claims. The other possible reason for such a low level of polymorphism might be due to the suppressed meiotic recombination in the *Vrs4* genomic region resulting in a genetic variation bottleneck.

In cultivated barley, the *intermedium* spike types with enlarged lateral spikelets/florets represent a large and diverse phenotypic row–type class. The phenotypic analysis of weak *vrs4* mutant alleles showed reduced determinacy of TSM and a row–type phenotype which is analogous with *intermedium* barleys (**Figure 3.1.3**). In the present study, the sequence variation at the *Vrs4* locus was not sampled in *intermedium* barleys. It might be possible that the weaker natural mutant alleles of *vrs4*, which do not show a major effect on determinate nature of TSM, are still hidden in *intermedium* barleys.

5.0. Outlook

Unlike barley, the sorghum and rice panicles are branched. The *RAMOSA2* expression in these species starts after the initiation of primary branch meristems (Bortiri et al., 2006). In branchless barley inflorescence, *HvRA2* expression initiates as early as double ridge stage, which is regarded as the first reproductive phase (temporally ahead compared with rice and Sorghum *RA2* expression), whereas at triple mound stage the *HvRA2* expression is localized in lateral spikelet meristems and also within the boundary domain between central and lateral spikelet meristems, most likely confining the TSM to three spikelets (Koppolu et al., 2013). This indicates that the expression pattern of *HvRA2* is important for the number of spikelet meristems at each rachis internode and subsequently TSM identity in barley. Based on such spatial and temporal expression pattern regulation of *RA2* in rice (*OsRA2*), sorghum (*SbRA2*), and barley (*HvRA2*) one could hypothesize that timing of *RA2* expression is crucial for the confinement of number of spikelet meristems in these species. Such hypothesis can be tested by promoter swapping experiments. For example, the barley *RA2* coding sequence (CDs) can be swapped with *SbRA2* or *OsRA2* promoter and complemented into a *vrs4* mutant to see whether the barley CDs driven by these heterologous promoters could completely recover a functional *Vrs4* phenotype

(determinate TSM and two-rowed spike). If the expression of *HvRA2* is delayed under Sorghum or rice *RA2* promoter, the wild type phenotype (determinate TSM and two-rowed spike) may be partially restored. Within the tribe Triticeae, the TSM is only seen in barley, whereas the other species in this tribe including wheat, rye, and triticale possess single spikelet meristem at each rachis internode. The double ridge stage seen in barley is also evident in the spike development of wheat; however, the double ridge in wheat differentiates into one spikelet meristem instead of three as seen in barley. Such a difference in number of spikelets per rachis internode in closely related species (wheat and barley) could be due to the dosage effect of *RA2* expression at double ridge stage in these two species (*HvRA2* starts to express from double ridge stage, **Figure 4.1.2-1.C**). It could be hypothesized that expression of *RA2* in wheat at double ridge is much stronger than in barley, which results in only one spikelet per rachis internode. This can be simply tested by driving *RA2* expression in barley under wheat *RA2* promoter to validate the promoter activity differences of wheat and barley *RA2*. These experiments will give an understanding about the correlation between inflorescence morphology and gene expression pattern and also whether the changes in gene expression pattern are causative of observed morphological changes. Results obtained from such studies would provide a better understanding and a deeper insight into the origin of different inflorescence architectures in grasses.

Two independent and elegant studies, conducted by Gendron et al. (2012) and Bell et al. (2012) demonstrated the importance of brassinosteroid (BR) homeostasis in organ boundary formation in Arabidopsis. Bell et al. (2012) showed that the *Arabidopsis* LOB domain transcription factor negatively regulates BR accumulation by directly activating a BR inactivating enzyme (*BAS1*) thereby down-regulating the BR levels in the boundary domain between organ primordia and SAM, promoting organ boundary formation. The expanded LOB expression domain in

brassinazole resistant1 (*bzr1*) mutants with elevated BR concentrations lead to organ fusion (Bell et al., 2012). Consistent with this several members of the LBD gene family were identified as *BZR1* target genes (Sun et al., 2010). In line with these findings, the mRNA *in situ* data showed that *HvRA2* (a LBD family transcription factor) localizes with in Lateral Spikelet primordia (LS) and the boundary between LS and central spikelets (CS) at triple mound stage (**Figure 4.1.2-1.E**). Because *HvRA2* activity is lost in barley *vrs4* mutant inflorescences, the boundary formation between the SMs within the TSM is affected; probably due to the disturbed brassinosteroid homeostasis (brassinosteriod homeostasis might be under the control of HvRA2). It has also been shown that accumulation of *DWARF4*, a key brassinosteroid biosynthetic gene is stimulated by auxin response (Chung et al., 2011). The expression analysis revealed elevated expression of *PIN1-LIKE* gene in *vrs4* mutants, which may probably elevate auxin transport, activity and subsequently more BR accumulation in *vrs4* inflorescences resulting in failure of boundary formation between the SMs within the TSM. However, a more detailed future work is needed to confirm this phenomenon in barley *vrs4* mutants by conducting experiments such as (1) measurement of brassinosteroid and auxin concentrations in *vrs4* mutants, WTs and also the transgenic lines over-expressing *HvRA2*. (2) Independently, the brassinosteriod accumulation can be manipulated in *vrs4* mutants, (for example suppression of excessive brassinosteriod accumulation) and the corresponding phenotypes can be evaluated.

It would be important to understand the molecular gene regulatory networks underlying *HvRA2* that shape the architecture of barley inflorescence. *HvRA2* encodes a LOB domain transcription factor. Transcription factors are known to modulate gene expression by binding to the *cis*-regulatory regions of their target genes. The global binding targets of the transcription factors can be identified by methods like chromatin immune precipitation sequencing (Chip seq). This

method has already been proven useful for identifying binding targets and molecular networks of maize TFs like *RAMOSA1* (Eveland et al., 2014), *KNOTTED1* (Bolduc et al., 2012) and *IDEAL PLANT ARCHITECTURE1* (Lu et al., 2013) of rice. Elucidation of gene regulatory networks underlying *HvRA2* using chipseq would provide a molecular mechanism underlying inflorescence development in barley and probably other closely related species (Triticeae). In the present study, the microarray analysis was conducted to identify the differentially regulated genes between *vrs4* mutants and wild types. However, the current 60 K microarray does not represent a complete barley gene set, which can potentially lead to missing of important gene regulation. This problem can be circumvented by using RNA sequencing by which the global expression differences between *vrs4* mutants and wild types can be assessed on a rather complete scale. By using methods like chipseq and RNA seq it would be possible to identify the direct targets of *Vrs4*. Elucidation of the mechanisms of interaction among these targets and further functional evaluation of these targets in *HvRA2* gene regulatory network forms an important and exciting follow up study to the present work.

6.0. Summary

Inflorescence architecture of barley (*Hordeum vulgare* L.) is commonly observed among Triticeae species, which bear one to many spikelets at each rachis internode. The triple spikelet meristem (TSM) is one of the unique features during barley spike development, in which three spikelets (one central and two lateral spikelets) are produced at each rachis internode. Based on the fertility of the lateral spikelets, the barley spikes can be categorized into two- and six-rowed spikes. The two-rowed spikes possess sterile lateral spikelets (two kernel rows); whereas the six-rowed spikes show fertile lateral spikelets (six kernel rows) and produce increased grain yield per spike compared to two-rowed spikes. The conversion from a two-rowed spike to a six-rowed spike is majorly controlled by *Vrs1*, which encodes a homeodomain-leucine zipper class I homeobox protein (Komatsuda et al., 2007). Lateral spikelet fertility and floret size is quantitatively regulated by another locus, *int-c*, which encodes the barley ortholog of maize TEOSINTE BRANCHED1 (Ramsay et al., 2011.)

In the present study, with the help of genetic mapping and mutant analysis, the genetic determinant underlying another row-type locus, Six-rowed spike 4 (*Vrs4*), has been identified as the barley ortholog of the maize (*Zea mays* L.) inflorescence architecture gene *RAMOSA2* (*RA2*). The *RA2* had already been implicated in the control of inflorescence branch architecture in maize and is one of the important regulators of the maize *RAMOSA* pathway (Vollbrecht et al. 2005; Bortiri et al. 2006; Satoh-Nagasawa et al. 2006). The *vrs4* mutant analysis showed that eighteen coding mutations (out of 20 allelic mutants) in barley *RA2* (*HvRA2*) were specifically associated with lateral spikelet fertility and loss of spikelet meristem determinacy. Expression analyses through mRNA *in situ* hybridization and microarray showed that *Vrs4* (*HvRA2*) controls the row-type pathway through *Vrs1* (*HvHox1*), a negative regulator of lateral spikelet fertility in barley.

Moreover, *Vrs4* may also regulate transcripts of barley's *SISTER OF RAMOSA3* (*HvSRA*), a putative trehalose-6-phosphate phosphatase (TPP), involved in T6P homeostasis. The T6P homeostasis has already been implicated to control spikelet determinacy in maize; a similar mechanism might be responsible inflorescence development in barley. The global gene expression data obtained by microarray analysis illustrated that although *RA2* is conserved among different grass species, its down-stream target genes appear to be modified in barley and possibly other species of tribe Triticeae giving rise to various inflorescence architectures in different species.

7.0. Zusammenfassung

Die Blütenstandsarchitektur der Gerste (*Hordeum vulgare* L.) ist ein typisches Merkmal vieler Triticeae-Arten, wobei i.d.R. ein bis mehrere Ährchen pro Spindelstufe gebildet werden. Das sog. Dreifache-Ährchen-Meristem (Triple-Spikelet-Meritem, TSM) ist ein Alleinstellungs-merkmal der Gattung *Hordeum*, wodurch es der Gerste ermöglicht wird, drei Ährchen pro Spindelstufe zu bilden (ein sog. Zentral- und zwei Lateral-Ährchen). Basierend auf der Fertilität der Lateral-Ärchen wird Gerste i.d.R. in zwei Zeiligkeitsklassen unterteilt: zwei- und sechszeilige Gerste. Zweizeilige Gerstenähren zeigen dabei sterile Lateral-Ährchen (nur zwei Körner), wohingegen sechszeilige Ähren fertile Lateral-Ärchen besitzen (sechs Körner) und daher im Vergleich mit zweizeiligen Ähren einen erhöhten Kornertrag pro Ähre aufweisen. In Kulturgersten ist der Unterschied zwischen zwei- und sechzeiliger Gerste i.d.R. durch das *Vrs1* Gen bestimmt, welches für ein HD-Leucin zipper class I homeo box Protein kodiert (Komatsuda et al. 2007). Allerdings kann die Fertilität der Lateral-Ährchen sowie die Grösse der Lateral-Blütchen auch durch den *Int-c* Lokus, für welchen das Gersten-Orthololog des Mais *TEOSINTE BRANCHED1* kodiert (Ramsay et al. 2011), in quantitativer Weise reguliert werden.

In der vorliegenden Arbeit wurde mit Hilfe von Kartierungs- und Mutantenanalysen die genetische Grundlage des Zeiligkeitslokus Six-rowed spike 4 (*Vrs4*) als Gersten-Ortholog des Mais (*Zea mays* L.) Blütenstandgens *RAMOSA2* (*RA2*) idenfiziert. *RA2* ist ein wichtiger Teil des in Mais vorkommenden RAMOSA-Pathways (Vollbrecht et al. 2005; Bortiri et al. 2006; Satoh-Nagasawa et al. 2006). Die *vrs4*-Mutantenanalyse in Gerste zeigte, dass 18 Mutationen im kodierenden Bereich des Gersten-*RA2* (*HvRA2*) Gens spezifisch mit der Fertilität der Lateral-Ährchen und dem Verlust der Ährchenmeristem-Determinierung assoziiert waren. Expressionanalysen mittels mRNA *in situ*-Hybridisierung und Microarrays zeigten, dass *Vrs4*

(*HvRA2*) über das Zeiligkeitsgen *Vrs1* (*HvHox1*), einem negativen Regulator der Fertilität der Lateral-Ährchen in Gerste, den sog. Zeiligkeits-Pathway kontrolliert. Desweiteren zeigten die Arbeiten, dass *Vrs4* möglicherweise auch die Transkripte einer putativen Trehalose-6-Phosphat Phosphatase (TPP), das Gerstengen *SISTER OF RAMOSA3* (*HvSRA*), reguliert und hierüber u.U. an der T6P-Homeostase beteiligt ist. Dass die T6P-Homeostase bereits die Anzahl der Ährchen determinieren kann, wurde bereits in Mais gezeigt; ein ähnlicher Mechanismus könnte auch in Gerste für die Blütenstandsentwicklung vorliegen. Die durchgeführte globale Genexpressionsanalyse mittels Microarray in Gerste illustrierte dabei deutlich, dass sich, obwohl das RA2 Protein in vielen verschiedenen Gras-Arten vorkommt, die gefundenen Geninteraktionen in Gerste, und auch möglicherweise anderer Triticeae-Arten, klar von denen in Mais unterscheiden. Die so detektierten Geninteraktionsunterschiede tragen möglicherweise zur Diversität der Blütenständsbildung verschiedener Gräserarten bei.

8.0. References

Albinsky D., Kusano M., Higuchi M., Hayashi N., Kobayashi M., Fukushima A., Mori M., Ichikawa T., Matsui K., Kuroda H., Horii Y., Tsumoto Y., Sakakibara H., Hirochika H., Matsui M., Saito K. (2010) Metabolomic screening applied to rice fox Arabidopsis lines leads to the identification of a gene-changing nitrogen metabolism. Molecular Plant 3:125-142.

Amasino R. (2010) Seasonal and developmental timing of flowering. The Plant Journal 61:1001-1013.

Ashikari M., Sakakibara H., Lin S., Yamamoto T., Takashi T., Nishimura A., Angeles E.R., Qian Q., Kitano H., Matsuoka M. (2005) Cytokinin oxidase regulates rice grain production. Science 309:741-745.

Baena-Gonzalez E., Rolland F., Thevelein J.M., Sheen J. (2007) A central integrator of transcription networks in plant stress and energy signalling. Nature 448:938-942.

Bai F., Reinheimer R., Durantini D., Kellogg E.A., Schmidt R.J. (2012) TCP transcription factor, BRANCH ANGLE DEFECTIVE 1 (BAD1), is required for normal tassel branch angle formation in maize. Proceedings of the National Academy of Sciences 109:12225-12230.

Baik B.K., Ullrich S.E. (2008) Barley for food: Characteristics, improvement, and renewed interest. Journal of Cereal Science 48:233-242.

Bartrina I., Otto E., Strnad M., Werner T., Schmülling T. (2011) Cytokinin regulates the activity of reproductive meristems, flower organ size, ovule formation, and thus seed yield in *Arabidopsis thaliana*. The Plant Cell 23:69-80.

Bell E.M., Lin W.-c., Husbands A.Y., Yu L., Jaganatha V., Jablonska B., Mangeon A., Neff M.M., Girke T., Springer P.S. (2012) Arabidopsis LATERAL ORGAN BOUNDARIES negatively regulates brassinosteroid accumulation to limit growth in organ boundaries. Proceedings of the National Academy of Sciences 109:21146-21151.

Blázquez M.A., Santos E., Flores C.-l., Martínez-Zapater J.M., Salinas J., Gancedo C. (1998) Isolation and molecular characterization of the Arabidopsis TPS1 gene, encoding trehalose-6-phosphate synthase. The Plant Journal 13:685-689.

Boch J., Scholze H., Schornack S., Landgraf A., Hahn S., Kay S., Lahaye T., Nickstadt A., Bonas U. (2009) Breaking the code of DNA binding specificity of TAL-type III Effectors. Science 326:1509-1512.

Boddu J., Cho S., Kruger W.M., Muehlbauer G.J. (2006) Transcriptome analysis of the barley-*Fusarium graminearum* interaction. Molecular Plant-Microbe Interactions 19:407-417.

Bolduc N., Yilmaz A., Mejia-Guerra M.K., Morohashi K., O'Connor D., Grotewold E., Hake S. (2012) Unraveling the *KNOTTED1* regulatory network in maize meristems. Genes & Development 26:1685-1690.

Bommert P., Satoh-Nagasawa N., Jackson D., Hirano H.-Y. (2005) Genetics and evolution of inflorescence and flower development in grasses. Plant and Cell Physiology 46:69-78.

Bommert P., Je B., Goldshmidt A., Jackson D. (2013) The maize *Gα* gene *COMPACT PLANT2* functions in *CLAVATA* signalling to control shoot meristem size. Nature 502:555-558.

Bortiri E., Chuck G., Vollbrecht E., Rocheford T., Martienssen R., Hake S. (2006) *ramosa2* encodes a LATERAL ORGAN BOUNDARY domain protein that determines the fate of stem cells in branch meristems of maize. Plant Cell 18:574-585.

Bossinger G., Lundqvist U., Rohde W., Salamini F. (1992) Genetics of plant development in barley, in: L. Munck (Ed.), Barley Genetics VI, Munksgaard International Publishers, Copenhagen, DK. pp. 989-1017.

Brueggeman R., Rostoks N., Kudrna D., Kilian A., Han F., Chen J., Druka A., Steffenson B., Kleinhofs A. (2002) The barley stem rust-resistance gene *Rpg1* is a novel disease-resistance gene with homology to receptor kinases. Proceedings of the National Academy of Sciences 99:9328-9333.

Brueggeman R., Druka A., Nirmala J., Cavileer T., Drader T., Rostoks N., Mirlohi A., Bennypaul H., Gill U., Kudrna D., Whitelaw C., Kilian A., Han F., Sun Y., Gill K., Steffenson B., Kleinhofs A. (2008) The stem rust resistance gene *Rpg5* encodes a protein with nucleotide-binding-site, leucine-rich, and protein kinase domains. Proceedings of the National Academy of Sciences 105:14970-14975.

Burge C., Karlin S. (1997) Prediction of complete gene structures in human genomic DNA. Journal of Molecular Biology 268:78-94.

Buschges R., Hollricher K., Panstruga R., Simons G., Wolter M., Frijters A., vanDaelen R., vanderLee T., Diergaarde P., Groenendijk J., Topsch S., Vos P., Salamini F., Schulze-Lefert P. (1997) The barley *mlo* gene: A novel control element of plant pathogen resistance. Cell 88:695-705.

Cabib E., Leloir L.F. (1958) The biosynthesis of trehalose phosphate. Journal of Biological Chemistry 231:259-275.

Caldo R.A., Nettleton D., Wise R.P. (2004) Interaction-dependent gene expression in *Mla*-specified response to barley powdery mildew. Plant Cell 16:2514-2528.

Caldo R.A., Nettleton D., Peng J.Q., Wise R.P. (2006) Stage-specific suppression of basal defense discriminates barley plants containing fast- and delayed-acting *Mla* powdery mildew resistance alleles. Molecular Plant-Microbe Interactions 19:939-947.

Campoli C., Pankin A., Drosse B., Casao C.M., Davis S.J., von Korff M. (2013) *HvLUX1* is a candidate gene underlying the *early maturity 10* locus in barley: phylogeny, diversity, and interactions with the circadian clock and photoperiodic pathways. New Phytologist 199:1045-1059.

Carillo P., Feil R., Gibon Y., Satoh-Nagasawa N., Jackson D., Blasing O.E., Stitt M., Lunn J.E. (2013) A fluorometric assay for trehalose in the picomole range. Plant Methods 9:21.

Carroll S.B. (2005) Evolution at two levels: On genes and form. Plos Biology 3:1159-1166.

Chalfun A., Franken J., Mes J.J., Marsch-Martinez N., Pereira A., Angenent G.C. (2005) *ASYMMETRIC LEAVES2-LIKE1* gene, a member of the *AS2/LOB* family, controls proximal-distal patterning in Arabidopsis petals. Plant Molecular Biology 57:559-575.

Chen J., Moreau C., Liu Y., Kawaguchi M., Hofer J., Ellis N., Chen R. (2012) Conserved genetic determinant of motor organ identity in Medicago truncatula and related legumes. Proceedings of the National Academy of Sciences 109:11723-11728.

Chono M., Honda I., Zeniya H., Yoneyama K., Saisho D., Takeda K., Takatsuto S., Hoshino T., Watanabe Y. (2003) A semidwarf phenotype of barley *uzu* results from a nucleotide substitution in the gene encoding a putative brassinosteroid receptor. Plant Physiology 133:1209-1219.

Chu H., Qian Q., Liang W., Yin C., Tan H., Yao X., Yuan Z., Yang J., Huang H., Luo D., Ma H., Zhang D. (2006) The *FLORAL ORGAN NUMBER4* gene encoding a putative ortholog of Arabidopsis CLAVATA3 regulates apical meristem size in rice. Plant Physiology 142:1039-1052.

Chuck G., Meeley R.B., Hake S. (1998) The control of maize spikelet meristem fate by the *APETALA2-like* gene *indeterminate spikelet1*. Genes & Development 12:1145-1154.

Chuck G., Meeley R., Hake S. (2008) Floral meristem initiation and meristem cell fate are regulated by the maize *AP2* genes *ids1* and *sid1*. Development 135:3013-3019.

Chuck G., Muszynski M., Kellogg E., Hake S., Schmidt R.J. (2002) The control of spikelet meristem identity by the *branched silkless1* gene in maize. Science 298:1238-1241.

Chung Y., Maharjan P.M., Lee O., Fujioka S., Jang S., Kim B., Takatsuto S., Tsujimoto M., Kim H., Cho S., Park T., Cho H., Hwang I., Choe S. (2011) Auxin stimulates *DWARF4* expression and brassinosteroid biosynthesis in Arabidopsis. The Plant Journal 66:564-578.

Clifford H. (1987) Spikelet and floral morphology, in: K. Hilu, et al. (Eds.), Grass Systematics and Evolution, Smithsonian Institution Press, Washington DC. pp. 21-30.

Close T.J., Wanamaker S.I., Caldo R.A., Turner S.M., Ashlock D.A., Dickerson J.A., Wing R.A., Muehlbauer G.J., Kleinhofs A., Wise R.P. (2004) A new resource for cereal genomics: 22K barley GeneChip comes of age. Plant Physiology 134:960-968.

Close T.J., Bhat P.R., Lonardi S., Wu Y.H., Rostoks N., Ramsay L., Druka A., Stein N., Svensson J.T., Wanamaker S., Bozdag S., Roose M.L., Moscou M.J., Chao S.A.M., Varshney R.K., Szucs P., Sato K., Hayes P.M., Matthews D.E., Kleinhofs A., Muehlbauer G.J., DeYoung J., Marshall D.F., Madishetty K., Fenton R.D., Condamine P., Graner A., Waugh R. (2009) Development and implementation of high-throughput SNP genotyping in barley. BMC Genomics 10:582.

Cockram J., White J., Zuluaga D.L., Smith D., Comadran J., Macaulay M., Luo Z., Kearsey M.J., Werner P., Harrap D., Tapsell C., Liu H., Hedley P.E., Stein N., Schulte D., Steuernagel B., Marshall D.F., Thomas W.T.B., Ramsay L., Mackay I., Balding D.J., Consortium T.A., Waugh R., O'Sullivan D.M. (2010) Genome-wide association mapping to candidate polymorphism resolution in the unsequenced barley genome. Proceedings of the National Academy of Sciences 107:21611-21616.

Collins N.C., Thordal-Christensen H., Lipka V., Bau S., Kombrink E., Qiu J.L., Huckelhoven R., Stein M., Freialdenhoven A., Somerville S.C., Schulze-Lefert P. (2003) SNARE-protein-mediated disease resistance at the plant cell wall. Nature 425:973-977.

Comadran J., Kilian B., Russell J., Ramsay L., Stein N., Ganal M., Shaw P., Bayer M., Thomas W., Marshall D., Hedley P., Tondelli A., Pecchioni N., Francia E., Korzun V., Walther A., Waugh R. (2012) Natural variation in a homolog of Antirrhinum *CENTRORADIALIS* contributed to spring growth habit and environmental adaptation in cultivated barley. Nature Genetics 44:1388-1392.

Dolezel J., Greilhuber J., Lucretti S., Meister A., Lysak M.A., Nardi L., Obermayer R. (1998) Plant genome size estimation by flow cytometry: Inter-laboratory comparison. Annals of Botany 82:17-26.

Doyle J.J., Doyle J.L. (1990) Isolation of plant DNA from fresh tissue. Focus 12:13-15.

Druka A., Potokina E., Luo Z.W., Jiang N., Chen X.W., Kearsey M., Waugh R. (2010) Expression quantitative trait loci analysis in plants. Plant Biotechnology Journal 8:10-27.

Druka A., Franckowiak J., Lundqvist U., Bonar N., Alexander J., Houston K., Radovic S., Shahinnia F., Vendramin V., Morgante M., Stein N., Waugh R. (2011) Genetic dissection of barley morphology and development. Plant Physiolology 155:617-627.

Druka A., Muehlbauer G., Druka I., Caldo R., Baumann U., Rostoks N., Schreiber A., Wise R., Close T., Kleinhofs A., Graner A., Schulman A., Langridge P., Sato K., Hayes P.,

McNicol J., Marshall D., Waugh R. (2006) An atlas of gene expression from seed to seed through barley development. Functional & Integrative Genomics 6:202-211.

Edgar R.C. (2004) MUSCLE: multiple sequence alignment with high accuracy and high throughput. Nucleic Acids Research 32:1792-1797.

Elbaum R., Zaltzman L., Burgert I., Fratzl P. (2007) The role of wheat awns in the seed dispersal unit. Science 316:884-886.

Elbein A.D., Pan Y.T., Pastuszak I., Carroll D. (2003) New insights on trehalose: a multifunctional molecule. Glycobiology 13:17-27.

Eveland A.L., Goldshmidt A., Pautler M., Morohashi K., Liseron-Monfils C., Lewis M.W., Kumari S., Hiraga S., Yang F., Unger-Wallace E., Olson A., Hake S., Vollbrecht E., Grotewold E., Ware D., Jackson D. (2014) Regulatory modules controlling maize inflorescence architecture. Genome Research 24:431-443.

Faure S., Turner A.S., Gruszka D., Christodoulou V., Davis S.J., von Korff M., Laurie D.A. (2012) Mutation at the circadian clock gene *EARLY MATURITY 8* adapts domesticated barley (*Hordeum vulgare*) to short growing seasons. Proceedings of the National Academy of Sciences 109:8328-8333.

Forster B.P., Franckowiak J.D., Lundqvist U., Lyon J., Pitkethly I., Thomas W.T.B. (2007) The barley phytomer. Annals of Botany 100:725-733.

Franckowiak J.D., Lundqvist U. (2011) Descriptions of barley genetic stocks for 2011. Barley Genetics Newsletter 40:45-177.

Franckowiak J.D., Foster A.E., Pederson V.D., Pyler R.E. (1985) Registration of bowman barley. Crop Science 25:883-883.

Fukuyama T., Takahashi R., Hayashi J. (1982) Genetic studies on the induced six-rowed mutants in barley. Ber. Ohara Inst. landw. Biol., Okayama Univ. 18:99-113.

Furukawa J., Yamaji N., Wang H., Mitani N., Murata Y., Sato K., Katsuhara M., Takeda K., Ma J.F. (2007) An aluminum-activated citrate transporter in barley. Plant and Cell Physiology 48:1081-1091.

Gallavotti A., Long J.A., Stanfield S., Yang X.A., Jackson D., Vollbrecht E., Schmidt R.J. (2010) The control of axillary meristem fate in the maize *ramosa* pathway. Development 137:2849-2856.

Gallavotti A., Zhao Q., Kyozuka J., Meeley R.B., Ritter M.K., Doebley J.F., Enrico Pe M., Schmidt R.J. (2004) The role of *barren stalk1* in the architecture of maize. Nature 432:630-635.

Galweiler L., Guan C.H., Muller A., Wisman E., Mendgen K., Yephremov A., Palme K. (1998) Regulation of polar auxin transport by *AtPIN1* in Arabidopsis vascular tissue. Science 282:2226-2230.

Gaut B.S. (2002) Evolutionary dynamics of grass genomes. New Phytologist 154:15-28.

Gawroński P., Ariyadasa R., Himmelbach A., Poursarebani N., Kilian B., Stein N., Steuernagel B., Hensel G., Kumlehn J., Sehgal S.K., Gill B.S., Gould P., Hall A., Schnurbusch T. (2014) A distorted circadian clock causes early flowering and temperature-dependent variation in spike development in the *Eps-3A*^{m} mutant of einkorn wheat. Genetics.

Gendron J.M., Liu J.-S., Fan M., Bai M.-Y., Wenkel S., Springer P.S., Barton M.K., Wang Z.-Y. (2012) Brassinosteroids regulate organ boundary formation in the shoot apical meristem of Arabidopsis. Proceedings of the National Academy of Sciences 109:21152-21157.

Gottwald S., Bauer P., Komatsuda T., Lundqvist U., Stein N. (2009) TILLING in the two-rowed barley cultivar 'Barke' reveals preferred sites of functional diversity in the gene *HvHox1*. BMC Research Notes 2:1-14.

Graner A., Jahoor A., Schondelmaier J., Siedler H., Pillen K., Fischbeck G., Wenzel G., Herrmann R.G. (1991) Construction of an RFLP map of barley. Theoretical and Applied Genetics 83:250-256.

Gurushidze M., Hensel G., Hiekel S., Schedel S., Valkov V., Kumlehn J. Designer nuclease-mediated heritable gene knockout in barley – a TALEN approach. Unpublished.

Hearnden P.R., Eckermann P.J., McMichael G.L., Hayden M.J., Eglinton J.K., Chalmers K.J. (2007) A genetic map of 1,000 SSR and DArT markers in a wide barley cross. Theoretical and Applied Genetics 115:383-391.

Hein I., Pacak M.B., Hrubikova K., Williamson S., Dinesen M., Soenderby I.E., Sundar S., Jarmolowski A., Shirasu K., Lacomme C. (2005) Virus-induced gene silencing-based functional characterization of genes associated with powdery mildew resistance in barley. Plant Physiology 138:2155-2164.

Hensel G., Himmelbach A., Chen W., Douchkov D.K., Kumlehn J. (2011) Transgene expression systems in the Triticeae cereals. Journal of Plant Physiology 168:30-44.

Hoheisel J.D. (2006) Microarray technology: beyond transcript profiling and genotype analysis. Nature Reviews Genetics 7:200-210.

Holzberg S., Brosio P., Gross C., Pogue G.P. (2002) Barley stripe mosaic virus-induced gene silencing in a monocot plant. Plant Journal 30:315-327.

Houston K., Druka A., Bonar N., Macaulay M., Lundqvist U., Franckowiak J., Morgante M., Stein N., Waugh R. (2012) Analysis of the barley bract suppression gene *Trd1*. Theoretical and Applied Genetics 125:33-45.

Houston K., McKim S.M., Comadran J., Bonar N., Druka I., Uzrek N., Cirillo E., Guzy-Wrobelska J., Collins N.C., Halpin C., Hansson M., Dockter C., Druka A., Waugh R. (2013) Variation in the interaction between alleles of *HvAPETALA2* and *microRNA172* determines the density of grains on the barley inflorescence. Proceedings of the National Academy of Sciences 110:16675-16680.

Huang X., Qian Q., Liu Z., Sun H., He S., Luo D., Xia G., Chu C., Li J., Fu X. (2009) Natural variation at the *DEP1* locus enhances grain yield in rice. Nature Genetics 41:494-497.

Husbands A., Bell E., Shuai B., Smith H., Springer P. (2007) LATERAL ORGAN BOUNDARIES defines a new family of DNA-binding transcription factors and can interact with specific bHLH proteins. Nucleic Acids Research 35:6663-6671.

IBSC. (2012) A physical, genetic and functional sequence assembly of the barley genome. Nature 491:711-716.

Ikeda-Kawakatsu K., Ito M., Nagasawa N., Kyozuka J., Nagato Y. (2007) Rice *ABERRANT PANICLE ORGANIZATION 1*, encoding an F-box protein, regulates meristem fate. The Plant Journal 51:1030-1040.

Ikeda-Kawakatsu K., Maekawa M., Izawa T., Itoh J.-I., Nagato Y. (2012) *ABERRANT PANICLE ORGANIZATION 2/RFL*, the rice ortholog of Arabidopsis *LEAFY*, suppresses the transition from inflorescence meristem to floral meristem through interaction with *APO1*. The Plant Journal 69:168-180.

Irish V.F. (2010) The flowering of Arabidopsis flower development. The Plant Journal 61:1014-1028.

Isidore E., Scherrer B., Bellec A., Budin K., Faivre-Rampant P., Waugh R., Keller B., Caboche M., Feuillet C., Chalhoub B. (2005) Direct targeting and rapid isolation of BAC clones spanning a defined chromosome region. Functional & Integrative Genomics 5:97-103.

Jeon J.-S., Jang S., Lee S., Nam J., Kim C., Lee S.-H., Chung Y.-Y., Kim S.-R., Lee Y.H., Cho Y.-G., An G. (2000) *leafy hull sterile1* Is a homeotic mutation in a rice *MADS BOX* gene affecting rice flower development. Plant Cell 12:871-884.

Jiao Y., Wang Y., Xue D., Wang J., Yan M., Liu G., Dong G., Zeng D., Lu Z., Zhu X., Qian Q., Li J. (2010) Regulation of *OsSPL14* by *OsmiR156* defines ideal plant architecture in rice. Nature Genetics 42:541-544.

Joung J.K., Sander J.D. (2013) INNOVATION TALENs: a widely applicable technology for targeted genome editing. Nature Reviews Molecular Cell Biology 14:49-55.

Kaplinsky N.J., Freeling M. (2003) Combinatorial control of meristem identity in maize inflorescences. Development 130:1149-1158.

Kellogg E. (2007) Floral displays: genetic control of grass inflorescences. Current Opinion in Plant Biollogy 10:26-31.

Kellogg E.A. (2001) Evolutionary history of the grasses. Plant Physiology 125:1198-1205.

Kleinhofs A., Kilian A., Maroof M.A.S., Biyashev R.M., Hayes P., Chen F.Q., Lapitan N., Fenwick A., Blake T.K., Kanazin V., Ananiev E., Dahleen L., Kudrna D., Bollinger J., Knapp S.J., Liu B., Sorrells M., Heun M., Franckowiak J.D., Hoffman D., Skadsen R., Steffenson B.J. (1993) A molecular, isozyme and morphological map of the barley (*Hordeum vulgare*) genome. Theoretical and Applied Genetics 86:705-712.

Komatsu K., Maekawa M., Ujiie S., Satake Y., Furutani I., Okamoto H., Shimamoto K., Kyozuka J. (2003a) *LAX* and *SPA*: Major regulators of shoot branching in rice. Proceedings of the National Academy of Sciences 100:11765-11770.

Komatsu M., Chujo A., Nagato Y., Shimamoto K., Kyozuka J. (2003b) *FRIZZY PANICLE* is required to prevent the formation of axillary meristems and to establish floral meristem identity in rice spikelets. Development 130:3841-3850.

Komatsuda T., Pourkheirandish M., He C.F., Azhaguvel P., Kanamori H., Perovic D., Stein N., Graner A., Wicker T., Tagiri A., Lundqvist U., Fujimura T., Matsuoka M., Matsumoto T., Yano M. (2007) Six-rowed barley originated from a mutation in a homeodomain-leucine zipper I-class homeobox gene. Proceedings of the National Academy of Sciences 104:1424-1429.

Komiya R., Ikegami A., Tamaki S., Yokoi S., Shimamoto K. (2008) *Hd3a* and *RFT1* are essential for flowering in rice. Development 135:767-774.

Koppolu R., Anwar N., Sakuma S., Tagiri A., Lundqvist U., Pourkheirandish M., Rutten T., Seiler C., Himmelbach A., Ariyadasa R., Youssef H.M., Stein N., Sreenivasulu N., Komatsuda T., Schnurbusch T. (2013) *Six-rowed spike4* (*Vrs4*) controls spikelet determinacy and row-type in barley. Proceedings of the National Academy of Sciences 110:13198-13203.

Kurakawa T., Ueda N., Maekawa M., Kobayashi K., Kojima M., Nagato Y., Sakakibara H., Kyozuka J. (2007) Direct control of shoot meristem activity by a cytokinin-activating enzyme. Nature 445:652-655.

Laudencia-Chingcuanco D., Hake S. (2002) The *indeterminate floral apex1* gene regulates meristem determinacy and identity in the maize inflorescence. Development 129:2629-2638.

Lazakis C.M., Coneva V., Colasanti J. (2011) *ZCN8* encodes a potential orthologue of Arabidopsis FT florigen that integrates both endogenous and photoperiod flowering signals in maize. Journal of Experimental Botany 62:4833-4842.

Lee D.-Y., An G. (2012) Two *AP2* family genes, *SUPERNUMERARY BRACT* (*SNB*) and *OsINDETERMINATE SPIKELET 1* (*OsIDS1*), synergistically control inflorescence architecture and floral meristem establishment in rice. The Plant Journal 69:445-461.

Lee D.-Y., Lee J., Moon S., Park S.Y., An G. (2007) The rice heterochronic gene *SUPERNUMERARY BRACT* regulates the transition from spikelet meristem to floral meristem. The Plant Journal 49:64-78.

Li H., Liang W., Jia R., Yin C., Zong J., Kong H., Zhang D. (2010) The *AGL6-like* gene *OsMADS6* regulates floral organ and meristem identities in rice. Cell Research 20:299-313.

Livak K.J., Schmittgen T.D. (2001) Analysis of relative gene expression data using real-time quantitative PCR and the 2−ΔΔCT Method. Methods 25:402-408.

Lu Z., Yu H., Xiong G., Wang J., Jiao Y., Liu G., Jing Y., Meng X., Hu X., Qian Q., Fu X., Wang Y., Li J. (2013) Genome-wide binding analysis of the transcription activator *IDEAL PLANT ARCHITECTURE1* reveals a complex network regulating rice plant architecture. The Plant Cell 25:3743-3759.

Lundqvist U. (2009) Eighty years of Scandinavian barley mutation genetics and breeding, in: Q.Y.Shu (Ed.), Induced plant mutations in the genomics era. , Food and agricultural organization of the united nations, Rome. pp. 39-43.

Lundqvist U., Lundqvist A. (1988) Induced intermedium mutants in barley: origin, morphology and inheritance. Hereditas 108:13-26.

Lundqvist U., Franckowiak J.D. (2003) Diversity of barley mutants, in: R. vonBothmer, et al. (Eds.), Developments in Plant Genetics and Breeding, Elsevier. pp. 77-96.

Lundqvist U., Franckowiak J.D., Konishi T. (1997) New and revised descriptions of barley genes. Barley Genetics Newsletter 26:22-516.

Luo Z.W., Potokina E., Druka A., Wise R., Waugh R., Kearsey M.J. (2007) SFP genotyping from affymetrix arrays is robust but largely detects cis-acting expression regulators. Genetics 176:789-800.

Malcomber S.T., Preston J.C., Reinheimer R., Kossuth J., Kellogg E.A. (2006) Developmental gene evolution and the origin of grass inflorescence diversity, in: E. S. Douglas, et al. (Eds.), Advances in Botanical Research, Academic Press. pp. 425-481.

Mameaux S., Cockram J., Thiel T., Steuernagel B., Stein N., Taudien S., Jack P., Werner P., Gray J.C., Greenland A.J., Powell W. (2012) Molecular, phylogenetic and comparative genomic analysis of the cytokinin oxidase/dehydrogenase gene family in the Poaceae. Plant Biotechnology Journal 10:67-82.

Marcel T.C., Varshney R.K., Barbieri M., Jafary H., de Kock M.J.D., Graner A., Niks R.E. (2007) A high-density consensus map of barley to compare the distribution of QTLs for partial resistance to *Puccinia hordei* and of defence gene homologues. Theoretical and Applied Genetics 114:487-500.

Martinez-Barajas E., Delatte T., Schluepmann H., de Jong G.J., Somsen G.W., Nunes C., Primavesi L.F., Coello P., Mitchell R.A.C., Paul M.J. (2011) Wheat grain development is characterized by remarkable trehalose 6-phosphate accumulation pregrain filling: Tissue distribution and relationship to SNF1-related protein kinase1 activity. Plant Physiology 156:373-381.

Marton M.L., Cordts S., Broadhvest J., Dresselhaus T. (2005) Micropylar pollen tube guidance by *EGG APPARATUS 1* of maize. Science 307:573-576.

Marwat S.K., Hashimi M., Usman Khan K., Aslam Khan M., Shoaib M., Rehman F. (2012) Barley (*Hordeum vulgare* L.) a prophetic food mentioned in ahadith and its ethnobotanical importance. American-Eurasian Journal of Agricultural & Environmental Sciences 12:835-841.

Mascher M., Richmond T.A., Gerhardt D.J., Himmelbach A., Clissold L., Sampath D., Ayling S., Steuernagel B., Pfeifer M., D'Ascenzo M., Akhunov E.D., Hedley P.E., Gonzales A.M., Morrell P.L., Kilian B., Blattner F.R., Scholz U., Mayer K.F.X., Flavell A.J., Muehlbauer G.J., Waugh R., Jeddeloh J.A., Stein N. (2013) Barley whole exome capture: a tool for genomic research in the genus *Hordeum* and beyond. The Plant Journal 76:494-505.

Mayer K., Martis M., Hedley P., Simková H., Liu H., Morris J., Steuernagel B., Taudien S., Roessner S., Gundlach H., Kubaláková M., Suchánková P., Murat F., Felder M., Nussbaumer T., Graner A., Salse J., Endo T., Sakai H., Tanaka T., Itoh T., Sato K., Platzer M., Matsumoto T., Scholz U., Dolezel J., Waugh R., Stein N. (2011) Unlocking the barley genome by chromosomal and comparative genomics. Plant cell 23:1249-1263.

McSteen P., Malcomber S., Skirpan A., Lunde C., Wu X.T., Kellogg E., Hake S. (2007) *barren inflorescence2* encodes a co-ortholog of the PINOID serine/threonine kinase and is required for organogenesis during inflorescence and vegetative development in maize. Plant Physiology 144:1000-1011.

Meyer M., Stenzel U., Hofreiter M. (2008) Parallel tagged sequencing on the 454 platform. Nature Protocols 3:267-278.

Miller M.B., Tang Y.W. (2009) Basic concepts of microarrays and potential applications in clinical microbiology. Clinical Microbiology Reviews 22:611-633.

Miura K., Ikeda M., Matsubara A., Song X.-J., Ito M., Asano K., Matsuoka M., Kitano H., Ashikari M. (2010) *OsSPL14* promotes panicle branching and higher grain productivity in rice. Nature Genetics 42:545-549.

Mrizova K., Jiskrova E., Vyroubalova S., Novak O., Ohnoutkova L., Pospisilova H., Frebort I., Harwood W.A., Galuszka P. (2013) Overexpression of cytokinin dehydrogenase genes in barley (*Hordeum vulgare* cv. Golden Promise) fundamentally affects morphology and fertility. PLoS ONE 8:11.

Muller K.J., Romano N., Gerstner O., Garcia-Marotot F., Pozzi C., Salamini F., Rohde W. (1995) The barley *Hooded* mutation caused by a duplication in a homeobox gene intron. Nature 374:727-730.

Nair S.K., Wang N., Turuspekov Y., Pourkheirandish M., Sinsuwongwat S., Chen G., Sameri M., Tagiri A., Honda I., Watanabe Y., Kanamori H., Wicker T., Stein N., Nagamura Y., Matsumoto T., Komatsuda T. (2010) Cleistogamous flowering in barley arises from the suppression of *microRNA*-guided *HvAP2* mRNA cleavage. Proceedings of the National Academy of Sciences 107:490-495.

Neff M.M., Turk E., Kalishman M. (2002) Web-based primer design for single nucleotide polymorphism analysis. Trends in Genetics 18:613-615.

Newman C.W., Newman R.K. (2006) A brief history of barley foods. Cereal Foods World 51:4-7.

O'Hara L.E., Paul M.J., Wingler A. (2013) How do sugars regulate plant growth and development? New insight into the role of trehalose-6-phosphate. Molecular Plant 6:261-274.

Ohmori S., Kimizu M., Sugita M., Miyao A., Hirochika H., Uchida E., Nagato Y., Yoshida H. (2009) *MOSAIC FLORAL ORGANS1*, an *AGL6-Like MADS Box* gene, regulates floral organ identity and meristem fate in rice. Plant Cell 21:3008-3025.

Okushima Y., Fukaki H., Onoda M., Theologis A., Tasaka M. (2007) *ARF7* and *ARF19* regulate lateral root formation via direct activation of *LBD/ASL* genes in Arabidopsis. Plant Cell 19:118-130.

Okushima Y., Overvoorde P.J., Arima K., Alonso J.M., Chan A., Chang C., Ecker J.R., Hughes B., Lui A., Nguyen D., Onodera C., Quach H., Smith A., Yu G.X., Theologis A. (2005) Functional genomic analysis of the *AUXIN RESPONSE FACTOR* gene family members in *Arabidopsis thaliana*: Unique and overlapping functions of *ARF7* and *ARF19*. Plant Cell 17:444-463.

Ori N., Eshed Y., Chuck G., Bowman J.L., Hake S. (2000) Mechanisms that control *KNOX* gene expression in the Arabidopsis shoot. Development 127:5523-5532.

Paul M.J., Jhurreea D., Zhang Y., Primavesi L.F., Delatte T., Schluepmann H., Wingler A. (2010) Up-regulation of biosynthetic processes associated with growth by trehalose 6-phosphate. Plant Signaling & Behavior 5:386-392.

Pautler M., Tanaka W., Hirano H.-Y., Jackson D. (2013) Grass Meristems I: Shoot Apical Meristem Maintenance, Axillary Meristem Determinacy and the Floral Transition. Plant and Cell Physiology 54:302-312.

Potokina E., Druka A., Luo Z.W., Wise R., Waugh R., Kearsey M. (2008) Gene expression quantitative trait locus analysis of 16,000 barley genes reveals a complex pattern of genome-wide transcriptional regulation. Plant Journal 53:90-101.

Poursarebani N. (2012) A genetically anchored physical map of barley chromosome 2H, Agriculture, Martin Luther University of Halle, Halle. pp. 107.

Pozzi C., Faccioli P., Terzi V., Stanca A.M., Cerioli S., Castiglioni P., Fink R., Capone R., Müller K.J., Bossinger G., Rohde W., F S. (2000) Genetics of mutations affecting the development of a barley floral bract. Genetics 154:1335-1346.

Pramanik M.H.R., Imai R. (2005) Functional identification of a trehalose 6-phosphate phosphatase gene that is involved in transient induction of trehalose biosynthesis during chilling stress in rice. Plant Molecular Biology 58:751-762.

Ramsay L., Comadran J., Druka A., Marshall D.F., Thomas W.T.B., Macaulay M., MacKenzie K., Simpson C., Fuller J., Bonar N., Hayes P.M., Lundqvist U., Franckowiak J.D., Close T.J., Muehlbauer G.J., Waugh R. (2011) *INTERMEDIUM-C*, a modifier of lateral spikelet fertility in barley, is an ortholog of the maize domestication gene *TEOSINTE BRANCHED 1*. Nat. Genet. 43:169-172.

Rao N.N., Prasad K., Kumar P.R., Vijayraghavan U. (2008) Distinct regulatory role for *RFL*, the rice *LFY* homolog, in determining flowering time and plant architecture. Proceedings of the National Academy of Sciences 105:3646-3651.

Rijavec T., Kovač M., Kladnik A., Chourey P.S., Dermastia M. (2009) A comparative study on the role of cytokinins in caryopsis development in the maize *miniature1* seed mutant and its wild type. Journal of Integrative Plant Biology 51:840-849.

Robertson D.W. (1967) Linkage studies of various barley mutations (*Hordeum Species*). Crop Science 7:41-42.

Rossini L., Vecchietti A., Nicoloso L., Stein N., Franzago S., Salamini F., Pozzi C. (2006) Candidate genes for barley mutants involved in plant architecture: an in silico approach. Theoretical and Applied Genetics 112:1073-1085.

Rostoks N., Schmierer D., Mudie S., Drader T., Brueggeman R., Caldwell D., Waugh R., Kleinhofs A. (2006) Barley *necrotic locus, nec1* encodes the cyclic nucleotide-gated ion channel 4 homologous to the Arabidopsis *HLM1*. Molecular Genetics and Genomics 275:159-168.

Rostoks N., Mudie S., Cardle L., Russell J., Ramsay L., Booth A., Svensson J.T., Wanamaker S.I., Walia H., Rodriguez E.M., Hedley P.E., Liu H., Morris J., Close T.J., Marshall D.F., Waugh R. (2005) Genome-wide SNP discovery and linkage analysis in barley based on genes responsive to abiotic stress. Molecular Genetics and Genomics 274:515-527.

Rubin G., Tohge T., Matsuda F., Saito K., Scheible W.R. (2009) Members of the LBD family of transcription factors repress anthocyanin synthesis and affect additional nitrogen responses in Arabidopsis. Plant Cell 21:3567-3584.

Rupp H.-M., Frank M., Werner T., Strnad M., Schmülling T. (1999) Increased steady state mRNA levels of the *STM* and *KNAT1* homeobox genes in cytokinin overproducing *Arabidopsis thaliana* indicate a role for cytokinins in the shoot apical meristem. Plant Journal 18:557-563.

Saisho D., Myoraku E., Kawasaki S., Sato K., Takeda K. (2007) Construction and characterization of a bacterial artificial chromosome (BAC) library from the japanese malting barley variety 'Haruna Nijo'. Breeding Science 57:29-38.

Sakamoto T., Sakakibara H., Kojima M., Yamamoto Y., Nagasaki H., Inukai Y., Sato Y., Matsuoka M. (2006) Ectopic expression of *KNOTTED1-Like* homeobox protein induces expression of cytokinin biosynthesis genes in rice. Plant Physiology 142:54-62.

Sakuma S., Salomon B., Komatsuda T. (2011) The domestication syndrome genes responsible for the major changes in plant form in the triticeae crops. Plant and Cell Physiology 52:738-749.

Sakuma S., Pourkheirandish M., Matsumoto T., Koba T., Komatsuda T. (2010) Duplication of a well-conserved homeodomain-leucine zipper transcription factor gene in barley generates a copy with more specific functions. Functional & Integrative Genomics 10:123-133.

Sakuma S., Pourkheirandish M., Hensel G., Kumlehn J., Stein N., Tagiri A., Yamaji N., Ma J.F., Sassa H., Koba T., Komatsuda T. (2013) Divergence of expression pattern contributed to neofunctionalization of duplicated HD-Zip I transcription factor in barley. New Phytologist 197:939-948.

Sato K., Nankaku N., Takeda K. (2009) A high-density transcript linkage map of barley derived from a single population. Heredity 103:110-117.

Satoh-Nagasawa N., Nagasawa N., Malcomber S., Sakai H., Jackson D. (2006) A trehalose metabolic enzyme controls inflorescence architecture in maize. Nature 441:227-230.

Scheible W.R., Morcuende R., Czechowski T., Fritz C., Osuna D., Palacios-Rojas N., Schindelasch D., Thimm O., Udvardi M.K., Stitt M. (2004) Genome-wide reprogramming of primary and secondary metabolism, protein synthesis, cellular growth processes, and the regulatory infrastructure of Arabidopsis in response to nitrogen. Plant Physiology 136:2483-2499.

Schluepmann H., Berke L., Sanchez-Perez G. (2012) Metabolism control over growth: a case for trehalose-6-phosphate in plants. Journal of Experimental Botany 63:3379-3390.

Schluepmann H., Pellny T., van Dijken A., Smeekens S., Paul M. (2003) Trehalose 6-phosphate is indispensable for carbohydrate utilization and growth in *Arabidopsis thaliana*. Proceedings of the National Academy of Sciences 100:6849-6854.

Schnable P.S., Ware D., Fulton R.S., Stein J.C., Wei F., Pasternak S., Liang C., Zhang J., Fulton L., Graves T.A., Minx P., Reily A.D., Courtney L., Kruchowski S.S., Tomlinson C., Strong C., Delehaunty K., Fronick C., Courtney B., Rock S.M., Belter E., Du F., Kim K., Abbott R.M., Cotton M., Levy A., Marchetto P., Ochoa K., Jackson S.M., Gillam B., Chen W., Yan L., Higginbotham J., Cardenas M., Waligorski J., Applebaum E., Phelps L., Falcone J., Kanchi K., Thane T., Scimone A., Thane N., Henke J., Wang T., Ruppert J., Shah N., Rotter K., Hodges J., Ingenthron E., Cordes M., Kohlberg S., Sgro J., Delgado B., Mead K., Chinwalla A., Leonard S., Crouse K., Collura K., Kudrna D., Currie J., He R., Angelova A., Rajasekar S., Mueller T., Lomeli R., Scara G., Ko A., Delaney K., Wissotski M., Lopez G., Campos D., Braidotti M., Ashley E., Golser W., Kim H., Lee S., Lin J., Dujmic Z., Kim W., Talag J., Zuccolo A., Fan C., Sebastian A., Kramer M., Spiegel L., Nascimento L., Zutavern T., Miller B., Ambroise C., Muller S., Spooner W., Narechania A., Ren L., Wei S., Kumari S., Faga B., Levy M.J., McMahan L., Van Buren P., Vaughn M.W., *et al.* (2009) The B73 maize genome: Complexity, diversity, and dynamics. Science 326:1112-1115.

Schnurbusch T., Hayes J., Hrmova M., Baumann U., Ramesh S.A., Tyerman S.D., Langridge P., Sutton T. (2010) Boron toxicity tolerance in barley through reduced expression of the multifunctional aquaporin *HvNIP2;1*. Plant Physiology 153:1706-1715.

Scholz F., Lehmann C. (1961) Die gaterslebener mutanten der saatgerste in beziehung zur formenmannigfaltigkeit der art *Hordeum vulgare* L.s.l. III. Die Kulturpflanze 9:230-272.

Schulte D., Ariyadasa R., Shi B.J., Fleury D., Saski C., Atkins M., deJong P., Wu C.C., Graner A., Langridge P., Stein N. (2011) BAC library resources for map-based cloning and physical map construction in barley (*Hordeum vulgare* L.). BMC Genomics 12:247.

Semiarti E., Ueno Y., Tsukaya H., Iwakawa H., Machida C., Machida Y. (2001) The *asymmetric leaves2* gene of *Arabidopsis thaliana* regulates formation of a symmetric lamina, establishment of venation and repression of meristem-related homeobox genes in leaves. Development 128:1771-1783.

Shahinnia F., Druka A., Franckowiak J., Morgante M., Waugh R., Stein N. (2012) High resolution mapping of *Dense spike-ar* (*dsp.ar*) to the genetic centromere of barley chromosome 7H. Theoretical and Applied Genetics 124:373-384.

Shi B.J., Sutton T., Collins N.C., Pallotta M., Langridge P. (2010) Construction of a barley bacterial artificial chromosome library suitable for cloning genes for boron tolerance, sodium exclusion and high grain zinc content. Plant Breeding 129:291-296.

Shima S., Matsui H., Tahara S., Imai R. (2007) Biochemical characterization of rice trehalose-6-phosphate phosphatases supports distinctive functions of these plant enzymes. FEBS Journal 274:1192-1201.

Shirasu K., Lahaye T., Tan M.-W., Zhou F., Azevedo C., Schulze-Lefert P. (1999) A novel class of eukaryotic zinc-binding proteins is required for disease resistance signaling in barley and development in *C. elegans*. Cell 99:355-366.

Shuai B., Reynaga-Pena C.G., Springer P.S. (2002) The *LATERAL ORGAN BOUNDARIES* gene defines a novel, plant-specific gene family. Plant Physiology 129:747-761.

Sigmon B., Vollbrecht E. (2010) Evidence of selection at the *ramosa1* locus during maize domestication. Molecular Ecology 19:1296-1311.

Sreenivasulu N., Schnurbusch T. (2012) A genetic playground for enhancing grain number in cereals. Trends in Plant Science 17:91-101.

Stein N., Perovic D., Kumlehn J., Pellio B., Stracke S., Streng S., Ordon F., Graner A. (2005) The eukaryotic translation initiation factor 4E confers multiallelic recessive Bymovirus resistance in *Hordeum vulgare* (L.). The Plant Journal 42:912-922.

Stein N., Prasad M., Scholz U., Thiel T., Zhang H., Wolf M., Kota R., Varshney R., Perovic D., Grosse I., Graner A. (2007) A 1,000-loci transcript map of the barley genome: new anchoring points for integrative grass genomics. Theoretical and Applied Genetics 114:823-839.

Steuernagel B., Taudien S., Gundlach H., Seidel M., Ariyadasa R., Schulte D., Petzold A., Felder M., Graner A., Scholz U., Mayer K.F.X., Platzer M., Stein N. (2009) *De novo* 454 sequencing of barcoded BAC pools for comprehensive gene survey and genome analysis in the complex genome of barley. BMC Genomics 10:547.

Sun Y., Fan X.-Y., Cao D.-M., Tang W., He K., Zhu J.-Y., He J.-X., Bai M.-Y., Zhu S., Oh E., Patil S., Kim T.-W., Ji H., Wong W.H., Rhee S.Y., Wang Z.-Y. (2010) Integration of brassinosteroid signal transduction with the transcription network for plant growth regulation in Arabidopsis. Developmental Cell 19:765-777.

Sutton T., Baumann U., Hayes J., Collins N.C., Shi B.-J., Schnurbusch T., Hay A., Mayo G., Pallotta M., Tester M., Langridge P. (2007) Boron-toxicity tolerance in barley arising from efflux transporter amplification. Science 318:1446-1449.

Suzaki T., Sato M., Ashikari M., Miyoshi M., Nagato Y., Hirano H.-Y. (2004) The gene *FLORAL ORGAN NUMBER1* regulates floral meristem size in rice and encodes a leucine-rich repeat receptor kinase orthologous to Arabidopsis *CLAVATA1*. Development 131:5649-5657.

Suzaki T., Toriba T., Fujimoto M., Tsutsumi N., Kitano H., Hirano H.-Y. (2006) Conservation and diversification of meristem maintenance mechanism in *Oryza sativa*: Function of the *FLORAL ORGAN NUMBER2* Gene. Plant and Cell Physiology 47:1591-1602.

Taguchi-Shiobara F., Yuan Z., Hake S., Jackson D. (2001) The *fasciated ear2* gene encodes a leucine-rich repeat receptor-like protein that regulates shoot meristem proliferation in maize. Genes & Development 15:2755-2766.

Taketa S., Yuo T., Sakurai Y., Miyake S., Ichii M. (2011) Molecular mapping of the *short awn 2* (*lks2*) and *dense spike 1* (*dsp1*) genes on barley chromosome 7H. Breeding Science 61:80-85.

Taketa S., Amano S., Tsujino Y., Sato T., Saisho D., Kakeda K., Nomura M., Suzuki T., Matsumoto T., Sato K., Kanamori H., Kawasaki S., Takeda K. (2008) Barley grain with adhering hulls is controlled by an ERF family transcription factor gene regulating a lipid biosynthesis pathway. Proceedings of the National Academy of Sciences 105:4062-4067.

Talamè V., Bovina R., Sanguineti M.C., Tuberosa R., Lundqvist U., Salvi S. (2008) TILLMore, a resource for the discovery of chemically induced mutants in barley. Plant Biotechnology Journal 6:477-485.

Tamaki S., Matsuo S., Wong H.L., Yokoi S., Shimamoto K. (2007) Hd3a protein is a mobile flowering signal in rice. Science 316:1033-1036.

Tamura K., Peterson D., Peterson N., Stecher G., Nei M., Kumar S. (2011) MEGA5: Molecular evolutionary genetics analysis using maximum likelihood, evolutionary distance, and maximum parsimony methods. Molecular Biology and Evolution 28:2731-2739.

Tanaka W., Pautler M., Jackson D., Hirano H.-Y. (2013) Grass Meristems II: Inflorescence architecture, flower development and meristem fate. Plant and Cell Physiology 54:313-324.

Thompson J.D., Higgins D.G., Gibson T.J. (1994) CLUSTAL W: improving the sensitivity of progressive multiple sequence alignment through sequence weighting, position-specific gap penalties and weight matrix choice. Nucleic Acids Research 22:4673-4680.

Tommasini L., Svensson J.T., Rodriguez E.M., Wahid A., Malatrasi M., Kato K., Wanamaker S., Resnik J., Close T.J. (2008) Dehydrin gene expression provides an indicator of low temperature and drought stress: transcriptome-based analysis of Barley (*Hordeum vulgare* L.). Functional & Integrative Genomics 8:387-405.

Trevaskis B., Tadege M., Hemming M.N., Peacock W.J., Dennis E.S., Sheldon C. (2007) Short Vegetative Phase-like *MADS-box* genes inhibit floral meristem identity in barley. Plant Physiology 143:225-235.

True J.R., Carroll S.B. (2002) Gene co-option in physiological and morphological evolution. Annual Review of Cell and Developmental Biology 18:53-80.

Turner A., Beales J., Faure S., Dunford R.P., Laurie D.A. (2005) The pseudo-response regulator *Ppdh1* provides adaptation to photoperiod in barley. Science 310:1031-1034.

Van Ooijen J.W., Voorrips R.E. (2001) JoinMap 3.0, Software for the calculation of genetic linkage maps. Plant Research International, Wageningen, the Netherlands.

Vandesteene L., López-Galvis L., Vanneste K., Feil R., Maere S., Lammens W., Rolland F., Lunn J.E., Avonce N., Beeckman T., Van Dijck P. (2012) Expansive evolution of the *TREHALOSE-6-PHOSPHATE PHOSPHATASE* gene family in Arabidopsis. Plant Physiology 160:884-896.

Varshney R.K., Grosse I., Hahnel U., Siefken R., Prasad M., Stein N., Langridge P., Altschmied L., Graner A. (2006) Genetic mapping and BAC assignment of EST-derived SSR markers shows non-uniform distribution of genes in the barley genome. Theoretical and Applied Genetics 113:239-250.

Vincze T., Posfai J., Roberts R.J. (2003) NEBcutter: a program to cleave DNA with restriction enzymes. Nucleic Acids Research 31:3688-3691.

Vollbrecht E., Springer P.S., Goh L., Buckler E.S., Martienssen R. (2005) Architecture of floral branch systems in maize and related grasses. Nature 436:1119-1126.

vonBothmer R. (1992) The wild species of Hordeum: Relationships and potential use for improvement of cultivated barley, in: P. R. Shewry (Ed.), Barley: Genetics, biochemistry, molecular biology and biotechnology, CAB International, Oxford. pp. 3-18.

Wahl V., Ponnu J., Schlereth A., Arrivault S., Langenecker T., Franke A., Feil R., Lunn J.E., Stitt M., Schmid M. (2013) Regulation of flowering by trehalose-6-phosphate signaling in *Arabidopsis thaliana*. Science 339:704-707.

Walia H., Wilson C., Condamine P., Liu X., Ismail A.M., Close T.J. (2007) Large-scale expression profiling and physiological characterization of jasmonic acid-mediated adaptation of barley to salinity stress. Plant Cell and Environment 30:410-421.

Ward S.P., Leyser O. (2004) Shoot branching. Current Opinion in Plant Biology 7:73-78.

Wei F., Gobelman-Werner K., Morroll S.M., Kurth J., Mao L., Wing R., Leister D., Schulze-Lefert P., Wise R.P. (1999) The *mla* (powdery mildew) resistance cluster is associated with three *nbs-lrr* gene families and suppressed recombination within a 240-kb DNA interval on chromosome 5S (1HS) of barley. Genetics 153:1929-1948.

Wendt T., Holm P.B., Starker C.G., Christian M., Voytas D.F., Brinch-Pedersen H., Holme I.B. (2013) TAL effector nucleases induce mutations at a pre-selected location in the genome of primary barley transformants. Plant Molecular Biology 83:279-285.

Wenzl P., Li H.B., Carling J., Zhou M.X., Raman H., Paul E., Hearnden P., Maier C., Xia L., Caig V., Ovesna J., Cakir M., Poulsen D., Wang J.P., Raman R., Smith K.P., Muehlbauer G.J., Chalmers K.J., Kleinhofs A., Huttner E., Kilian A. (2006) A high-density consensus map of barley linking DArT markers to SSR, RFLP and STS loci and agricultural traits. BMC Genomics 7:206.

Whipple C.J., Hall D.H., DeBlasio S., Taguchi-Shiobara F., Schmidt R.J., Jackson D.P. (2010) A conserved mechanism of bract suppression in the grass family. Plant Cell 22:565-578.

Whipple C.J., Kebrom T.H., Weber A.L., Yang F., Hall D., Meeley R., Schmidt R., Doebley J., Brutnell T.P., Jackson D.P. (2011) *grassy tillers1* promotes apical dominance in maize and responds to shade signals in the grasses. Proceedings of the National Academy of Sciences 108:506-512.

Yan L., Loukoianov A., Tranquilli G., Helguera M., Fahima T., Dubcovsky J. (2003) Positional cloning of the wheat vernalization gene *VRN1*. Proceedings of the National Academy of Sciences 100:6263-6268.

Yan L., Fu D., Li C., Blechl A., Tranquilli G., Bonafede M., Sanchez A., Valarik M., Yasuda S., Dubcovsky J. (2006) The wheat and barley vernalization gene *VRN3* is an orthologue of *FT*. Proceedings of the National Academy of Sciences 103:19581-19586.

Yan L.L., Loukoianov A., Blechl A., Tranquilli G., Ramakrishna W., SanMiguel P., Bennetzen J.L., Echenique V., Dubcovsky J. (2004) The wheat *VRN2* gene is a flowering repressor down-regulated by vernalization. Science 303:1640-1644.

Yanai O., Shani E., Dolezal K., Tarkowski P., Sablowski R., Sandberg G., Samach A., Ori N. (2005) Arabidopsis KNOXI proteins activate cytokinin biosynthesis. Current Biology 15:1566-1571.

Yang Y., Yu X., Wu P. (2006) Comparison and evolution analysis of two rice subspecies *LATERAL ORGAN BOUNDARIES* domain gene family and their evolutionary characterization from Arabidopsis. Molecular Phylogenetics and Evolution 39:248-262.

Yoshida A., Ohmori Y., Kitano H., Taguchi-Shiobara F., Hirano H.-Y. (2012a) *ABERRANT SPIKELET AND PANICLE1*, encoding a TOPLESS-related transcriptional co-repressor, is involved in the regulation of meristem fate in rice. The Plant Journal 70:327-339.

Yoshida A., Sasao M., Yasuno N., Takagi K., Daimon Y., Chen R., Yamazaki R., Tokunaga H., Kitaguchi Y., Sato Y., Nagamura Y., Ushijima T., Kumamaru T., Iida S., Maekawa M., Kyozuka J. (2012b) *TAWAWA1*, a regulator of rice inflorescence architecture, functions through the suppression of meristem phase transition. Proceedings of the National Academy of Sciences 110:767-772.

Yoshida H., Nagato Y. (2011) Flower development in rice. Journal of Experimental Botany 62:4719-4730.

Yu Y., Tomkins J.P., Waugh R., Frisch D.A., Kudrna D., Kleinhofs A., Brueggeman R.S., Muehlbauer G.J., Wise R.P., Wing R.A. (2000) A bacterial artificial chromosome library for barley (*Hordeum vulgare* L.) and the identification of clones containing putative resistance genes. Theoretical and Applied Genetics 101:1093-1099.

Yuo T., Yamashita Y., Kanamori H., Matsumoto T., Lundqvist U., Sato K., Ichii M., Jobling S.A., Taketa S. (2012) A *SHORT INTERNODES* (*SHI*) family transcription factor gene

regulates awn elongation and pistil morphology in barley. Journal of Experimental Botany 63:5223-5232.

Zakhrabekova S., Gough S.P., Braumann I., Müller A.H., Lundqvist J., Ahmann K., Dockter C., Matyszczak I., Kurowska M., Druka A., Waugh R., Graner A., Stein N., Steuernagel B., Lundqvist U., Hansson M. (2012) Induced mutations in circadian clock regulator *Mat-a* facilitated short-season adaptation and range extension in cultivated barley. Proceedings of the National Academy of Sciences 109:8328-8333.

Zalewski W., Orczyk W., Gasparis S., Nadolska-Orczyk A. (2012) *HvCKX2* gene silencing by biolistic or Agrobacterium-mediated transformation in barley leads to different phenotypes. BMC Plant Biology 12:206.

Zalewski W., Galuszka P., Gasparis S., Orczyk W., Nadolska-Orczyk A. (2010) Silencing of the *HvCKX1* gene decreases the cytokinin oxidase/dehydrogenase level in barley and leads to higher plant productivity. Journal of Experimental Botany 61:1839-1851.

Zang B., Li H., Li W., Deng X., Wang X. (2011) Analysis of trehalose-6-phosphate synthase (TPS) gene family suggests the formation of TPS complexes in rice. Plant Molecular Biology 76:507-522.

Zhang L., Castell-Miller C., Dahl S., Steffenson B., Kleinhofs A. (2008) Parallel expression profiling of barley-stem rust interactions. Functional & Integrative Genomics 8:187-198.

Zhang L., Fetch T., Nirmala J., Schmierer D., Brueggeman R., Steffenson B., Kleinhofs A. (2006) *Rpr1*, a gene required for *Rpg1*-dependent resistance to stem rust in barley. Theoretical and Applied Genetics 113:847-855.

Zhang Y.-C., Yu Y., Wang C.-Y., Li Z.-Y., Liu Q., Xu J., Liao J.-Y., Wang X.-J., Qu L.-H., Chen F., Xin P., Yan C., Chu J., Li H.-Q., Chen Y.-Q. (2013a) Overexpression of *microRNA OsmiR397* improves rice yield by increasing grain size and promoting panicle branching. Nature Biotechnology 31:848-852.

Zhang Y., Zhang F., Li X.H., Baller J.A., Qi Y.P., Starker C.G., Bogdanove A.J., Voytas D.F. (2013b) Transcription Activator-Like Effector Nucleases enable efficient plant genome engineering. Plant Physiology 161:20-27.

Zhang Y.H., Primavesi L.F., Jhurreea D., Andralojc P.J., Mitchell R.A.C., Powers S.J., Schluepmann H., Delatte T., Wingler A., Paul M.J. (2009) Inhibition of SNF1-Related Protein Kinase1 Activity and Regulation of Metabolic Pathways by Trehalose-6-Phosphate. Plant Physiology 149:1860-1871.

9.0. Supplementary Information

Supplementary Table 1a. List of markers used for genetic mapping of *vrs4*.

Marker	Rice Orthologue	Forward sequence (5'-3')	Reverse sequence (5'-3')	Tm (˚C)	Fragment size (bp)	Method of genotyping	CAPS Enzyme	*vrs4.k* × Golden Promise	Barke × *vrs4.k*
Hv04140	LOC_Os01g07320	TACTTTTCCTGCACCCTGC	CTATAACTAGACTAGCTCTGCAATCATC	55	436	CAPS	*Sau96I*	Monomorphic	Polymorphic
Hv04130	LOC_Os01g07310	GTGAAGGAAGGCGAATCAGAC	GGAGATGTTCATATTAGTGTAGCAAGT	55	1058	CAPS	*Hpy188I*	Monomorphic	Polymorphic
Hv0167800	LOC_Os01g07350	GCTCAATCCTCGTAACCGTG	GCACGCAAAGAATCTTCATCG	55	1400	CAPS	*Sau96I*	Monomorphic	Polymorphic
Hv04180BV	LOC_Os01g07370	CTGAGCCACAGAAGTCCTG	CTCCAGATGCACTCATCAGAG	55	1206	CAPS	*Kpn2I* or *MspI*	Monomorphic	Polymorphic
Hv03717	LOC_Os01g73910	CAGAACACCTTGCTGCTCAA	CATGATCGCACTTGAGGTGA	55	500	CAPS	*TaqI*	Polymorphic	Polymorphic
Hv04380	LOC_Os01g07590	TGTGTTCATCTGAGCTTTGCAG	CTACTACTGTTCTTGCAGACGG	55	1106	CAPS	*HincII*	Polymorphic	Polymorphic
DQ327702	LOC_Os01g07480	AGTAGTTAGCATTCGGAAGAAACG	CTCATGAAGCTAGCATATATACACGC	55	964	CAPS	*Sau96I* or *MwoI*	Polymorphic	Polymorphic
Hv04317	LOC_Os01g07540	TCCTGTGCGTGAAGTTCATC	CCAATGAGTCCATGTCCTCG	55	1583	CAPS	*MvaI* or *DrdI*	Monomorphic	Polymorphic
Hv45740	LOC_Os01g47340	CCACTACAACAACCCGCGGAA	TGGTGGAAGTGACAAGTGCTTTGC	55	2400	CAPS	*HinfI*	Polymorphic	Polymorphic
Hv49520	LOC_Os01g54020	GAGTAGTTTCTGGTGTACAGCC	GGATGTCAGAAGCCATTAGAACAG	55	2100	CAPS	*AseI*	Polymorphic	Polymorphic
Hv49560	LOC_Os01g54050	CACTCGTTCATTCATATAAATGG	GGAAATAGGATTCTAGTTTCTGC	50	1470	CAPS	*EcoRV*	Monomorphic	Polymorphic
12_31529	LOC_Os01g54550	AACCACAAATCTGAGAAATATCACCA	CGATATAGCAGAGTCCGCC	55	600	CAPS	*BstUI*	Polymorphic	Polymorphic
Hv49870	LOC_Os01g54560	GAAAGTGCTTTGGTGTGGC	AGCATGGTGGCCACTTC	55	1100	CAPS	*BccI*	Polymorphic	Monomorphic
Hv04430	LOC_Os01g07700	TGCTTACGGATATGGTGTTTTGG	ATCAAATGGTGGGGTGTCAC	55	1780	CAPS	*HpyF10VI*	Polymorphic	Monomorphic
Hv03800	LOC_Os01g74650	GTATCTCAACAGGATCGTCAAGG	GAATAACAGGCACAATTCAGCTG	55	1324	CAPS	*NsiI*	Polymorphic	Monomorphic
101_102	LOC_Os01g55740	GATCAGATCCAGCCCTTCCTAATTC	GCCATTGTGCTTCTTCACATTTTTC	55	800	CAPS	*HaeIII*	Polymorphic	Monomorphic
103_104	LOC_Os05g22614	GAAGAACCCCTTCTTTGTCGACTT	TAGTCTTCAGTGAGTGACGCCTTG	55	663	CAPS	*NGOMIV*	Polymorphic	Polymorphic
139_140	LOC_Os01g65080	GAGGAAGAACTGAGACGGTCATACA	TCATTTCTGTGTGATATGTGGCAAG	55	800	CAPS	*BmgBI*	Monomorphic	Polymorphic
149_150	LOC_Os02g53420	TCAACTGCACAGACTGAGATCAACC	CACAAGATCAAACTCGCCAAGAAGT	55	1100	CAPS	*HhaI*	Polymorphic	Polymorphic
Hv07640	LOC_Os01g07640	GGGAAAGGCTACTACCGTGAAGG	CACTCTCACACGTCGGCACTTG	60	1359	CAPS	*BtScI*	Polymorphic	Monomorphic
Hv04290	LOC_Os01g07500	GGTGGGACTTCATTACTTGCCGTAAC	CCTTTTCTAGTGTGAGAACCAGCCCAC	60	229	Size polymorhism	-	Polymorphic	Monomorphic
Hv45400	LOC_Os01g46590	GACCTGCTTGAGAATCTACCC	GCCAGAATTAGTGGCACCATA	55	1317	Size polymorhism	-	Polymorphic	Polymorphic
53_54	LOC_Os02g21660	TGCGCAGGAACAGTGCTC	GTGAGGAAGCTTGACAGAACCACT	55	800	Size polymorhism		Polymorphic	Polymorphic
Hv04360	LOC_Os01g07570	GCACTGTTCCATGCTTTCC	GTCAGTTCATGAACAGCAAGC	55	1320	Size polymorhism or CAPS	*AvaI*	Polymorphic	Polymorphic
Hv07610	LOC_Os01g07610	GCTGAGAAGTTTGTGTATGTGATGG	GGAAGTTAACTGTGGACTGAAATGAG	55	1105	Size polymorhism	-	Polymorphic	Monomorphic
Hv04180VG	LOC_Os01g07370	CAAGTTCTGCAGGGCCACAAGAG	ACTGACTGCAAGGAACGTAGGTAAGC	60	1017	Sanger sequencing	-	Polymorphic	Monomorphic
Hv04080	LOC_Os01g07212	GTGCCGTGGACTCCTGAATAGTTC	GCTAGCGTTGGATGTCGTCTTCC	60	1258	Sanger sequencing	-	Polymorphic	Monomorphic
2_0976	LOC_Os01g04010	-	-	-	-	Veracode beads	-	Polymorphic	Polymorphic
2_0595	LOC_Os01g03520	-	-	-	-	Veracode beads	-	Polymorphic	Polymorphic
2_1145	LOC_Os01g07370	-	-	-	-	Veracode beads	-	Monomorphic	Polymorphic
3_0953	LOC_Os01g74650	-	-	-	-	Veracode beads	-	Polymorphic	Polymorphic
1_1401	LOC_Os01g46720	-	-	-	-	Veracode beads	-	Polymorphic	Polymorphic
1_0225	LOC_Os01g46980	-	-	-	-	Veracode beads	-	Polymorphic	Polymorphic
1_0728	LOC_Os06g51060	-	-	-	-	Veracode beads	-	Polymorphic	Polymorphic
1_0281	LOC_Os05g22614	-	-	-	-	Veracode beads	-	Polymorphic	Polymorphic
2_1502	LOC_Os01g51360	-	-	-	-	Veracode beads	-	Polymorphic	Polymorphic
1_1391	LOC_Os01g51890	-	-	-	-	Veracode beads	-	Polymorphic	Polymorphic
1_0335	LOC_Os01g52110	-	-	-	-	Veracode beads	-	Polymorphic	Polymorphic
3_1153	LOC_Os01g52230	-	-	-	-	Veracode beads	-	Polymorphic	Polymorphic
2_1305	-	-	-	-	-	Veracode beads	-	Monomorphic	Polymorphic
3_0616	LOC_Os01g52920	-	-	-	-	Veracode beads	-	Polymorphic	Polymorphic
3_0788	LOC_Os01g52970	-	-	-	-	Veracode beads	-	Polymorphic	Polymorphic
1_1394	LOC_Os01g52550	-	-	-	-	Veracode beads	-	Monomorphic	Polymorphic
2_0931	LOC_Os01g52640	-	-	-	-	Veracode beads	-	Polymorphic	Polymorphic
3_1242	LOC_Os01g53610	-	-	-	-	Veracode beads	-	Polymorphic	Polymorphic

3_0170	LOC_Os01g56360	-	-	-	-	Veracode beads	-	Polymorphic	Polymorphic
3_0278	LOC_Os01g57420	-	-	-	-	Veracode beads	-	Polymorphic	Polymorphic
2_0063	LOC_Os01g57920	-	-	-	-	Veracode beads	-	Polymorphic	Polymorphic
3_0250	LOC_Os01g65380	-	-	-	-	Veracode beads	-	Polymorphic	Polymorphic
2_0999	LOC_Os01g65070	-	-	-	-	Veracode beads	-	Polymorphic	Polymorphic
2_1381	LOC_Os01g63820	-	-	-	-	Veracode beads	-	Polymorphic	Polymorphic
1_0662	LOC_Os01g63420	-	-	-	-	Veracode beads	-	Polymorphic	Polymorphic
3_0927	LOC_Os05g33380	-	-	-	-	Veracode beads	-	Polymorphic	Polymorphic
2_0252	-	-	-	-	-	Veracode beads	-	Polymorphic	Monomorphic
2_0742	LOC_Os01g04190	-	-	-	-	Veracode beads	-	Polymorphic	Monomorphic
3_0571	LOC_Os01g05500	-	-	-	-	Veracode beads	-	Polymorphic	Monomorphic
2_0276	LOC_Os01g48190	-	-	-	-	Veracode beads	-	Polymorphic	Monomorphic
3_1011	-	-	-	-	-	Veracode beads	-	Polymorphic	Monomorphic
3_1393	LOC_Os01g47740	-	-	-	-	Veracode beads	-	Polymorphic	Monomorphic
1_0653	LOC_Os03g50850	-	-	-	-	Veracode beads	-	Polymorphic	Monomorphic
1_1016	LOC_Os01g48810	-	-	-	-	Veracode beads	-	Polymorphic	Monomorphic
1_1314	LOC_Os01g53910	-	-	-	-	Veracode beads	-	Polymorphic	Monomorphic
2_0017	LOC_Os01g53720	-	-	-	-	Veracode beads	-	Polymorphic	Monomorphic
1_0609	LOC_Os01g55190	-	-	-	-	Veracode beads	-	Polymorphic	Monomorphic
2_1161	LOC_Os01g62260	-	-	-	-	Veracode beads	-	Polymorphic	Monomorphic

Supplementary Table 1b. Primer pairs for *HvRA2* resequencing and haplotype analysis.

Primer Name	Forward sequence (5'-3')	Reverse sequence (5'-3')	Tm (˚C)	Fragment size (bp)
AS12	CCATCCCCCACCCTTTTG	GGAGGAGATTAGGGTTTCTGATC	55	896
AS34	CCCACTGCTATGAATGAATCTACAG	TCCAGCGTTGTTGTTGCTC	55	910
AS56	GGCTTGTGGACGCGATAG	GTGATGCCCTCCATAGAAAACTG	55	983

Supplementary Table 1c. qRT-PCR primer pairs used in the present study.

Primer Name	HarvEST/Affymetrix ID/FLc ID	Forward sequence (5'-3')	Reverse sequence (5'-3')	Tm (˚C)	Fragment size (bp)
EA1-LIKE	35_15636	TGTCCTCTAAGATGTTGTGTGTGTCA	CGCTAGTGTCGATCTTCATTCCTGA	58	122
LOG1-LIKE	35_9790	GATCCTGTTGGTGAAGTTCGAGC	GCAACTCCTCCAAGGTTCCG	58	118
LOG1-LIKE	35_10423	AGATGGAATGTGCTAGTCCTTGTCG	AACGCCATCATCAACCCAATGC	58	111
TPP (HvSRA)	35_7759	CTCAACATGGAGAGCGAGCAG	CGATCCCAACACGCATGCA	58	125
TPS	Contig12019_at	GCTCAACTCGTCGGAGGAC	GAAACTTGGCTTACTGCCTATCCAA	58	131
KNOX	35_10104	CACGCCACACAGGGAGAAATAAG	ACGCATATGCAAAGTGGTCAGAC	58	119
VRS1	35_34639	CCGAGATAGCTGCTGCCGCC	TGCATCGCGGGCAATGGAGA	58	121
HvRA2	DQ327702	ATTACCACCACCTCAGGATCA	GAGTAGGAGAGGTAATCCACA	55	114
HvSRA	AK366852.1	GTGAAGAGCAACGGGACGAAGAAG	CAACACCGGGTCCAAAAGGGAAAC	60	140
HvCKX2	AK373850	GTTCGTGGAGCGGAAGAGGAAG	CGGGGCCAATCGATTAACTTCGTG	60	107
HvPIN1-LIKE	AK369028.1	CTGCTGGGCCTCTGAACTCAC	TCCATTCTAATCTGGGATCAACCGAC	60	133

Supplementary Table 2. Monocot RAMOSA2 orthologs, RAMOSA2-LIKE proteins from dicots and LBD proteins used for phylogenetic analysis.

#	Annotation	Query cover (%)	E-value	Max identity (%)	Accession/ Morex contig	Phylogenetic clade
1	RAMOSA2 [*Hordeum vulgare*]	100	0	100	ABC54561.1/ Ctg2547112_3HS	RAMOSA2 ortholog/homolog
2	RAMOSA2 [*Triticum durum*]	100	5.00E-165	93	ADJ67794.1	RAMOSA2 ortholog/homolog
3	RAMOSA2 [*Aegilops tauschii*]	100	2.00E-169	95	EMT25999.1	RAMOSA2 ortholog/homolog
4	RAMOSA2 [*Oryza sativa Japonica* Group]	93	2.00E-125	79	ABU44495.1	RAMOSA2 ortholog/homolog
6	RAMOSA2 [*Chrysopogon gryllus*]	93	6.00E-112	72	AFJ42327.1	RAMOSA2 ortholog/homolog
7	RAMOSA2 [*Triticum aestivum*]	100	3.00E-158	94	ABK79907.1	RAMOSA2 ortholog/homolog
8	RAMOSA2 [*Schizachyrium sanguineum var. hirtiflorum*]	93	2.00E-101	69	AFJ42332.1	RAMOSA2 ortholog/homolog
9	RAMOSA2 [*Sorghum bicolor*]	94	3.00E-104	69	AFJ42334.1	RAMOSA2 ortholog/homolog
10	RAMOSA2 [*Andropogon hallii*]	94	1.00E-99	69	AFJ42331.1	RAMOSA2 ortholog/homolog
11	RAMOSA2 [*Zea mays*]	100	2.00E-112	73	NP_001131918.1	RAMOSA2 ortholog/homolog
12	RAMOSA2 [*Phacelurus digitatus*]	100	1.00E-110	73	AFJ42333.1	RAMOSA2 ortholog/homolog
13	RAMOSA2 [*Andropterum stolzii*]	94	8.00E-103	70	AFJ42330.1	RAMOSA2 ortholog/homolog
14	RAMOSA2 [*Brachypodium distachyon*]	100	5.00E-117	77	XP_003569245.1	RAMOSA2 ortholog/homolog
15	RAMOSA2 [*Brachypodium sylvaticum*]	100	1.00E-108	75	CCF55439.1	RAMOSA2 ortholog/homolog
16	RAMOSA2 [*Cymbopogon flexuosus*]	100	2.00E-101	67	AFJ42328.1	RAMOSA2 ortholog/homolog
17	ELONGATED PETIOULE1 (ELP1) - [*Glycine max*]	48	2.00E-67	77	AFK81066.1	RAMOSA2 ortholog/homolog
18	LBD PROTEIN-LIKE [*Glycine max*]	48	3.00E-67	77	XP_003527004.1	RAMOSA2 ortholog/homolog
19	ELONGATED PETIOULE2 - [*Glycine max*]	48	7.00E-67	75	XP_003523096.1	RAMOSA2 ortholog/homolog
20	LBD PROTEIN-LIKE [*Cicer arietinum*]	45	5.00E-67	81	XP_004515877.1	RAMOSA2 ortholog/homolog
21	LBD PROTEIN-LIKE [*Glycine max*]	49	5.00E-66	77	ACU23406.1	RAMOSA2 ortholog/homolog
22	SLEEPLESS (SLP) - ortholog of ELP1 - [*Lotus japonicus*]	63	5.00E-68	63	AFK81064.1	RAMOSA2 ortholog/homolog
23	ELONGATED PETIOULE1 (ELP1) - [*Medicago truncatula*]	45	4.00E-66	79	AFK81063.1	RAMOSA2 ortholog/homolog
24	LBD PROTEIN-LIKE [*Cicer arietinum*]	45	4.00E-64	78	XP_004501886.1	RAMOSA2 ortholog/homolog
25	APULVINIC (APU) - ortholog of ELP1 - [*Pisum sativum*]	45	4.00E-65	78	AFK81065.1	RAMOSA2 ortholog/homolog
26	LBD PROTEIN-LIKE [*Cucumis sativus*]	45	2.00E-67	81	XP_004173060.1	RAMOSA2 ortholog/homolog
27	LBD PROTEIN-LIKE [*Ricinus communis*]	51	9.00E-69	78	XP_002511341.1	RAMOSA2 ortholog/homolog
28	LBD PROTEIN-LIKE [*Populus trichocarpa*]	48	1.00E-68	81	XP_002318660.1	RAMOSA2 ortholog/homolog
29	LBD PROTEIN-LIKE [*Theobroma cacao*]	48	2.00E-68	81	EOY20851.1	RAMOSA2 ortholog/homolog
30	LBD PROTEIN-LIKE [*Prunus persica*]	47	3.00E-67	79	EMJ12162.1	RAMOSA2 ortholog/homolog
31	LBD PROTEIN-LIKE [*Fragaria vesca subsp. vesca*]	50	1.00E-67	75	XP_004298984.1	RAMOSA2 ortholog/homolog
32	LBD PROTEIN-LIKE [*Solanum lycopersicum*]	49	1.00E-66	77	XP_004236250.1	RAMOSA2 ortholog/homolog
33	LBD PROTEIN-LIKE [*Capsella rubella*]	57	3.00E-63	67	EOA15040.1	RAMOSA2 ortholog/homolog
34	ASSYMETRIC LEAVES2-LIKE4 (ASL4) [*Arabidopsis thaliana*]	43	4.00E-63	81	BAH10548.1	RAMOSA2 ortholog/homolog
35	LBD PROTEIN-LIKE [*Solanum lycopersicum*]	45	2.00E-61	74	XP_004242158.1	RAMOSA2 ortholog/homolog
36	LBD PROTEIN-LIKE [*Vitis vinifera*]	46	2.00E-68	82	XP_002281358.1	RAMOSA2 ortholog/homolog
37	LBD PROTEIN25-LIKE [*Cucumis sativus*]	45	2.00E-64	79	XP_004169034.1	RAMOSA2 ortholog/homolog
38	LBD PROTEIN25-LIKE [*Cucumis sativus*]	49	5.00E-63	75	XP_004156730.1	RAMOSA2 ortholog/homolog
39	LBD PROTEIN-LIKE [*Arabidopsis thaliana*]	45	2.00E-57	74	BAB02689.1	RAMOSA2 ortholog/homolog
40	LBD PROTEIN-LIKE [*Vitis vinifera*]	45	3.00E-63	76	XP_002273053.1	RAMOSA2 ortholog/homolog
41	LBD PROTEIN-LIKE [*Theobroma cacao*]	45	2.00E-66	79	EOY02489.1	RAMOSA2 ortholog/homolog
42	LBD PROTEIN-LIKE [*Prunus persica*]	45	6.00E-63	80	EMJ18120.1	RAMOSA2 ortholog/homolog
43	LBD PROTEIN-LIKE [*Ricinus communis*]	46	1.00E-64	78	XP_002521459.1	RAMOSA2 ortholog/homolog

44	LBD PROTEIN-LIKE [*Populus trichocarpa*]	45	2.00E-65	79	XP_002300051.1	RAMOSA2 ortholog/homolog
45	LBD PROTEIN25-LIKE [*Glycine max*]	46	1.00E-62	75	XP_003554815.1	RAMOSA2 ortholog/homolog
46	LBD PROTEIN25-LIKE [*Glycine max*]	45	2.00E-65	79	XP_003548568.1	RAMOSA2 ortholog/homolog
47	LBD PROTEIN25 [*Glycine max*]	45	6.00E-65	78	XP_003553820.1	RAMOSA2 ortholog/homolog
48	LBD PROTEIN-LIKE [*Cucumis sativus*]	47	5.00E-61	74	XP_004157828.1	RAMOSA2 ortholog/homolog
49	LBD PROTEIN-LIKE [*Prunus persica*]	45	7.00E-48	66	EMJ13351.1	LBD protein (CLASS I)
50	LBD PROTEIN4-LIKE [*Fragaria vesca subsp. vesca*]	45	4.00E-49	66	XP_004293726.1	LBD protein (CLASS I)
51	LBD PROTEIN-LIKE [*Populus trichocarpa*]	45	2.00E-47	65	XP_002304584.1	LBD protein (CLASS I)
52	LBD PROTEIN4 isoform 1 [*Theobroma cacao*]	45	2.00E-48	66	EOY27472.1	LBD protein (CLASS I)
53	LBD PROTEIN4 [*Vitis vinifera*]	45	8.00E-48	64	XP_002270650.1	LBD protein (CLASS I)
54	LBD PROTEIN4-LIKE [*Cicer arietinum*]	45	2.00E-47	64	XP_004505337.1	LBD protein (CLASS I)
55	LBD PROTEIN-LIKE - LOC100790989 [*Glycine max*]	47	6.00E-48	60	NP_001241363.1	LBD protein (CLASS I)
56	LBD PROTEIN4-LIKE [*Solanum lycopersicum*]	45	1.00E-48	65	XP_004250781.1	LBD protein (CLASS I)
57	LBD PROTEIN-LIKE [*Ricinus communis*]	50	3.00E-50	60	XP_002513395.1	LBD protein (CLASS I)
58	LBD PROTEIN4 [*Theobroma cacao*]	46	2.00E-48	64	EOY13865.1	LBD protein (CLASS I)
59	LBD PROTEIN-LIKE [*Medicago truncatula*]	45	3.00E-47	64	XP_003616690.1	LBD protein (CLASS I)
60	LBD PROTEIN-LIKE [*Theobroma cacao*]	47	3.00E-49	63	EOY34594.1	LBD protein (CLASS I)
61	LBD PROTEIN-LIKE [*Vitis vinifera*]	47	4.00E-48	64	CAN68873.1	LBD protein (CLASS I)
62	LBD PROTEIN-LIKE [*Prunus persica*]	47	4.00E-48	64	EMJ07197.1	LBD protein (CLASS I)
63	LBD PROTEIN6-like [*Cucumis sativus*]	50	8.00E-55	65	XP_004152887.1	LBD protein (CLASS I)
64	LBD PROTEIN6-like [*Glycine max*]	61	6.00E-48	57	XP_003545810.1	LBD protein (CLASS I)
65	LBD PROTEIN-LIKE [*Capsella rubella*]	51	3.00E-47	64	EOA35742.1	LBD protein (CLASS I)
66	LBD PROTEIN-LIKE [*Populus trichocarpa*]	59	5.00E-49	58	XP_002307250.1	LBD protein (CLASS I)
67	LBD PROTEIN36-like [*Cucumis sativus*]	51	1.00E-47	62	XP_004148465.1	LBD protein (CLASS I)
68	LBD PROTEIN-LIKE [*Prunus persica*]	53	1.00E-47	61	EMJ04878.1	LBD protein (CLASS I)
69	LBD PROTEIN1-LIKE *[Hordeum vulgare*]	—	8.00E-57	—	Ctg135924_5HL	LBD protein (CLASS I)
70	LBD PROTEIN15-LIKE [*Hordeum vulgare*]	—	3.00E-23	—	Ctg1572307_3HL	LBD protein (CLASS I)
71	LBD PROTEIN1-LIKE [*Hordeum vulgare*]	—	9.00E-18	—	Ctg62778_4HL	LBD protein (CLASS I)
72	LBD PROTEIN11-LIKE [*Hordeum vulgare*]	—	2.00E-52	—	Ctg54974_1H	LBD protein (CLASS I)
73	LBD PROTEIN18-LIKE [*Hordeum vulgare*]	—	9.00E-12	—	Ctg1591863_7HS	LBD protein (CLASS I)
74	LBD PROTEIN16-LIKE [*Hordeum vulgare*]	—	2.00E-27	—	Ctg46032_6HL	LBD protein (CLASS I)
75	LBD PROTEIN24-LIKE [*Hordeum vulgare*]	—	9.00E-18	—	Ctg47723_4HL	LBD protein (CLASS I)
76	LBD PROTEIN6-LIKE [*Hordeum vulgare*]	—	2.00E-76	—	Ctg61827_3HL	LBD protein (CLASS I)
77	LBD PROTEIN6-LIKE [*Hordeum vulgare*]	—	3.00E-81	—	Ctg45166_1H	LBD protein (CLASS I)
78	LBD PROTEIN6-LIKE [*Hordeum vulgare*]	—	2.00E-76	—	Ctg51474_4HS	LBD protein (CLASS I)
79	LBD PROTEIN7-LIKE [*Hordeum vulgare*]	—	4.00E-09	—	Ctg98873_3HL	LBD protein (CLASS I)
80	LBD PROTEIN-LIKE [*Hordeum vulgare*]	—	4.00E-10	—	Ctg38897_5HL	LBD protein (CLASS I)
81	LBD PROTEIN41-LIKE; Class II [*Hordeum vulgare*]	—		—	Ctg42541_2HL	LBD protein (CLASS II)
82	LBD PROTEIN38-LIKE; Class II [*Hordeum vulgare*]	—		—	Ctg36895	LBD protein (CLASS II)
83	LBD PROTEIN39-LIKE; Class II [*Hordeum vulgare*]	—		—	Ctg1561909	LBD protein (CLASS II)
84	LBD PROTEIN41-LIKE; Class II [*Hordeum vulgare*]	—		—	Ctg50476_4HL	LBD protein (CLASS II)

Supplementary Text

Allelism test for *int-e.4* and *int-e.20* (Performed by Dr.Udda Lundqvist).

Since the *int-e.4* and *int-e.20* mutant alleles of *vrs4* did not show any molecular lesion within the ORF the allelism test data is presented below which confirms that these two mutants are in fact allelic to *vrs4* locus. The *int-e.4* and *int-e.20* were crossed to *vrs4.m* and the phenotypes were recorded for F_1 and F_2 stages.

Crossing analyses were done at Svalöv 1989 – 1990.

F_1 : *vrs4.m* × *int-e.4* − *Intermedium* types

F_2: *vrs4.m* × *int-e.4* − 22 *vrs4.m*: 26 *int-e.4*: 61 *Intermedium* types stronger than int-e.4 but not so pronounced than *vrs4.m*

F_1 : *vrs4.m* × *int-e.20* − *Intermedium* types

F_2: *vrs4.m* × *int-e.20* − 48 *vrs4.m*: 34 *int-e.20*: 68 *Intermedium* types stronger than *int-e.20* but not so pronounced than *vrs4.m*

10.0. Curriculum vitae

Name:	Ravi Koppolu
Institution/Employer:	Research group Plant Architecture, Genebank Department, Leibniz Institute of Plant Genetics and Crop Plant Research (IPK), Correns str.3, 06466 Stadt Seeland, OT Gatersleben, Germany.
Phone:	+49-39482-5694
E-mail:	koppolu@ipk-gatersleben.de, ravikoppolu@gmail.com
Nationality:	Indian
Date of Birth, PoB:	12.08.1982, in Santanutalapadu, India
Gender:	Male
Marital status:	Married
Children:	One (2012)

Education

PhD – Agriculture, Martin-Luther-University-Halle, Germany (March 2010 – October 2014), the thesis work has been carried out at the Leibniz Institute of Plant Genetics and Crop Plant Research (IPK.)

M.Sc – Agricultural Biotechnology, Acharya NG Ranga Agricultural University (ANGRAU), Hyderabad, India (2005 – 2007). Thesis work was conducted at ANGRAU and National Bureau of Plant Genetic Resources (NBPGR), Hyderabad, India.

B.Sc – Agriculture, Acharya NG Ranga Agricultural college, Bapatla, India (2000 – 2004.)

Research

- Functional analysis of *RAMOSA2* gene regulatory regions from grass species in barley *vrs4* (*HvRA2*) mutants (In continuation to the PhD work.)
- Cloning and characterization of barley Six-rowed spike 4 (*vrs4*) locus (PhD thesis.)
- Development of genetic linkage maps and quantitative trait loci analysis (QTL) for drought tolerance in peanut (*Arachis hypogaea* L.), at International Crops Research Institute for the Semi-arid Tropics (ICRISAT), Hyderabad, India (2007 – 2010.)
- Determination of genetic variability among chilli (*Capsicum annum* L.) germplasm using molecular markers – M.Sc. thesis (2005 – 2007.)

Achievements

- Awarded PhD with summa cum laude (excellent) by Martin-Luther-University-Halle-Wittenberg – Germany.
- Awarded Gold medal by Acharya NG Ranga Agricultural University (ANGRAU), Hyderabad – India for securing highest OGPA in M.Sc (2008.)
- Received AP – NL fellowship supported by the *Netherlands' Ministry of Foreign Affairs* during Masters Programme (2005 – 2007.)
- Secured 21st rank in national PhD entrance conducted by University of Hyderabad, Hyderabad, India in Plant Sciences division (2007.)

- Secured 3rd rank in state wide (Andhra Pradesh) M.Sc Agricultural Biotechnology entrance conducted by Acharya NG Ranga Agricultural University, Hyderabad – Andhra Pradesh, India (2004.)
- Secured 53rd rank in Indian Council of Agricultural Research (ICAR), M.Sc Entomology national entrance exam (2004.)

Peer-reviewed publication, oral or poster presentations based on the present thesis

Koppolu R., Anwar N., Sakuma S., Tagiri A., Lundqvist U., Pourkheirandish M., Rutten T., Seiler C., Himmelbach A., Ariyadasa R., Youssef H.M., Stein N., Sreenivasulu N., Komatsuda T., Schnurbusch T. (2013). Six-rowed spike 4 (*vrs4*) controls spikelet determinacy and row-type in barley. *Proceedings of the National Academy of Sciences 110:13198-13203* (***Koppolu R**., and **Anwar N.** contributed equally*.)

Koppolu R., Anwar N., Sakuma S., Tagiri A., Lundqvist U., Pourkheirandish M., Rutten T., Seiler C., Himmelbach A., Ariyadasa R., Youssef H.M., Stein N., Sreenivasulu N., Komatsuda T., Schnurbusch T. Genetic Control of Spikelet Determinacy and Lateral Spikelet Fertility in Barley. *Plant and Animal Genome conference XXII, 10-15 January 2014, San Diego, USA* (*Poster presentation.*)

Koppolu R., Anwar N., Sakuma S., Tagiri A., Lundqvist U., Pourkheirandish M., Rutten T., Seiler C., Himmelbach A., Ariyadasa R., Youssef H.M., Stein N., Sreenivasulu N., Komatsuda T., Schnurbusch T. Six-rowed spike 4 (*Vrs4*) mediates spikelet architecture and row-type identity in barley. *VIPCA, Plant Genetics and Breeding Technologies, 18-20 February 2013, Vienna, Austria* (*Poster presentation.*)

Koppolu R., Anwar N., Sakuma S., Tagiri A., Lundqvist U., Pourkheirandish M., Rutten T., Seiler C., Himmelbach A., Ariyadasa R., Youssef H.M., Stein N., Sreenivasulu N., Komatsuda T., Schnurbusch T. Six-rowed spike 4 (*Vrs4*) mediates spikelet architecture and row-type identity in barley. *Plant and Animal Genome conference XXI, 11-16 January 2013, San Diego, USA* (*Poster presentation.*)

Koppolu R*, Anwar N, Sakuma S, Govind G, Ariyadasa R, Pourkheirandish M, Himmelbach A, Lundqvist U, Stein N, Sreenivasulu N, Komatsuda T, Schnurbusch T. *Vrs4* mediates determinacy of the triple spikelet meristem in barley. *11th International Barley Genetics Symposium, 15-20 April 2012, Hangzhou, China* (*presenting author, *Oral presentation.*)

Koppolu R., Komatsuda T., Schnurbusch T. Isolation and characterization of candidates for Six-rowed spike 4 (*vrs4*) gene in barley (*Hordeum vulgare* L.). *Genomics based breeding conference 26-28 October 2010, Giessen, Germany* (*Poster presentation.*)

Other peer-reviewed publications or poster presentations during PhD thesis work

Youssef, H.M., **Koppolu R**., Rutten T., Korzun V., Schweizer P. and Schnurbusch T. (2014). Genetic mapping of the *labile* (*lab*) gene: a recessive locus causing irregular spikelet fertility in *labile*-barley (*Hordeum vulgare* convar. *labile*). *Theoretical and Applied Genetics, DOI: 10.1007/s00122-014-2284-0.*

Youssef H., **Koppolu R**., Schnurbusch T. (2012). Re-sequencing of *vrs1* and *int-c* loci shows that *labile* barleys (*Hordeum vulgare* convar. *labile*) have a six-rowed genetic background. *Genetic Resources and Crop Evolution 59:1319-1328* (***Youssef H.,*** *and* ***Koppolu R.*** *contributed equally.*)

Youssef H.M., Fazeli Arash., **Koppolu R**., Rutten T., Ariyadasa Ruvini., Himmelbach A., Stein N., and Schnurbusch T (2013). Does Six-rowed spike2 (*vrs2*) play a role in regulating barley lateral spikelet fertility? *VIPCA, Plant Genetics and Breeding Technologies, 18-20 February 2013, Vienna, Austria* (*Poster presentation.*)

Previous peer-reviewed publications (prior to PhD thesis work)

Koppolu R., Vadez V., Isobe S., Mir R.R., Guo Y., Nigam S.N., Gowda M.V.C., Radhakrishnan T., Bertioli D.J., Knapp S.J., Varshney R.K. (2011). Identification of several small main-effect QTLs and a large number of epistatic QTLs for drought tolerance related traits in groundnut (*Arachis hypogaea* L.) *Theoretical and Applied Genetics 122:1119-1132.*

Koppolu R., Upadhyaya H., Dwivedi S., Hoisington D.A, Varshney R.K (2010). Genetic relationships among seven sections of genus *Arachis* studied by using SSR markers. *BMC Plant Biology 10:15.*

Varshney R.K., Bertioli D.J., Moretzsohn M.C., Vadez V., Krishnamurthy L., Aruna R., Nigam S.N., Moss B.J., Seetha K., **Koppolu R**., He G., Knapp S.J., Hoisington D.A. (2009). The first SSR-based genetic linkage map for cultivated groundnut (*Arachis hypogaea* L.). *Theoretical and Applied Genetics 118:729-739.*

Gautami B, **Koppolu R**., Lakshmi Narasu M., Hoisington D., Varshney R. (2009). Novel set of groundnut SSR markers for germplasm analysis and interspecific transferability. *International Journal of Integrative Biology 7:100-106.*

I hereby declare that all information stated above is true

[ ]
Ravi Koppolu

11.0. Eidesstattliche Erklärung

Herr. Ravi Koppolu
GH1, Selkeweg 4a
Gatersleben – 06466

Hiermit versichere ich an Eides Statt, dass ich die eingereichte Dissertation "**Six-rowed spike 4 (*Vrs4*) regulates spike architecture and lateral spikelet fertility in barley (*Hordeum vulgare* L.)"** selbstständig angefertigt und diese nicht bereits für eine Promotion oder andere Zwecke an einer anderen Universität eingereicht habe. Weiterhin versichere ich, dass ich die zur Erstellung der Dissertationsschrift verwendeten Arbeiten und Hilfsmittel genau und vollständig angegeben habe.

Des Weiteren erkläre ich, dass keine Strafverfahren gegen mich anhängig sind.

Gatersleben, den ----------

[ ]
Ravi Koppolu